NDX-070015

ALOS User Handbook

Earth Observation Research Center, Japan Aerospace Exploration Agency

Table of contents

1. Introduction

The Advanced Land Observing Satellite (ALOS) "Daichi" was launched a year and a half ago. Within this period, the initial mission check of satellite and sensors, initial calibration, and routine calibration have been carried out, to verify the performance of the satellite and sensors. It was confirmed that the satellite is operating properly, providing correct position, attitude, and time data to the sensors. This means that the satellite fulfills its task of serving as a backbone for the earth observation equipment. Accurate information helps the sensors to produce high quality images of a level that is among the best worldwide. The observation sensors consist of a high-resolution stereo mapping sensor (PRISM), a visible and near infrared radiometer (AVNIR-2), and an L-band synthetic aperture radar (PALSAR), all of which are high performance systems. Over the last 18 months, their performance was evaluated and image processing technology was applied to improve image accuracy (geometric accuracy and radiometric accuracy, including calibration and validation). Application research areas where extracted geophysical parameters have been used so far include the creation of numerical elevation models, finalizing of orthogonal projection methods, acquiring data about seismic and volcanic activity fluctuations, and detection of environmental changes such as deforestation. ALOS is expected to contribute to society in numerous ways. One such example is disaster monitoring, which requires the capability for establishing immediate observation plans, identifying affected areas, and instant distribution of data. These functions were successfully tested over the past year and a half. Of course, imaging accuracy is of utmost importance. In this area, a variety of feedback both on the technical and the application side was received and processed during the testing stage, which has helped us to develop an observation system that we believe is practical and easy to use. While the first edition of the Reference Handbook which was compiled before the launch was based on a prognosis of how the expected data could be used, this second edition reflects the results of various trials conducted over the past 18 months. There are still many areas that are incomplete, and the handbook should be considered as another step on the road to the final goal. It is hoped that the materials presented here will help clarify the potential of the satellite and serve as an incentive for further research and utilization (including calibration and validation). In this regard, the handbook should be considered an addition to the library of reference tools available to users.

Masanobu Shimada
Earth Observation Research Center

2. ALOS Science Program

2.1 Concept and Background

2.1.1 Diversification of Earth Environment Problems

Most analyses on Earth's environmental problems have focused on forecasting, evaluating and preventing of impacts of the global warming due to greenhouse gas effect. Greenhouse gas from a single country spreads in a short instance and accelerates global climate changes. Greenhouse gas emissions can be clearly recognized as a global problem. However, global environment problems also have natural resource problem aspects, such as food supply.

A global food crisis may not occur suddenly. Instead, sneaking shortage and resulting price rise of major crops may apply pressures to relatively vulnerable areas, which may slowly lead to instability in global food trade systems worldwide. For instance, the current civil wars in Africa are fundamentally related to long-term poverty due to land resource degradation and water resource deficiencies. Moreover, devastation from the wars causes additional problems such as large numbers of refugees. These land and water resource problem may lead to instability of the world political system and, therefore, cause difficulties to individual countries worldwide.

To alleviate and eventually solve these problems, it is necessary to continuously obtain local information on land, water, and vegetation resources at global scale. Ecosystem preservation and genetic resource protection are also influential subjects, which also require a steady flow of local data acquired globally. So far, it is widely believed that low-resolution data is enough for global problems. In fact, high-resolution data, which is useful for local area, should be acquired globally to cope with the problem. Moreover, this is now becoming technically possible.

2.1.2 Think Globally and Act Locally------Establishing Global Environment Measures Corresponding to Local Needs.

As shown by the Kyoto protocol of COP3, the focus of global environment problems has shifted from examining the influence and clarifying the mechanism to drafting countermeasures, forming mutual agreement and developing implementation strategies. In the area of greenhouse gas, effective countermeasures for controlling greenhouse gas generation include forest preservation, carbon storage and fixation, carbon emission taxes, emission trade, and energy saving technology development. Policies such as forest preservation and reforestation are expected to be directly linked to regional interests and should therefore be coordinated with regional needs, because a global policy that brings disadvantages to local people is not sustainable.

Consequently, it is necessary to obtain local data to conduct policy globally. In particular, policy issues such as preservation of land and water resources, stabilization of food production by sustainable use of land and water resources, disaster risk mitigation, and various species' preservation by ecosystem conservation should be addressed on a regional basis. Therefore regional data that covers the globe and reflects local needs is necessary to develop realizable policies balancing global viewpoints and regional needs.

2.1.3 Popularization of GIS (Geographic Information System)

Today utilizations of the Geographic information System are in the process of getting into full swing in the field of regional planning and development as well as many other fields such as facility management. Regional planning and development need a comprehensive appraisal of environmental resources with various information, and corroboration of planning alternatives by simulations. GIS is now an essential tool enabling to integrate information on environment, resources and human activities through digital base maps. However, in developing areas which need careful examination in the process of regional planning and development, even very basic data such as topography and vegetation do not exist at all, or even if they existed, they seldom become available due to several reasons such as national security reasons. On the other hand, since commercial GIS software has been widely used in recent years, if current data become ready for use, the data provision would have very great impacts. Especially, such information as topography that can be used in many application fields (so-called spatial data infrastructure (SDI)) is expected for distribution.

Popularization of GIS also means that ordinary users can have powerful data processing capability. If it becomes easy to obtain data together with necessary software and input parameters as well through the network, not a small part of the data processing can be conducted by users, which will greatly contribute to reducing processing load of the primary data distributors. High level processing software can be distributed over the net as well, to promote efficient and effective use of the data.

2.1.4 ALOS Mission Concept

To help resolve local issues such as food security, water resource scarcity, disaster prevention and biological diversity conservation that also require support and collaboration from the global viewpoint, what kinds of data should be developed.

Information on current status and changes of environmental resources such as soil, water, and vegetation (from forest to farmland) are the basis in analyzing these issues. Though quality of soil may not be easy to acquire by remote sensing, risk of soil degradation caused by erosion is governed by climatic and topographical factors. Regarding water circulation and vegetation, climatic and topographical factors are dominant as well. It is also the case with disaster risks. Of course, information on how people use land (land use Information) is indispensable. Although the climate data may be excluded just because it cannot be directly observed from satellite, it could be concluded that topographic information would be the core part of the common information basis.

Figure 2.1.4-1 illustrates the percentage cover of topographic maps by major regions. It can be found that the percentage cover of 1:1000 to 1:31,600 topographic maps is very low in developing areas such as Africa and Asia. As a matter of fact, topographic maps of this range of scales, mainly 1:25,000 maps are essential for environment conservation planning, resource management and development planning from regional to national scales. They also play central roles in formulating ODA for developing countries. So far, only "temporal" solutions have been explored to meet the information demand. Individual projects might generate a very minimum amount of data for their own purposes or could not help using out-of-dated paper maps might be used. In some cases, satellite imagery might be used as an insufficient substitute. On the other hands, topographic information equivalent to 1:25000 maps can be acquired by satellite observation very efficiently over the continents.

With these backgrounds, mission concept of ALOS (Advanced Land Observation Satellite) was defined as below.

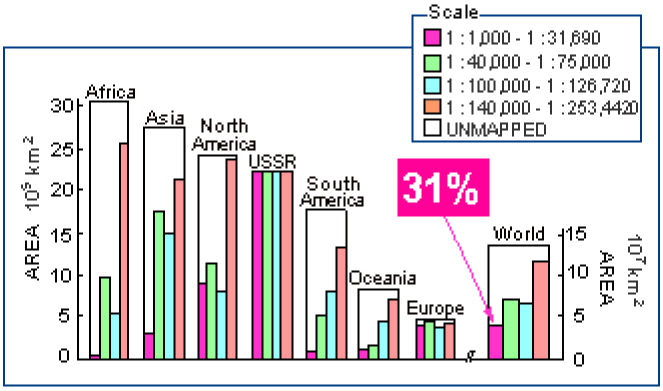

United Nations,"World Cartography vol.XX", 1990

Fig.2.1.4-1 The percentage cover of topographic maps by major regions
(Source: United Nations, "World Cartography vol. XX" 1990)

(1) Generate topographic data as SDI (Spatial Data Infrastructure) at the global scale.

DEM (Digital Elevation Model) data with less than 5-meter errors and with 10 meter grid spacing will be developed. Satellite imagery has advantages in generating DEM of this level, because the measurement techniques are relatively established and elevation data are not likely to change so frequently. By overlaying high-resolution optical sensor data and SAR data on the derived DEM, information on environmental resources like vegetation and soil can be provided. For the areas where the DEM was already developed, we can focus on changes of land surfaces. Combination of DEM and satellite imagery will contribute to the development of global spatial data infrastructure

(2) Support "sustainable" development at local to regional scale through monitoring global environmental resources.

In addition to the global spatial data Infrastructure, a variety of information on environmental resources provided through ALOS mission can help conservation of environmental resources and sustainable development at the local to regional scale.

(3) Monitor major disasters at the global scale.

Disaster such as drought, volcanic explosion and flooding can threaten sustainable and stable regional development. Being integrated with the other satellites and monitoring systems, ALOS will provide information on major disasters.

(4) Exploration of non-renewable resources

In parallel with the monitoring of land and water related resources, ALOS mission will provide information for exploring non-renewable resources to support regional development.

(5) Technological development for the future earth observation

ALOS is almost a single satellite, which aim at global observation with high-resolution sensors. It poses many challenging research and development topics for sensor development and data processing, which will make significant contributions to the development of next generation earth observation technologies.

2.1.5 The ALOS Kyoto & Carbon Initiative

The ALOS Kyoto & Carbon Initiative is an international collaborative project led by JAXA Earth Observation Research Center (EORC). It follows JAXA's Global Rain Forest and Global Boreal Forest Mapping project (GRFM/GBFM) which was carried out from 1995 to 2003 using the Synthetic Aperture Radar (SAR) carried on board the Japanese Earth Resources Satellite-1 (JERS-1), and continues this topic into the era of the Advanced Land Observation Satellite (ALOS).

The initiative encompasses an observation project using the global imager (GLI) carried on board the Advanced Earth Observation Satellite-II (ADEOS-II).

Related data and information will also be prepared in the following areas:

- UNFCCC Kyoto Protocol
- International contribution to an overall carbon cycle observation system as defined by IGOS-P

A second mission is cooperation with and direct or indirect support for international environmental conventions (Ramsar Convention on Wetlands, UN Convention to Combat

Desertification, Convention on Biological Diversity).

(1) Objectives

The objectives of the ALOS K & C Initiative fall into the following main categories.

- Extraction and quantification of changes in forest distribution and land cover
    - Identification of changes and assessment of affected areas
    - Quantification of changes in biomass
- Mapping and monitoring of methane discharge sources
    - Wetlands:
        - Mapping of wetland areas
        - Monitoring of inundation and flooding dynamics
    - Irrigated fields:
        - Mapping of rice paddy areas
        - Assessment of harvest timing and harvesting
    - Dynamics of freezing and thawing in cold zones

(2) Data acquisition strategy

Dedicated data acquisition strategies intended to meet requests for systematic and consistent observation data on a continental scale are currently being developed. The strategies are characterized as follows.

- Spatial uniformity on a continental scale (continuous observation without gaps)
- Chronological uniformity (area observation within a short time span)
- Multiple spatial resolution options (20 m, 100 m, 250 m)
- Appropriate repeat frequency (from once per month to once per year)
- Long-term continuity (for the life of the satellite)
- Global coverage observation

The L-band Synthetic Aperture Radar (PALSAR; 1,270 MHz/23.5 cm) carried on ALOS is in principle capable of observation with a large number of different combinations of polarization, off-nadir angles, and resolution. With the aim of ensuring chronological and spatial uniformity, the following three modes have been selected.

- HH polarization, off-nadir angle 34.3 degrees, 10 m resolution
- HH + HV polarization, off-nadir angle 34.3 degrees, 20 m resolution
- HH polarization ScanSAR, 100 m resolution

The GLI sensor on board ADEOS-II has multispectral scan capability in 36 bands. Six out of these bands have a spatial resolution of 250 m, and spectral observation is performed in the ETM+ and MODIS (B, G, R, NIR, MIR1, MIR2) bands.

Data acquisition strategies are determined using a series of observation simulations performed at JAXA. At this stage, it is planned to acquire 200,000 scenes per year for PALSAR HH + HAVE polarization. Each continent is to be covered at least twice per year.

It forms the continuation of JAXA's JERS-1 SAR Global Rain Forest and Global Boreal Forest Mapping project (GRFM/GBFM) into the era of the Advanced Land Observation Satellite (ALOS).

The ALOS K & C Initiative is set out to support explicit and implicit data and information needs raised by international environmental Conventions, Carbon Cycle Science and Conservation of the environment - referred below to as the CCCs. Led and coordinated by EORC JAXA, the Initiative is being undertaken by an international Science Team, and focuses primarily on defining and optimizing provision of data products and validated thematic information derived from in-situ and satellite sensor data, focusing particularly on that acquired by the Phased Array L-band Synthetic Aperture Radar (PALSAR) on-board the Advanced Land Observing Satellite (ALOS).

(3) Objective and Data acquisition strategy

The objective of the ALOS K & C Initiative is to define, develop and validate thematic products derived primarily from ALOS PALSAR data that can be used to meet the specific information requirements relating to the CCCs. A key component of this work has been the development of a systematic data acquisition strategy for ALOS which comprises fixed, systematic global observation plans for PALSAR. The strategy is implemented as a top-level foreground mission and with a priority level second only to that of emergency observations. With emphasis on acquiring repetitive and consistent data over continental scales, it ensures that adequate data will be collected to allow the required thematic output products to be developed on a timely basis.

The K & C Initiative is based on the three coordinated themes relating to global biomes; Forests, Wetlands, Deserts and Semi-Arid Regions, and a fourth theme dealing with the generation of regional ALOS PALSAR mosaics. A key word for the Initiative is regional-scale applications and product development, with data requirements in the order of hundreds or thousands of PALSAR scenes for each prototype area. Each theme has identified key products that can be generated from the PALSAR data including land cover (forest mapping), forest change mapping and forest biomass and structure (Forests), global wetlands inventory and change (Wetlands), freshwater resources and desertification (Deserts). Each of these products are generated using a combination of PALSAR, in situ and ancillary datasets.

(4) Scientific support

An international Scientific Advisory Panel has been established to assure scientific relevance in the project design and alignment with other relevant international efforts (e.g. GOFC/GOLD, IGOL, GTOS/TCO). The panel consists of scientists active in the fields of carbon modeling and biophysical parameter retrieval, SAR experts, and representatives from GOFC, TCO, FAO, space agencies, universities and public research institutions.

2.2 Goals

To achieve the ALOS mission, it is essential not only to distribute data products to users, but also to promote scientific and utilization research for ALOS data in broad categories ranging from the environmental and resource sciences to computer science. This Plan suggests research categories that are strongly related to acquisition and application of ALOS data and that will be promoted by association and efforts of PIs in this RA and EORC.

Among the suggested research categories, certain data products and associated algorithms which are considered especially important and for which JAXA resources should be allocated with high priority are referred to as strategic goals. These are selected from the general goals based on factors such as relevance to the ALOS mission, spin-off effects, and available resources. While general goals are mainly to be realized through the promotion of research activities, strategic goals are to be pursued systematically, with EORC and related institutions playing a central role.

2.2.1 General Goals

The general goals determine which categories to select, how to contribute to each category, and what kinds of data products and algorithms are required. The categories mentioned below are classified based on the categories of undergoing core projects of the International Geosphere- Biosphere Program (IGBP).

(1) Land Use and Land Cover Research

This research reveals land use and land cover changes, and contributes to clarifying the mechanism of such changes and the development of change models. It is important to develop the following products and algorithms for these purposes.

1) High-resolution Digital Elevation Model:

Topographical conditions strongly influence land use determination and its change process as well as environmental impacts such as soil erosion and runoff changes. In these research categories, a Digital Elevation Model (DEM) which corresponds to a 1: 25,000 to 1: 100,000 scale topographical map is useful. Algorithms for stereo matching and interferometric measurement need to be developed.

2) Orthophoto image (PRISM, AVNIR-2, PALSAR images) and land use and land cover data:

These can reveal sprawl of urban areas and villages, changes of agricultural land and agricultural practices, deforestation, etc. Radar images may also be able to detect tillage variations (variation of tillage surface roughness) and changes of cropping pattern. It is also necessary to promote research for integrating ALOS data with ADEOS-II data.

(2) Topography and Geology

This research contributes to measuring changes in terrain and watercourses due to soil erosion and slope failure as well as to classifying and analyzing terrain features with elevation data. It is thus essential that the following data products and algorithms be developed.

1) High-resolution DEM:

High-resolution DEM can be used for terrain classification and analysis as well as watercourse analysis.

2) Orthophoto image (particularly PALSAR image):

An orthophoto image can be used for extraction and classification of terrain features and so on.

3) Elevation change due to soil erosion and sedimentation:

Interferometric measurement is expected to provide a method for measuring time-series changes of land elevation. An area which a topographic condition changes remarkably due to soil erosion and sedimentation, such as the Yellow River basin, is selected as the objective area.

(3) Terrestrial (Vegetation) Ecosystem, Agriculture and Forestry Research

This research contributes to clarifying vegetation dynamics with emphasis on the carbon cycle, monitoring agricultural production, estimating productivity of pastures based on the vegetation dynamics, and investigating biomass changes caused by human activities. For this purpose, the following data products and algorithms need to be developed using AVNIR-2 data or other satellite data.

1) Forest distribution monitoring:

Methods for measuring global forestry distribution are expected to be advanced using PALSAR or AVNIR-2.

2) Vegetation biomass distribution measurement :

Vegetation biomass is a key parameter which describes vegetation dynamics. A method of measuring vegetation biomass with focus on forests with simultaneous observations by PRISM and AVNIR-2 is expected to be developed.

3) Application to forest management:

A method of monitoring deforestation and afforestation and estimating forest growth should also be developed concurrently with the development of a biomass measurement method.

4) Monitoring the productivity of pastures and crop land:

Developing a method for determining the crop planting area, estimating productivity of pastures and crop land in a specific area, based on intensive observation by both PALSAR and AVNIR-2, is expected. In addition, a method of monitoring the changes of agricultural production and productivity of pastures caused by drought should also be developed.

5) Monitoring vegetation change due to human activities such as biomass burning:

A method for measuring and monitoring the variation of biomass density and vegetation structure due to biomass burning in specific areas with intensive observations using PALSAR together with AVNIR-2 needs to be developed.

6) Desertification Monitoring:

This aims at monitoring the decline of land productivity and soil degradation due to excessive cultivation and pasturage and improper irrigation. Methods of indirectly monitoring desertification need to be developed by observing vegetative deterioration using PALSAR and AVNIR-2 as well as directly monitoring of salt accumulation on the soil surface using AVNIR-2.

(4) Climatic System, Hydrological Processes, and Water Resources Related Research

1) Surface process:

In research on surface processes, it will be useful to develop methods to understand vegetation distribution, to measure soil moisture, and to prepare soil moisture datasets.

① Vegetation monitoring:

Development of algorithms for measuring key parameters for water vapor estimation such as biomass density or Leaf Area Index (LAI) is expected. Development of methods for integrating other satellite data, such as ADEOS-II data, is also important.

② Estimating of soil moisture distribution:

Development of algorithms for measuring soil moisture with PALSAR need to be facilitated. Development methods for integrating other satellite data, such as ADEOS-II data, with PALSAR data may also be essential.

③ Run-off analysis:

ALOS data will contribute to run-off analysis under various conditions related to climate and land even in areas where there is insufficient available data.

a. High-resolution DEM:

A high-resolution DEM, having much higher resolution than the existing 1km DEM, has the potential of making the run-off analysis more accurate and reliable.

b. Datasets of land use / land cover and their changes:

These datasets will help analyze water valance and run-off variation due to land use and land cover changes. Using additional satellite data will make this research more successful.

2) Water pollution analysis:

This research aims at estimating the quantity of water pollutant load and analyzing flow-down conditions by providing more accurate topographical data, and land use and land cover datasets.

① High-resolution DEM:

A high-resolution DEM will enable more accurate analysis of the flow-down of the water pollutant load due to soil erosion and estimation of the amount.

② Datasets of land use / land cover and their change:

These datasets facilitate analyzing the quantity of the water pollutant load by land use and land cover changes. Combined with hydrological analysis, these datasets reveal the condition of the pollution effluent. Using additional satellite data will make this research more successful.

3) Snow and ice related analysis:

Accurately analyzing snow and ice in the following categories using high resolution sensor data from ALOS will contribute to understanding changes of climate and water resources (hydrological cycles), and so on.

① Estimating states and changes of snow cover and snow-water equivalent:

Analysis using the observation data from PALSAR and AVNIR-2 can help accurately predict and understand the seasonal or annual change of snow cover and snow-water equivalent.

② Measuring and analyzing variations of ice sheets and glaciers:

Analysis of Interferometric measurements by PALSAR and observation by AVNIR-2 will contribute to understanding the ice sheet mass balance and mountain glacier variation in the South Pole, Greenland, and so on.

③ Sea ice monitoring:

Analyzing the observation data from PALSAR and AVNIR-2 will contribute to determining the extent and seasonal or annual variation of ice sheets in the polar regions and coastal zones. Furthermore, using ScanSAR data from PALSAR will contribute to methodological development of extensive sea ice monitoring, and using polarimetric data of PALSAR will improve the accuracy of sea ice classification.

(5) Oceanography and Coastal Zone Related Research

1) Coastal zone related research:

Providing information on wave, sea surface wind, water current, sea ice, topographical change and sand drift in coastal areas can support economic activities in coastal areas such as sea traffic, pollution control and fisheries. For this purpose, it is necessary to develop and prepare the following algorithms and products.

① Oil spill datasets of coastal zones:

Techniques for extracting the polluted areas from PALSAR images is expected to be developed. It is necessary to analyze sea surface wind and the spectrum of ocean waves around the area to accurately extract polluted areas. At the same time, datasets which analyze these factors must be developed.

② High-resolution DEM of coastal zones:

High-resolution DEM of coastal zones combined with water depth data will contribute to analyzing transformation of sea wave and coastal topography and impacts of sea level rise.

③ Datasets of sea surface wind and wave height in coastal zones:

It is possible to prepare datasets for coastal sea-surface winds and waves using PALSAR data. A method which predicts coastal current by utilizing a numeric simulation model along with these datasets should be also developed. These are useful for giving of a boundary condition for analysis of coastal transformation and sand drift.

④ Datasets of sea ice:

Methods for monitoring coastal sea ice and for providing its data accurately using PALSAR and AVNIR-2 need to be developed. Coastal ice datasets are useful for various coastal activities of human beings.

2) Ocean dynamics:

Utilization of PALSAR or development methods using PALSAR together with other satellite data such as ADEOS-II data will contribute to studies on air-sea interaction, sea waves, and dynamics of various ocean phenomena in coastal zones and the open seas.

① Coastal topography-air-sea interaction:

Strong or weak wind zones are generated locally in a coastal sea because of coastal topography. Though such changes of sea-surface are essentially important to coastal waves and water currents, little research has been conducted in these areas. High-spatial resolution information collected by PALSAR on ocean waves and sea surface winds is expected to greatly contribute to studying the coastal topography-air-sea interaction and probing its mechanism.

② Wave-current interaction and various phenomena in the ocean:

Studies on the interactions between ocean waves and currents using data acquired in the ScanSAR mode of PALSAR need to be promoted. Based on these studies, large-scale ocean currents (like the Black Current), cold/warm water masses, coastal water currents, and internal waves can be visualized from ScanSAR images. This will help us to understand ocean dynamics.

(6) Disasters and Earthquakes

1) Diastrophism:

Methods for monitoring land surface deformations due to diastrophism employing interferometoric observation by PALSAR are needed to be developed.

2) Volcano monitoring:

A method for monitoring deformation of mountains caused by volcanic activities should be developed.

3) Slope failure:

It is necessary to develop a method for risk analysis of slope failure using high-resolution DEMs generated by PRISM and PALSAR. Datasets of land use and land cover in slope areas will contribute to estimating surface erosion and water infiltration as well as forecasting the damage of slope failure.

4) Analysis and simulation of flooding and inundation:

By applying high-resolution DEMs, we can conduct run-off (flooding) analysis and inundation in areas where we previously haven't had enough data. This will contribute to advancing methods for analyzing and investigating those phenomena. At the same time, land cover and land use data will improve the reliability of these analyses as well as damage forecasting and refuge planning.

5) Tidal wave analysis:

It is expected that tidal wave tracing analysis with high-resolution DEMs can be conducted in areas where we previously haven't had enough data. This will contribute to advancing the methods of analyzing and investigating these phenomena. Furthermore, land cover and land use data together with high-resolution DEMs will improve the reliability of these analyses as well as damage forecasting and refuge planning.

6) Disaster monitoring technique:

Disaster monitoring techniques reveal damage due to drought, flood, fire, slope failure, earthquake disaster. Furthermore, these techniques can be applied to quick and accurate damage assessment (for example, the effect on agricultural production).

(7) Resource Exploration

Resource exploration research techniques for mineral resource need to be developed. Analysis methods integrating PRISM, AVNIR-2, and PALSAR images with DEMs will be examined.

(8) Development of Spatial Data Infrastructure

1) Techniques for developing spatial data infrastructure:

Automatic recognition and three-dimensional measurement of terrain features need to be developed to efficiently generate high-resolution DEMs and spatial data on artificial structures, which are the basis of various scientific research and practical uses. For three-dimensional measurement, orientation methods and stereo matching methods for PRISM images need to be developed. Furthermore, an algorithm for interferometric measurement need to be developed for PALSAR. In addition, a method integrating images (from PRISM, AVNIR-2 and PALSAR) with DEM needs to be developed for automatic recognition and three-dimensional measurement of terrain features such as roads, large structures and urban areas.

2) Management and retrieval techniques for very large database:

Using ALOS data as a test case, techniques for very large spatial database are expected to be developed. Examples include data storage and management techniques, an efficient retrieval method based on a map or coordinates.

(9) Basic Studies on Scattering and Interferometric Characteristics

In order to expand the application fields of PALSAR data, including improvements of interferometric analysis, polarimetric analysis, and terrain correction methods, the following study will be performed.

1) Decomposition method for polarimetric SAR data

Decomposition methods for PALSAR polarimetric data should be studied and developed. This methodology will be applied to land cover classification using scattering characteristics of the targets.

2) Polarimetric and interferometric data analysis

Interferometric analysis is applied to the polarimetric data acquired from PALSAR repeat-pass observation. An applied field example is tree height estimation in forested areas.

(10) Basic studies for accurate observation with high resolution optical sensors

Research on the following topics needs to be conducted to develop the next-generation high-resolution optical sensors.

1) The accuracy of satellite position and attitude determination, including the rate of the variation of the attitude which will affect the pointing accuracy and resolution of the optical sensors, needs to be analyzed and evaluated.

2) Impacts of the shock during launch, temporal degradation, and temperature changes inside the instruments on optical alignment (including the optical benches and the structures with optical alignment), photoelectric transfer characteristics, and sensor resolution need to be analyzed and evaluated.

3) It is necessary to develop a code to analyze the effect of multiscattering of the atmosphere, especially regarding aerosols, whose spatial conditions fluctuate largely with time, and to estimate the surface albedo with high speed and high accuracy.

4) A suitable filter for the modulation transfer function (MTF) correction needs to be developed to restore observation data degraded by the MTF of each sensor or atmospheric influences.

2.2.2 Strategic Goals

We define development of specific data products and algorithms for promoting the other scientific researches as "strategic goals." These are selected considering the relevance to the ALOS mission and the goals of this plan, resource limitations, etc.

(1) Data products

1) Global High-resolution DEM and Orthophoto image (PRISM, AVNIR-2, and PALSAR):

These data products form the basis of many fields of research and practical applications. They are provided by only ALOS at the moment. However, resources required to generate these data are so large that the accuracy and resolution may change according to the objective area. Global coverage will be pursued by coordinating with other data node organizations.

2) Global Biomass density dataset (PALSAR and AVNIR-2):

Biomass is not only one of the most important parameters for estimating the carbon cycle, but also provides a basis for forestry management. However, it is difficult to measure on the ground and there is no data covering a large area. Since only ALOS is equipped with L-band, which favors biomass observation, it is expected that biomass density data will be generated using PALSAR images along with AVNIR-2 images and high resolution DEMs. These activities will allow us to conduct time series analysis with Global Forest Mapping (GFM) datasets from JERS-1 SAR data.

3) Land surface deformation dataset (Earthquake-prone areas only):

The distribution of deformed land surfaces can be extracted by interferometric measurement. Monitoring diastrophism is essential in the Pacific Rim area, including Japan, which is always threatened by earthquakes. Land surface deformation data will be collected by periodic satellite observation and continuous ground observation.

4) Coastal environment data

① Wave and sea surface wind data, oil spill area data Information about waves and sea surface winds in coastal areas is to be extracted from PALSAR data. Methods for improved extraction of reliable data regarding sea surface winds and wave height to create customized ALOS products are to be developed. The detection of oil spills which show up as darker sections in wave areas can be improved by performing parallel analysis of adjacent wave areas. Suitable methods for this are also to be developed.

② Coastal sea ice data Data regarding sea ice can be extracted reliably, and such data are of high importance. The development of methods for quickly extracting such data and reliably distributing them can therefore be expected to be highly beneficial to society.

(2) Algorithms

1) Automated generation of high-resolution DEM and orthophoto image:

A large computing capability is usually required to generate high-resolution DEMs and orthophoto images, and the quality of these products is affected strongly by the performance of the algorithms used. Algorithms for automated generation of high-resolution DEMs and orthophoto (including an algorithm to estimate satellite position and altitude) need to be developed.

2) Accuracy improvement of biomass measurement method:

Development of algorithms using DEMs and AVNIR-2 images together with other satellite images for measuring global biomass distribution with higher accuracy is solicited.

(3) Calibration and Validation for each Sensor and Related Basic Studies

Calibration and validation of each sensor is necessary for improving the quality of the data products such as high-resolution DEMs and biomass density data. In addition, basic studies on calibration and validation for improving the accuracy of each sensor should also be pursued as strategic goals.

1) Calibration and validation for optical Sensors

To generate high-quality products from optical sensors, AVNIR-2 and PRISM, basic study for very accurately evaluating radiance characteristics, geometric characteristics, spatial resolution, system noises, and other factors. is considered to be one of the strategic objectives.

① Accuracy improvement of radiance and brightness calibration

The radiance and brightness of optical sensors will be calibrated by using pre-flight test data, internal calibration source data, and external calibration data after launch. The main output of this study is to estimate absolute calibration coefficients. In particular, an important challenge will be the improvement of stability characteristics with ground-based experiments with calibration after launch and development of the radiative transfer model with high accuracy.

② Accuracy improvement of DEM

Algorithms for automatically evaluating and correcting registration and pointing accuracy, and for automatically producing high-resolution DEMs using stereo matching images will be developed.

③ Atmospheric correction

Algorithm should be improved to estimate the surface albedo on a heterogeneous surface using optical sensors data, taking into account the effect of multi-scattering in the atmosphere, especially spatial and temporal changes of aerosols.

2) Calibration and validation for PALSAR system

A basic study for achieving high radiometric accuracy of the PALSAR system is considered to be one of the strategic objectives.

① Accurate estimation of normalized radar cross section

The relation between the digital number and the normalized backscattering coefficient for PALSAR standard products will be determined by using the pre-flight test data, internal calibration source data, and external calibration data. The main outputs of this study are the estimated in-orbit antenna elevation patterns and the absolute calibration coefficients.

② Accuracy improvement of interferometric SAR data

In order to derive accurate digital elevation models as well as crustal movements, a study on achieving an accurate phase difference will be done by using repeat-pass interferometric datasets acquired by the PALSAR system.

③ Accuracy improvement of polarimetric SAR data

PALSAR's polarimetric observation mode is currently an experimental mode. However, this observation mode will be the main operation mode in future SAR systems. In order to prepare for the practical use of fully polarimetric data, polarimetric calibration with the data acquired from PALSAR polarimetric observation mode should be studied. The methodology to derive phase correction, cross talk, and gain imbalance will be developed and investigated.

2.3 Data Analysis and Utilization

2.3.1 Calibration and Validation of PALSAR

Since the PALSAR first image acquired on February 14, 2006, calibration of the PALSAR has been carried out. To each of the PALSAR operation mode, detailed characterization of the sensor data were conducted, processing algorithms were designed, image processing software were developed and optimized. After extensive evaluation of image accuracy, distribution of standard data began on October 24, 2006. Continued monitoring is being carried out, to determine whether calibration factors or sensor performance have changed over time. Tasks that were carried out include collection and analysis of PALSAR calibration mode data to calibrate the SAR algorithm, adjusting the filter bandwidth to exclude unwanted interference from the ground radars, comparing data from in-situ equipment to improve geometric accuracy, and defining a time delay constant. To improve radiometric accuracy, inter-beam deviation was minimized, and analysis of Amazon images was used to recalibrate range antenna patterns. Location information of corner reflectors installed on a global scale, and theoretical radar cross section were used to attain geometric and radiometric accuracy on the order of 9.3 meters and 0.2 dB, respectively. This means that accuracy goals were met, and accuracy is sufficient for standard product. (See Figure 2.3.1-1 for time-based stability of radiometric calibration factors and Figure 2.3.1-2 for results of geometric accuracy evaluation.)

With regard to the generation of the high-level products, Digital Elevation Models (DEM) and the crustal deformation maps were created by using the interferometric SAR processing, and demonstrating that performance of the system fully meets the initially planned PALSAR product requirements. Figure 2.3.1-3 shows a three-dimensional view of PALSAR image of the Mt. Daisen. This image was created by orthogonal projection of PALSAR image using the elevation data that was obtained by the averaging of the InSAR DEM.

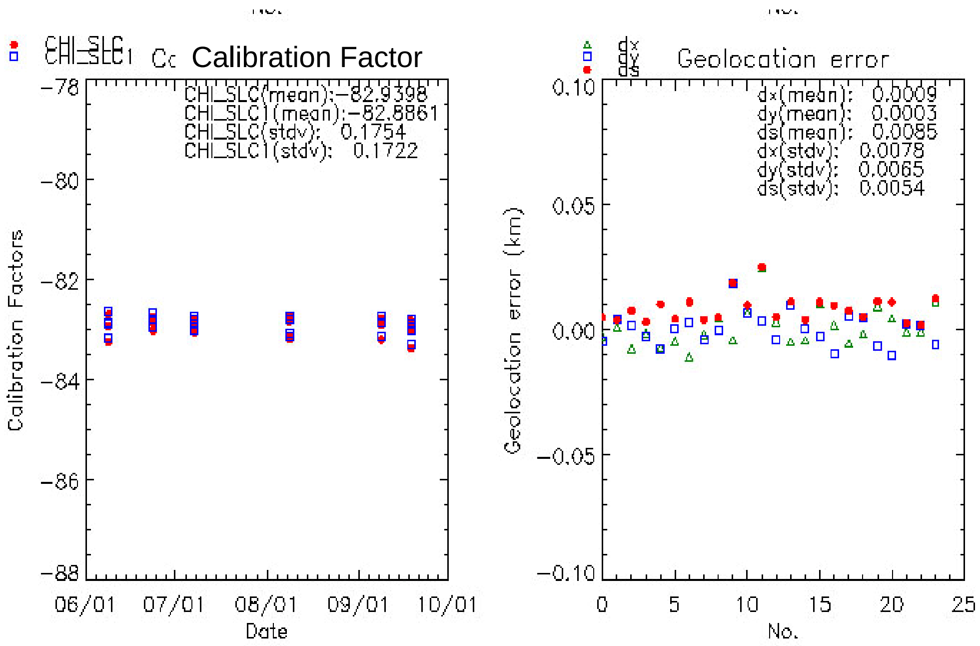

Fig. 2.3.1-1, Fig. 2.3.1-2 Time-based changes of radiometric accuracy Geometric accuracy distribution

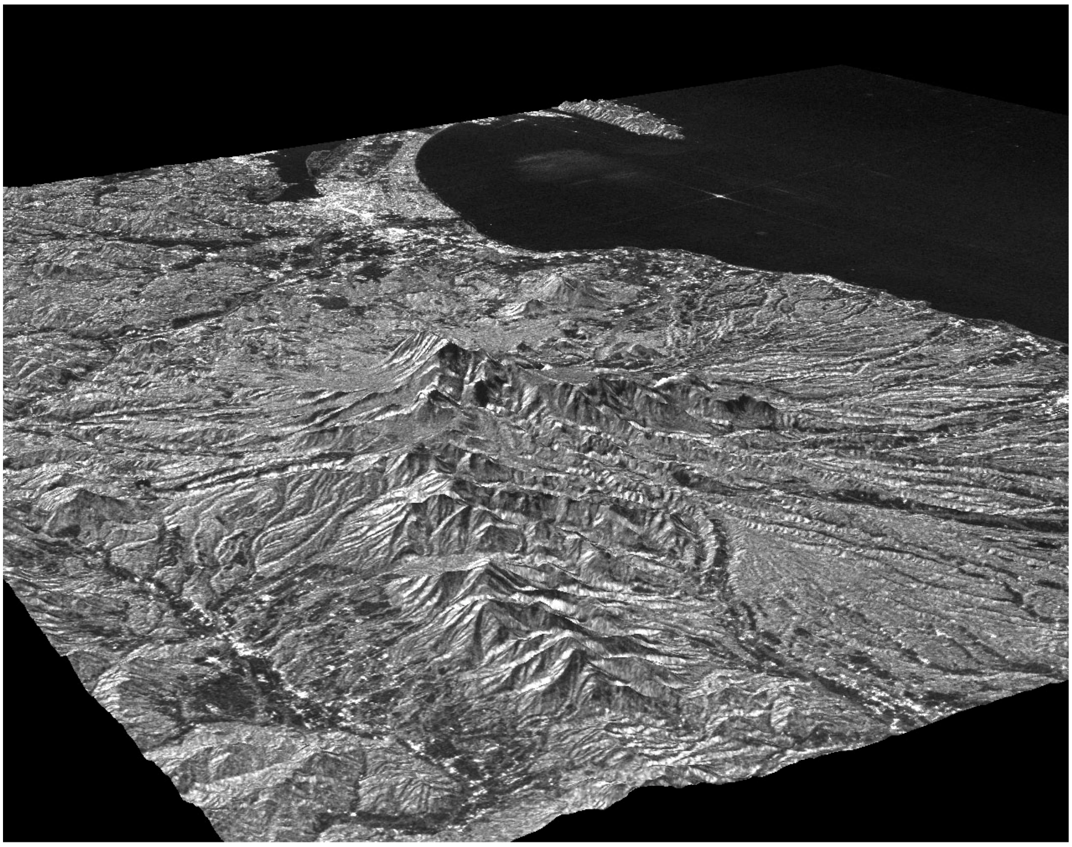

Fig. 2.3.1-3 Orthogonal projection image using DEM based on differential interferometric SAR and SAR ima

2.3.2 Calibration and Validation of PRISM and AVNIR-2

Relative calibration and absolute calibration of PRISM and AVNIR-2 for geometrical and radiometric accuracies are carried out on an ongoing basis. Regarding PRISM, crucial aspects are absolute geometric accuracy based on ALOS pointing management technology, and elevation data estimation accuracy for digital surface models (DEMs) using triplet observing images. For AVNIR-2, absolute radiometric calibration is an important aspect.

Relative geometric calibration of PRISM was performed by evaluating the alignment between CCD units and providing appropriate parameter compensation. As of August 2007, the system operates using version 3 parameters, thereby achieving a relative geometric accuracy of 4 m or less in all three radiometers. Absolute geometric accuracy is managed by updating the pointing alignment parameters (AP) and by continuously evaluating these parameters. Currently, standard products are generated using version 10 pointing AP. Absolute accuracy is 9.8 m (RMS) in the nadir looking direction, and 18.1 m (RMS) in the forward and backward looking directions. Figures 2.3.2-1 and 2.3.2-2 are time-series plots of geometric accuracy evaluation results for nadir looking radiometer from March 2006 onwards. The average error results obtained by evaluation using ground control points (GCPs) for each scene are shown in Figure 2.3.2-1, and the standard deviation values are shown in Figure 2.3.2-2. (a) and (b) are plots for the X (pixels) direction and Y (lines) direction, respectively. For convenience, the average error and standard deviations on the vertical axis are absolute values expressed in logarithmic notation. The horizontal axis shows the observation date of the data used for evaluation. The plots show the difference in the evaluation date, *i.e.*, the difference in parameters used for processing the evaluation data. Shortly after the launch of ALOS, the onboard time server had an error of one second, which resulted in an error of about 8 km on the Y axis. An incorrect setting for the sensor mounting angle in the processing software for the X axis also resulted in an error of about 8 km. The processing software problem was corrected quickly, which reduced the average error on the X axis to about 20 m. The onboard time server error was corrected through a firmware update performed in September 2006. As a result, there are no more errors on the order of several kilometers, but errors of about 100 m remain, due to pointing alignment parameter estimation errors. The parameters were subsequently updated several times, thereby gradually increasing accuracy on the Y axis, as can be seen from the graph.

Absolute radiometric calibration of AVNIR-2 was performed by cross calibration with the optical sensors of existing satellites, using homogenious earth surfaces. Figure 2.3.2-3 shows the results of cross calibration for AVNIR-2 and the medium spatial resolution optical sensor MODIS carried by the NASA earth observation satellite TERRA. Taking into account the resolution differences of AVNIR-2 observation images for the homogenious earth surfaces, spatial averaging was used to determine the top of atmosphere (TOA) reflectance from the radiances were calculated. These two values were then compared. The results give AVNIR-2 absolute radiometric accuracy as 4.6% (RMS) or less in bands 1 - 3 and 15.6% (RMS) or less in band 4.

For validation of high-level products, the accuracy of DSMs derived by PRISM and ortho rectified images, and of ortho rectified images derived by AVNIR-2 were evaluated. DSMs obtained with PRISM for a variety of terrain types and land cover conditions were evaluated in detail. It was confirmed that DSMs can be generated with elevation accuracy of 4.8 m (RMS) for flat terrain and of 5.8 to 7.5 m (RMS) for varied terrain. Both for PRISM and AVNIR-2, ortho rectified images could generally be generated with a horizontal accuracy of one pixel or better. Figure 2.3.2-4 shows a bird's eye view of the vicinity of Toi harbor on the Izu peninsula in Shizuoka Prefecture, Japan. The image was created by overlaying a DSM with pan sharpened and ortho rectified images derived from PRISM and AVNIR-2.

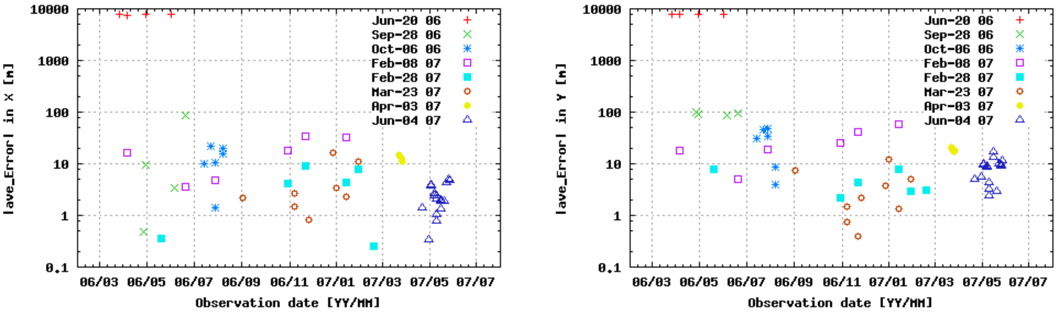

(a) Average geometrical error on X axis (b) Average geometrical error on Y axis

Fig. 2.3.2-1 Time series of PRISM nadir looking radiometer of geometric errors since launch of ALOS

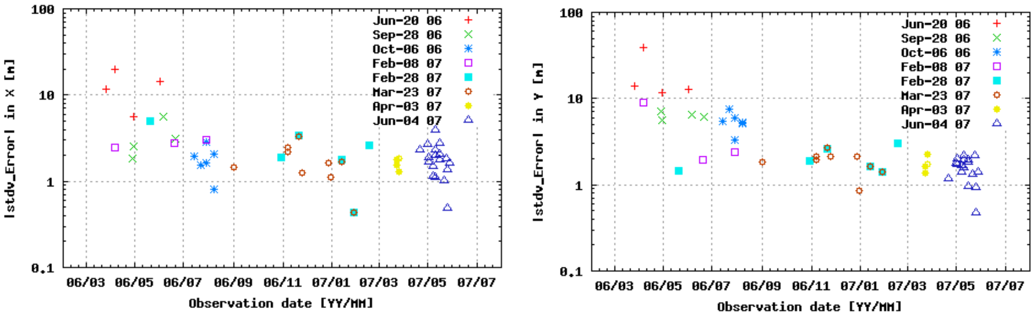

(a) Standard deviation of geometrical error on X axis (b) Standard deviation of geometrical error on Y axis

Fig. 2.3.2-2 Time series of standard deviation of PRISM nadir looking radiometer of geometric errors since launch of ALOS

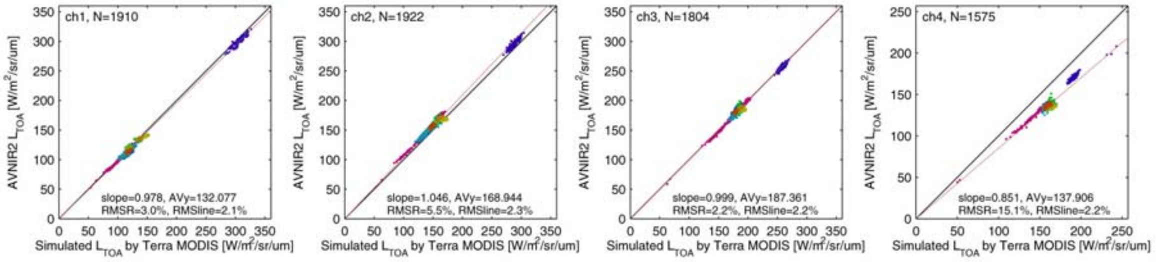

Fig. 2.3.2-3 Radiometric cross calibration results for AVNIR-2 and TERRA/MODIS

From left, images show AVNIR-2 bands 1, 2, 3 and 4 with horizontal axis representing AVNIR-2 equivalent surface reflectance determined from MODIS, and vertical axis representing surface reflectance observed by AVNIR-2.

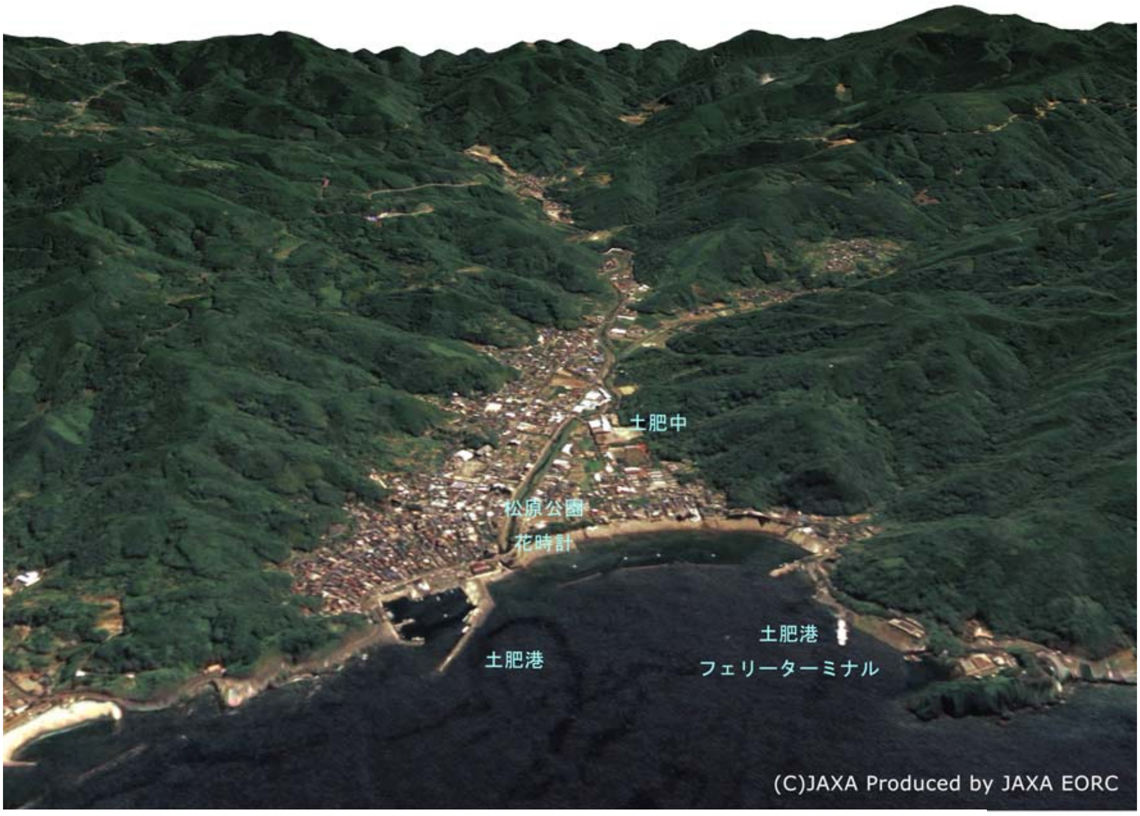

Advanced Land Observing Satellite (ALOS) "Daichi"

Bird's eye view of Toi area

Images: AVNIR-2 and PRISM ortho-rectified and pan-sharpened images

Elevation data: PRISM Digital Surface Model (DSM)

Observation date: August 20, 2007 (simultaneous observation with AVNIR-2 and PRISM)

Fig. 2.3.2-4 Bird's eye view of vicinity of Toi harbor in Shizuoka Pref., Japan based on PRISM/DSM and PRISM/AVNIR-2 ortho rectified and pan-sharpened images (observation date August 20, 2007)

2.3.3 Forest, wetlands and other vegetated areas

For monitoring and mapping of land cover and changes therein, AVNIR-2 and PALSAR are the main instruments of interest on ALOS. The multi-spectral AVNIR-2 provides an important tool for characterization of forest and wetlands, as it is sensitive to the spectral properties of vegetation. Optical techniques have been used widely and successfully for the past 35 years and their limitations are well established. As is the case with all sensors on ALOS, also AVNIR-2 is subject to global observation strategy, where all land areas on the Earth are acquired in a consistent and systematic manner on a repetitive basis several times per year. Notwithstanding cloud cover, the objective is to establish a homogeneous multi-annual global archive, from which time series of regional-scale AVNIR-2 (and PRISM and PALSAR) data can be found for any arbitrary region on the Earth.

Rather than being sensitive to the *spectral* features of the target, PALSAR is an active microwave instrument and is primarily sensitive to its roughness and structural composition (the more roughness or structure, the greater the backscatter) and dielectric properties (or moisture content; with less signal absorption in moist targets). Different land cover types thus typically produce different backscatter – a key feature in using microwave sensors for land cover analyses. With PALSAR, a smooth surface (e.g. still water or bare soil) will give rise to little backscatter as most of the transmitted signal will be reflected away from the sensor, while a more structurally complex target (e.g. a forest) will appear brighter as signal interaction with the leaves, branches and trunks will result in a higher proportion of the signal being transmitted back to the sensor.

As a general rule of thumb, SAR sensors are sensitive to features which are of about the same size, or larger than its particular wavelength, while objects smaller than the SAR wavelength generally render transparent. This explains why the small particles in clouds and smoke – which are visible in optical images – are invisible in microwave images. The relatively long L-band wavelength of PALSAR (23.6 cm) allows penetration of the radar signal below the vegetation canopy (leaves appear transparent), to reveal information about the physical structure of the vegetation.

The polarization channels can also be considered as “spectral bands” of PALSAR, where the co-polarised (HH and VV) and the cross-polarised (HV and VH) channels provide complementary information, as illustrated in Fig. 2.3.3-1. The HH and VV signals typically interact with branches, stems and the ground layer, while the cross-polarised HV and VH backscatter generally are results of multiple scattering within the vegetation canopies.

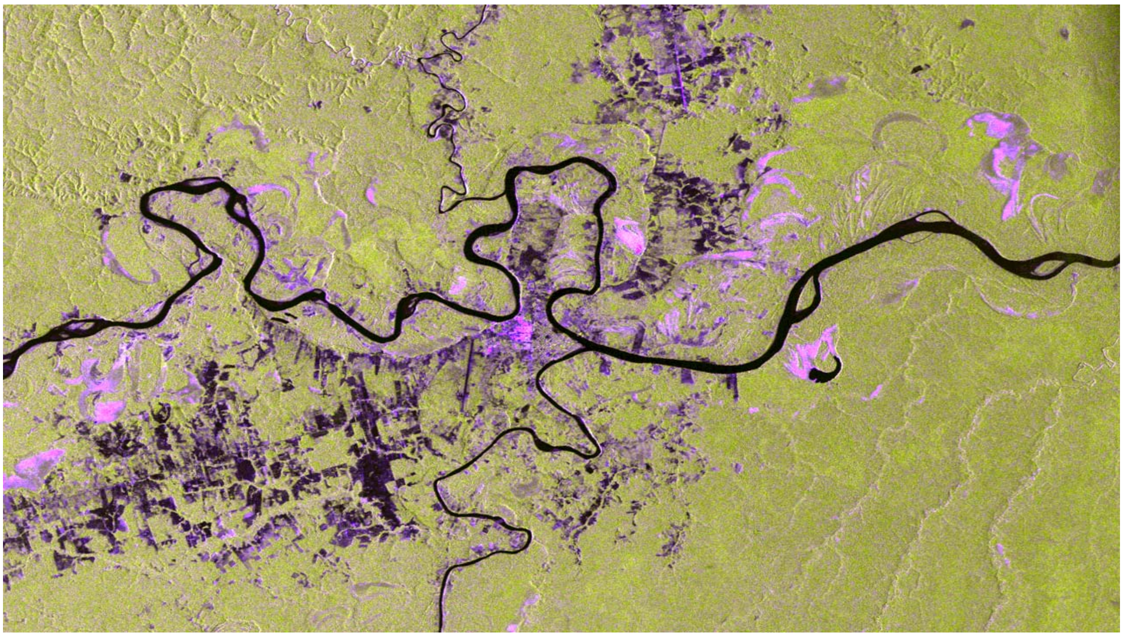

Fig. 2.3.3-1 ALOS PALSAR dual-polarization image.
(Western Amazon, 21 August, 2006.).

False colour composite where the co-polarisation (HH) band is displayed in the red channel, the cross-polarisation band (HV) in the green and the (HH-HV) difference in the blue channel. With the HH banc sensitive to direct and specular backscatter and the HV band to volume scattering, forest appears green, clear cut areas dark purple, open water black, and flooded vegetation light violet in this image.

(1) Forest change monitoring

Identification and monitoring of human-induced and natural disturbances in the global land cover is an important PALSAR application, where updated information about *where* changes have occurred, *when* they occurred, and the *area affected*, is crucial. As many forest and wetland areas are under threat of anthropogenic change, the capacity to monitor such areas on a regular basis regardless of cloud cover is of key importance. Multi-temporal SAR colour composites provide a simple, but effective means for disturbance mapping, yielding a clear indication of both the temporal and spatial characteristics of the disturbance.

Figure 2.3.3-2 shows a multi-temporal JERS-1 SAR colour composite of a mangrove area in Southeast Asia, with an image acquired in 1992 displayed in the red image channel, and images from 1995 and 1998 in the green and blue, respectively. Areas which have not changed in the periods between the acquisitions appear in shades of grey (dark grey - undisturbed mangrove; light grey – degenerated mangrove/dryland forest, white – urban areas; black – open water). Areas of change on the other hand, appear in colour, depending on when the change occurred, and the type of change.

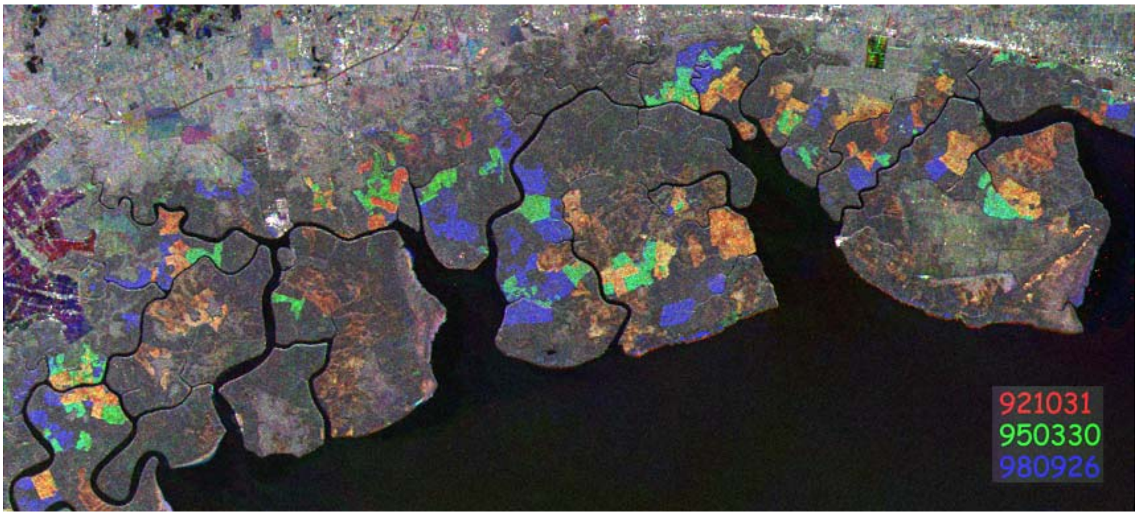

Figure 2.3.3-2 Disturbance monitoring of mangrove forest in Southeast Asia, using a multi-temporal time series of JERS-1 SAR data (Red:1992; Green:1995; Blue:1998).

Undisturbed/mature mangrove appears in dark grey. Clearings which occurred 1992-1995 and 1995-1998 are green and blue respectively, while regenerating areas since 1992 appear orange.

(2) Wetlands monitoring

Mapping of spatio-temporal characteristics of inundation phenomena in wetlands is of key interest both from an environmental viewpoint as well as for carbon cycle modelling. Detecting flooding below a closed forest canopy is one of the unique and spectacular applications of L-band SAR, such as PALSAR and JERS-1 SAR, which cannot be performed by any other sensor, neither optical nor shorter wavelength SARs. The reason for this particular sensitivity is that while parts of the L-band signal interacts with branches in the crown layer, a significant portion of the long wavelength signals penetrate *through* the forest canopy down to the ground, to perform a dihedral (“double-bounce”) reflection on the vertical trunks and the horizontal ground surface. As illustrated in Figure 2.3.3-3, the magnitude of the backscattered signal depends to a large extent on the ground media, which is the key parameter for detecting forest inundation by SAR. While a non-flooded forest floor usually causes diffuse scattering in various directions because of its roughness (a), a smooth water surface covering a flooded forest floor – even a mere centimetre of water covering the ground – provides optimal conditions for a nearly loss-less dihedral reflection between the vertical trunks and horizontal water surface. This results in a significantly enhanced return signal directed back towards the satellite (b and c), giving flooded areas a bright appearance in L-band imagery. In cases where the forest is completely submerged however, no part of the transmitted signal will scatter back towards the sensor (d); hence open water will appear dark.

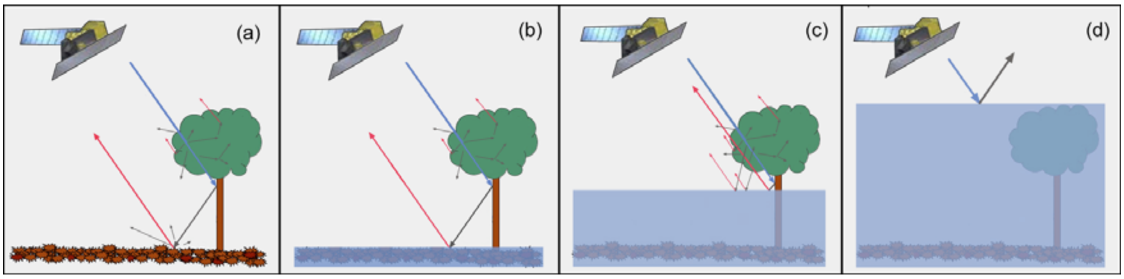

Figure 2.3.3-3. L-band (HH) backscattering mechanisms. Blue arrow – transmitted signal. Red - parts of the signal reflected back towards the satellite. Black – part of signal reflected away from the satellite.

(a): Non-flooded condition. Signal scattering in the crown and on the ground. Medium grey appearance in the image **(b and c)**: Flooded ground surface. Strong "double bounce" reflection between the tree trunks and the water surface occur for both shallow (b) and deep (c) water. Flooded areas appear bright in L-band imagery. **(d)**: Submerged forest/open water. A The microwave signal will reflect once on the open water surface and continue away from the satellite, hence giving open water a dark appearance in the image.

Figure 2.3.3-4 illustrates how flooded forest appears in L-band SAR data. The figure shows a section of two regional-scale mosaics over the central part of the Amazon, acquired by JERS-1 SAR in October 1995 (low water oseason) and July 1996 (hight water season). The bright areas visible in the right hand figure are areas which are flooded during the high water season, as described above.

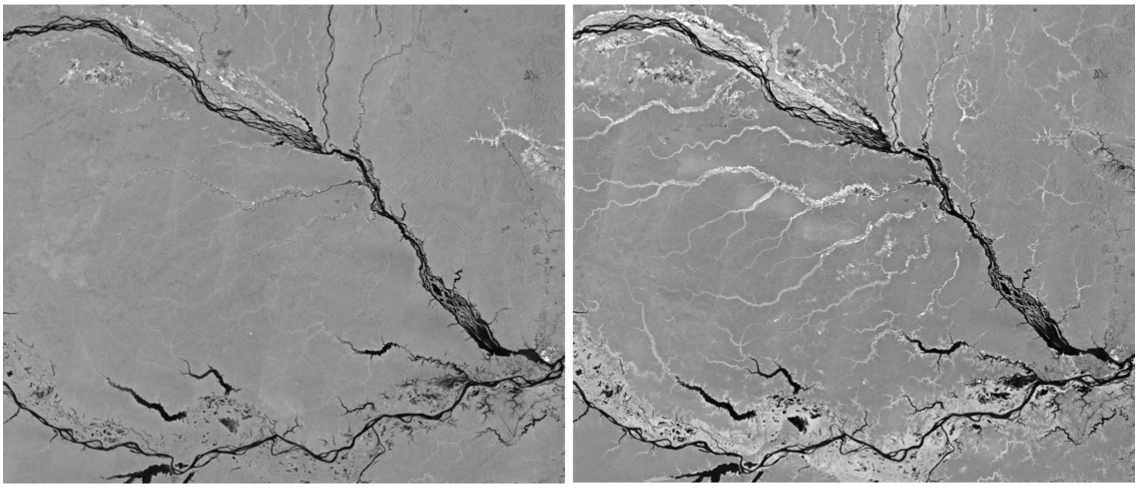

Figure 2.3.3-4 JERS-1 SAR (L-HH) sensitivity to forest inundation (left – Amazon basin at low water; right – high water). Bright areas - flooded forest, grey - non-flooded forest; black - open water.

Mapping of seasonal changes in the inundation extents of major global wetlands is a major purpose for ALOS PALSAR. With a wide-beam and co-polarisation, ScanSAR observations every cycle are undertaken to provide detailed information about both flooding dynamics and extreme flooding extents.

2.3.4 Topography and Geology

ALOS is capable of collecting high-resolution observation data with global coverage, enabling it to meet regional needs. ALOS data are expected to contribute to the measurement and assessment of geological shifts such as changes in terrain and watercourses due to soil erosion and slope failure. Elevation data from ALOS can be utilized in the classification and analysis of terrain features on a global scale.

Toward this aim, the following data products and algorithms are being developed.

(i) Digital Elevation Model (DEM): terrain classification and analysis, watercourse analysis.
(ii) Orthophoto image (particularly PALSAR image): classification of terrain features, etc.
(iii) Geological elevation change measurement: assessment of time-series changes due to soil erosion, sedimentation, and other factors.

Figure 2.3.4.-1 shows an overlay of several PALSAR orthophoto images with different incident angles. The orthogonal transformation compensates for terrain folds, allowing the use of observation data with different incident angles for terrain classification and for assessment of terrain changes.

Utilization of ALOS data is planned for the following projects in the areas of topography and geology:

(1) A correlation exists between underground mineral veins and surface shape of the terrain. For more than 10 years, an ongoing project for the Sudbury Basin in Canada has been aiming at the creation of high-resolution maps by overlaying DEMs with synthetic aperture radar data. Following the launch of ALOS, it is planned to use ALOS data for this project.

(2) A study of diastrophism and seismic damage in southern Tibet uses differential interferometric SAR measurement based on ALOS PALSAR, as well as DEMs derived from ALOS PRISM data to monitor land surface deformations and upheavals, and to perform detailed analysis of terrain changes due to erosion and other factors. The required accuracy of deformation measurement in the vertical direction is 1 mm to 1 cm per year.

(3) For the volcanic island of Cheju, Korea, various DEMs have been created using NASA/JPL AIRSAR, JERS-1 SAR, and KOMPSAT-1 EOC data. For the future, it is planned to perform monitoring of volcanic damage using ALOS PALSAR and PRISM data.

(4) SAR based surveys of the large land area of Brazil including the Amazon Basin have been carried for almost 30 years. ALOS PALSAR with its high spatial

resolution and distinct polarization characteristics as well as stereo mapping capability is expected to provide important data in this regard.

(5) In Korea, a project to use ALOS PALSAR for creating topographic charts of coastal areas is being prepared. Differential interferometric SAR will be used to create DEMs of tidal flats, and polarization SAR images are to be used for identifying sediment deposits.

(6) The high spatial resolution and good spectrographic characteristics of ALOS PRISM, AVNIR-2, and PALSAR are expected to provide relevant data for the study of terrain changes brought about by oil drilling in northwestern Russia.

(7) Differential interferometric SAR images are used in the observation of volcanic islands such as Hawaii, and it is expected that ALOS PALSAR will be utilized for continuing these observations. Monitoring of volcanic activity based on such data is also expected to be useful for Central America and the Caribbean region. Figure 2.3.4-2 shows the amount of diastrophism around Kilauea Caldera, Hawaii Island, as determined using PALSAR data. A rise of about 10 cm around the volcanic crater was detected successfully, thanks to PALSAR's excellent differential interferometric processing capability.

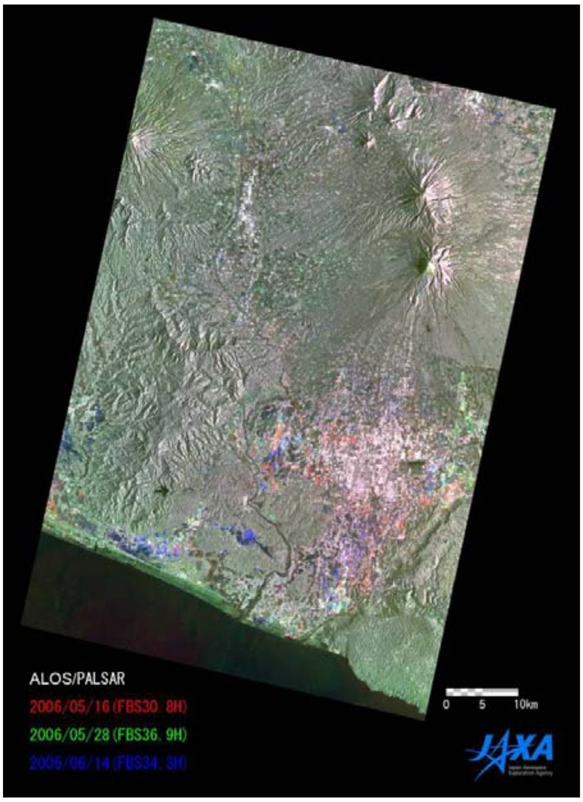

Fig. 2.3.4-1 Overlay of three PALSAR orthophoto images with different incident angles

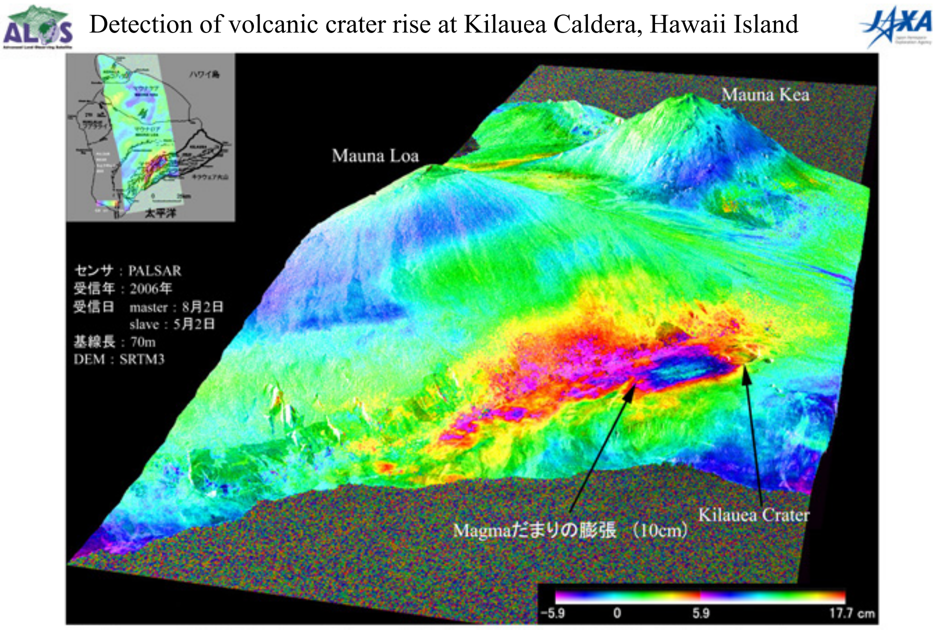

Detection of volcanic crater rise at Kilauea Caldera, Hawaii Island

センサ：PALSAR
受信年：2006年
受信日　master：8月2日
　　　　slave：5月2日
基線長：70m
DEM：SRTM3

Fig. 2.3.4-2 Diastrophism detection at Kilauea Caldera, Hawaii Island, using PALSAR

2.3.5 Hydrology, Water Resources, Snow and Ice

The field of hydrology is mainly concerned with water resources management. Precipitation such as rain and snow, feeds rivers and streams, after various stages including evapotranspiration and runoff. During this process, snow depth and soil moisture are important parameters, and runoff behavior is determined by topographic features. River management is an important activity with regard to managing water resources, as well as predicting droughts, floods, land slides, and other disasters. The water cycle comprised of evapotranspiration, watervapor transport, condensation, and precipitation at the same time performs efficient transport of thermal energy, and the mutual interaction between atmosphere and land greatly influences both local weather phenomena and weather systems on a global scale. Also, the distribution of sea ice in the winter season as well as sea ice and glacier distribution in the polar regions and cold climate zones is linked to global weather fluctuations and acts as an indicator of global warming. The many important topics in this area are not limited to glaciology but also touch the fields of meteorology and climatology. The following sections describe special products using ALOS data in the fields of hydrology, water resources, snow and ice.

(1) Extraction of topological data and river analysis

The basis for river management is an analysis of runoff. In recent years, the use of distributed runoff models has come to be regarded as an efficient approach to this task. When performing this kind of analysis, it is essential to have a thorough grasp of the topological features in the catchment area. A digital surface model (DSM) generated from PRISM data provides an elevation extraction accuracy of 5 m while covering a wide area of several 10 km^2. This makes it quite suitable for assessing the topological features of a catchment area. Using data for earth surface albedo, land cover classification, *etc.*, obtained from AVNIR-2, the surface heat budget, estimated evapotranspiration, and other important surface parameters can be determined, in order to analyze mutual atmosphere-land interaction phenomena (see Figure 2.3.2-4).

(2) Estimation of soil moisture and aerodynamic roughness

The soil moisture present at the land surface level is one of the major parameters that determine how much of the solar energy is transported into the atmosphere. The aerodynamic roughness of the surface in turn influences the evaporation efficiency. To measure such hydrological parameters, microwave based remote sensing is a valid approach. The active microwave sensor, PALSAR, is a synthetic aperture radar (SAR) which uses the L-band with comparatively long wavelengths with high spatial resolution. As a first for a satellite borne L-band SAR system, PALSAR allows fully polarization observation, and the incidence angle can be adjusted. The backscattering coefficient obtained from SAR is greatly influenced by specific inductive capacity which is dependent on water content, *etc.*, and by surface roughness.

The simultaneous fully-polarized or dual-polarized observation data from PALSAR are likely to improve estimation accuracy for soil moisture which so far was hampered by insufficient observation data for unknown quantities. The development of soil moisture estimation algorithms using multi-polarized SAR is already in progress. By using PALSAR, the suitability of these algorithms can be tested, and it is expected that tuning and operational use will become possible. If the estimation accuracy for soil moisture increases, the estimation accuracy for surface roughness in effect will also increase. Research into the estimation of aerodynamic roughness from this value is also being carried out. Figure 2.3.5-1 shows PALSAR images of the heavy rains that hit the Korean Peninsula at the beginning of August 2007. The color was synthesized by assigning the PALSAR ScanSAR HH polarization image of August 11 (after the rains) to red, and the ScanSAR HH polarization image of July 25 (before the rains) to blue and green. The blue parts in these images are thought to be flooded areas, while reddish parts suggest an increase in soil moisture due to the heavy rains.

Because DSMs created with PRISM data indicate the elevation of the top of buildings, they can be used to provide input values for hydrometeorological models of urban areas. Until now, detailed models of urban areas indicating the height of buildings (called city models) could only be produced by using aircraft borne laser scanners or photogrametry techniques. PRISM based DSMs allow the creation of city models with a spatial resolution of less than 10 m, and they are also considered to be useful for studying heat island phenomena. Figure 2.3.5-2 shows an example of such a city model. It is a bird's eye view created from a PRISM/DSM and ortho rectified and pan-sharpened images derived from PRISM/AVNIR-2.

(3) Estimation of snow related parameters and sea ice distribution

The snow cover on land surfaces in winter season is an important source of water, but it can also result in snow melting floods and other disasters. Meanwhile, information about the distribution of sea ice on the oceans is important for fisheries and for the control of maritime traffic. Both of these conditions are associated with high surface albedo, exerting a considerable influence on the global thermal energy cycle.

Regarding the distribution of sea ice, the presence of ice can to a certain extent be determined visually if suitable images can be obtained. The PALSAR ScanSAR and the pointing angle change function of AVNIR-2 are useful in this respect. Algorithms are currently being developed to determine the consistency of sea ice (one-year ice, multi-year ice, *etc.*) from the scattering characteristics of multi-polarization and multi-incidence angle SAR. Their application to PALSAR looks promising. The Japan Coast Guard has started to use PALSAR data for assessing the distribution of sea ice in the Okhotsk Sea in winter (see

Figure 2.3.5-3).

As for snow cover, the density and water content influence a large number of parameters including inductive capacity, snow particle size, snow cover depth, and scattering characteristics at the lower boundary surface. Increasing the amount of observation data is important to gain a more thorough understanding, and PALSAR multi-polarization and multi-incidence angle observation again look promising. With the longer wavelength of PALSAR, estimating the depth of the snow cover should also be possible.

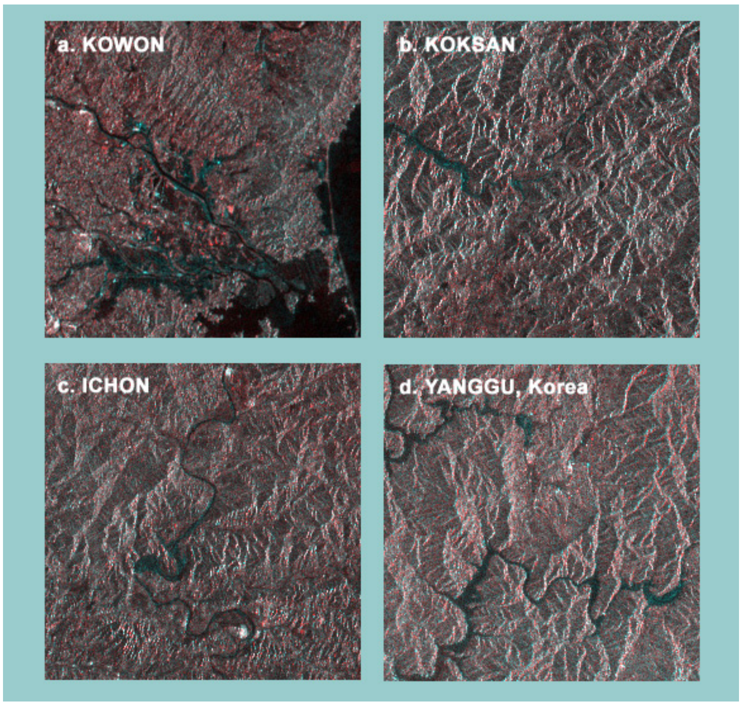

Fig. 2.3.5-1 Images of flooding on Korean Peninsula at beginning of August 2007

Color composite, with PALSAR ScanSAR image of August 11 (after flooding occurred) assigned to red, and ScanSAR image of July 25 (before flooding) assigned to blue and green. Blue parts indicate flooded areas, and red parts indicate increase in soil moisture due to heavy rains.

Fig. 2.3.5-2 Example for city model using PRISM/DSM

Bird's eye view created by overlaying DSM calculated from triplet PRISM images and ortho-rectified and pan-sharpened images derived from PRISM/AVNIR-2. The image shows the result of calculating height information for large buildings.

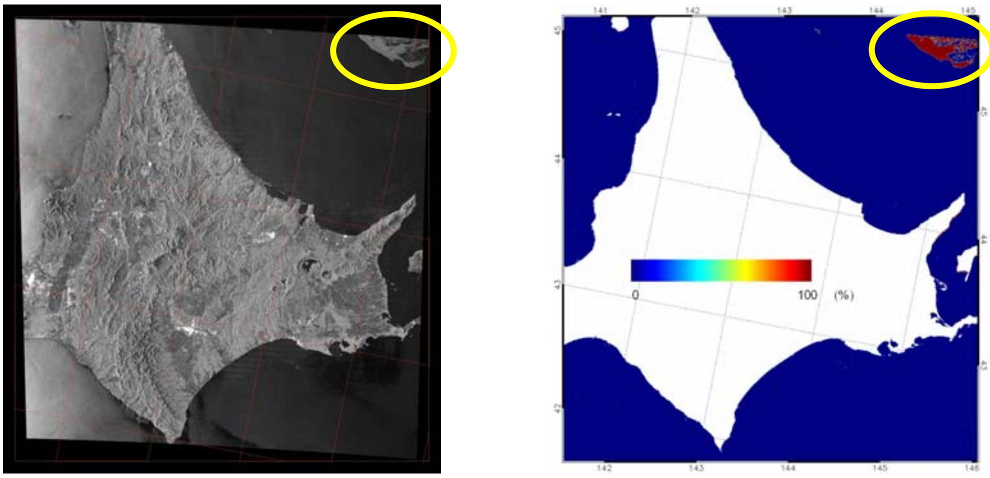

Fig. 2.3.5-3 PALSAR/ScanSAR images from observation on April 17, 2006

Estimation of sea ice distribution in Okhotsk Sea in winter. Left image is ScanSAR intensity image, and right image shows estimated sea ice concentration density.

2.3.6 Disaster Monitoring and Damage Management

(1) Introduction

For disaster monitoring, the pointing function of AVNIR-2 as well as the all-weather and day-and-night observation capabilities of PALSAR are highly effective. Observable and favorable targets by ALOS associated with disasters are the following:

- Seismic and volcanic activity
- Wind, water, snow damage
- Maritime disasters
- Hazardous substance disasters
- Forest fires

Table 2.3.6-1 shows relationships among various kinds of disaster, damages due to the disasters, and appropriate sensors for observing them. The section below discusses about observation data and analysis examples for different sensors, as well as expected results.

(2) Disaster monitoring and damage management by PALSAR

The PALSAR sensor can observe the earth surface at anytime of the day and night, regardless of weather or environmental conditions such as cloud, fog, dust, and volcanic ash. Therefore, it is an effective sensor system for disaster monitoring. In several applications of SAR data, satisfactory results of the detection of crustal deformation using differential interferometric (DInSAR) technique have so far been achieved by JERS-1/SAR data. Because the precision of orbit control and attitude determination of ALOS are significantly better than those of JERS-1, a larger number of coherent SAR images can be obtained, and the advantage of L-band SAR should allow highly precise detection of crustal deformation over an extensive area including mountainous areas. Monitoring the crustal deformation caused by seismic or volcanic activity is an important tool for exploring the mechanism of fault movements and volcanic eruptions, and it can be applied to the prevention and mitigation of disasters. Figures 2.3.6-1 show examples for crustal deformation detected using differential interferometric processing of PALSAR data. The image on the left shows the crustal deformation (change in distance between the satellite and the earth surface) due to the Noto Peninsula Earthquake which occurred on March 25, 2007, Japan Standard Time (JST, all dates and times hereinafter are in JST). The image on the right shows the crustal deformation associated with the earthquake that occurred on April 2, 2007 in the Solomon Islands. The color cycles in the interferograms represent the change in satellite-ground distance, that is the crustal deformation. By comparing amplitude images or coherence images from before and after the disaster, destruction of buildings, flood damage, lava flow, and area losses can be assessed, and providing data are useful for mapping disaster areas and creating hazard maps.

Figures 2.3.6-2 show amplitude images from before and after the eruption of the Tavurvur volcano near Rabaul in Papua New Guinea, which occurred on October 7, 2006. Compared to the left-side image (observed on July 17, 2006, before the eruption), it is possible to discern the lava flow clearly (in the red circle) in the right-side image (observed on October 17, 2006, after the eruption). Another example using amplitude images is shown in Figure 2.3.6-3, which represents the extent of an oil spill caused by a tanker accident. Such images can provide useful information for disaster management without a complicated analysis. In polarimetric technique, we use the combination of polarized waves and analyze the difference of backscattering characteristics. Using this technique, it is possible to extract the change in the surface condition, and it can be expected to allow the identification of disaster areas.

(3) Disaster monitoring and damage management by Optical sensors (AVNIR-2, PRISM)

Optical sensors provide high spatial resolution images (about 2.5 m for PRISM and about 10 m for AVNIR-2) that are well suited for detecting disaster conditions. Differences in brightness before and after a disaster and classification of color composite images can provide clues for liquefaction, landslides, flooding, structure damage, and area losses. Figures 2.3.6-4 represent a landslide or slope failure caused by the Noto Peninsula Earthquake mentioned earlier, detected by optical sensors. The image was created using data from two optical sensor systems (AVNIR-2 and PRISM), with the application of an advanced technique called the pan-sharpen method for creating a high-resolution color composite image. When conditions in the observed area change drastically, in the case of landslide, liquefaction, or a destruction of trees by a tsunami, the color composite image from before and after the disaster will allow detection by visual inspection, which should facilitate fast response to disasters.

Figures 2.3.6-5 show damages caused by the tsunami triggered by the above mentioned earthquake in the Solomon Islands. The images taken with AVNIR-2 indicate that trees have been decimated, which corresponds to actual observations on the ground, where large-scale destruction of houses and trees had occurred. Optical sensors are also capable of extracting data about disasters which are hard to spot in PALSAR based images. The sensors are therefore well-suited for monitoring of smaller scale disasters such as volcanic fumes, red tide, or blue tide which are undetectable by PALSAR (Figures 2.3.6-6). A combination of optical sensors and PALSAR can be expected to provide the best overall disaster detection and assessment performance. (See Table 2.3.6-1.)

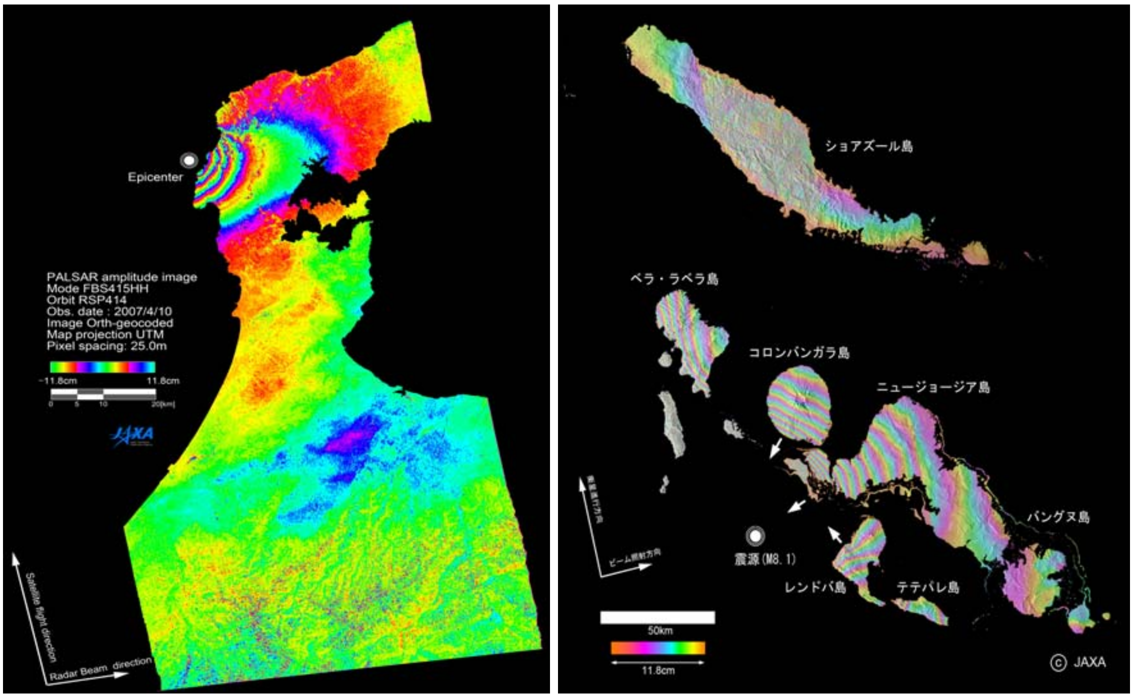

Fig. 2.3.6-1 Crustal deformation detected using differential interferometric technique of PALSAR data

Fig. 2.3.6-2 Before/after PALSAR amplitude images of Tavurvur volcano (red circle) eruption on October 7, 2006 (left: before eruption, right: after eruption)

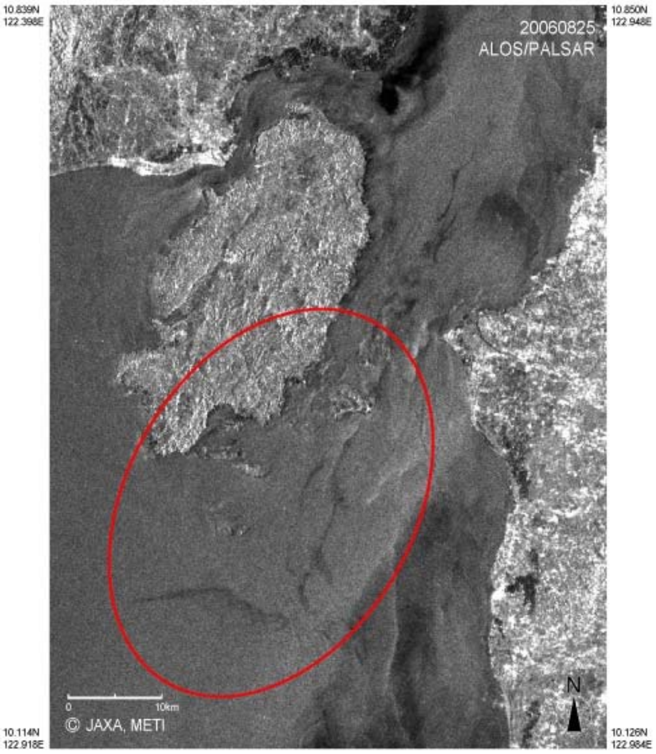

Fig. 2.3.6-3 PALSAR image of oil spill caused by tanker accident on August 11, 2006, near the island of Guimaras, Philippines (darker swath within red oval is believed to be leaked oil)

Before disaster (taken on August 10, 2006; left: Monzen area of Wajima city, right: Wajimazaki area of Wajima city)

After disaster (taken on March 28, 2007; left: Monzen area of Wajima city, right: Wajimazaki area of Wajima city)

Fig. 2.3.6-4 Before/after AVNIR-2 color composite images of the Solomon Islands earthquake on April 2, 2007
(false color image; red area [trees] within black circle is reduced)

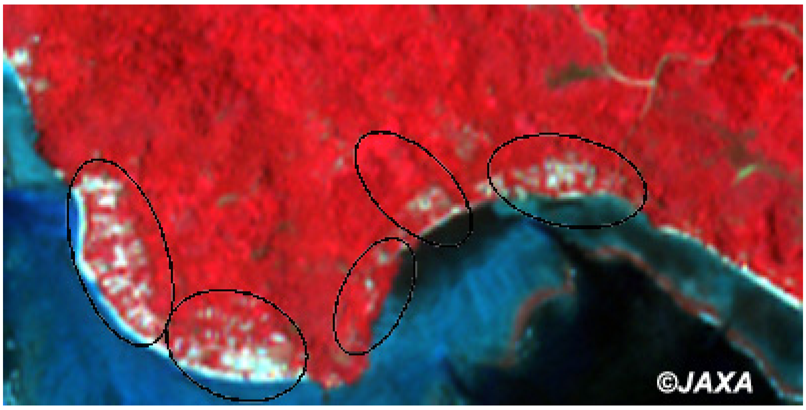

Before disaster (taken on March 8, 2007; Solomon Islands, southern part of Gizo Island)

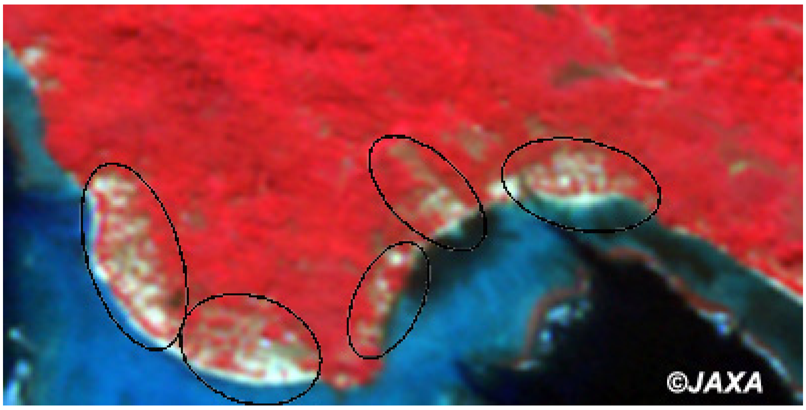

After disaster (taken on April 8, 2007; Solomon Islands, southern part of Gizo Island)

Fig. 2.3.6-5 Before/after AVNIR-2 color composite images of the Solomon Islands earthquake on April 2, 2007
(false color image; red area [trees] within black circle is reduce)

Before white tide occurrence (taken on May 4, 2006, Hakata Bay, Fukuoka city)

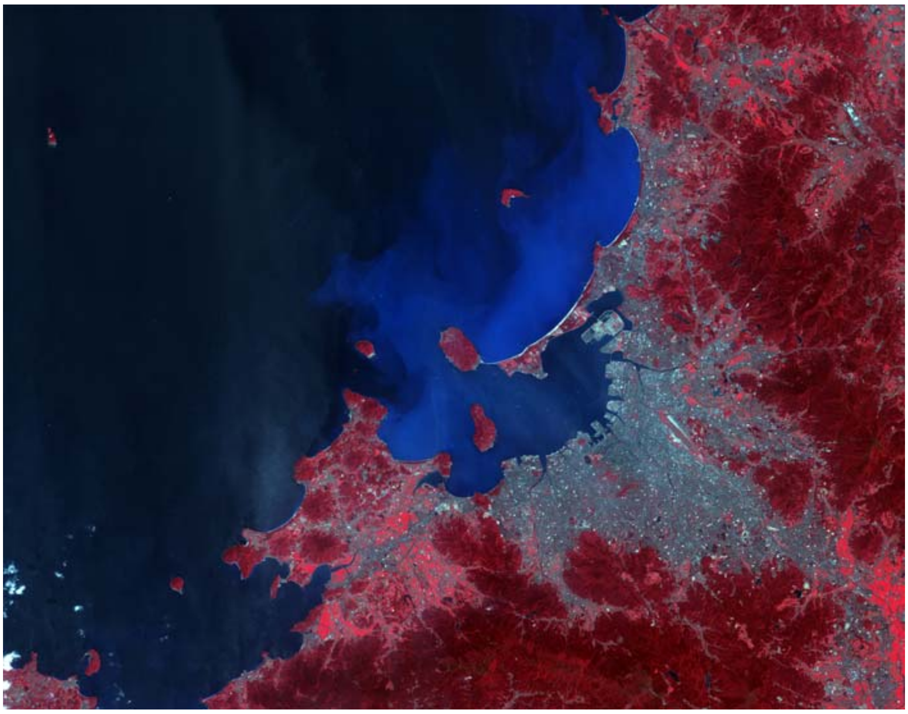

After white tide occurrence (taken on April 20, 2007, Hakata Bay, Fukuoka city)

Fig. 2.3.6-6 Case of red tide (so-called "white tide") which occurred in March 2007

Table 2.3.6-1 Correlation between disaster types and presumed observable damage

	Crustal deformation	volcanic activity	damage: road & railroad	damage: structure	geohazard	landslide	flood	fire disaster	oil spil	Tsunami	sea ice	avalanche
Earthquake	PAL	－	PAL/AV2/PRI	PAL/AV2/PRI	PAL/AV2/PRI	PAL/AV2/PRI	PAL/AV2/PRI	PAL/AV2/PRI	－	PAL/AV2/PRI	－	PAL/AV2/PRI
Typhoon	－	－	PAL/AV2/PRI	PAL/AV2/PRI	－	－	－	－	－	PAL/AV2/PRI	－	－
Wind damage	－	－	－	PAL/AV2/PRI	－	－	－	－	－	PAL/AV2/PRI	－	－
Heavy rain damage	－	－	－	PAL/AV2/PRI	－	PAL/AV2/PRI	PAL/AV2/PRI	－	－	－	－	－
Slope damege	－	－	PAL/AV2/PRI	PAL/AV2/PRI	－	PAL/AV2/PRI	－	－	－	－	－	－
Volcanic damage	PAL	PAL/AV2/PRI	PAL/AV2/PRI	PAL/AV2/PRI	PAL/AV2/PRI	PAL/AV2/PRI	－	PAL/AV2/PRI	－	－	－	－
Snow damege	－	－	PAL/AV2/PRI	PAL/AV2/PRI	－	PAL/AV2/PRI	－	－	－	－	－	PAL/AV2/PRI
Maritime disaster	－	－	－	－	－	－	－	PAL/AV2/PRI	PAL/AV2/PRI	－	PAL/AV2/PRI	－
Hazardous substance disaster	－	－	PAL/AV2/PRI	PAL/AV2/PRI	－	－	－	PAL/AV2/PRI	－	－	－	－
Forest fire	－	－	PAL/AV2/PRI	PAL/AV2/PRI	PAL/AV2/PRI	－	－	PAL/AV2/PRI	－	－	－	－
Others												

PAL: PALSAR,AV2: AVNIR-2,PRI: PRISM

2.3.7 Land Use, Land Cover, Agriculture

When utilizing satellite data in the fields of land use and agriculture, optical sensor band information and SAR polarized wave data are helpful in investigating earth surface conditions. Judging from analysis results of satellite images from previous systems, a few representative examples for cases where ALOS products can be expected to prove useful are discussed below.

(1) Assessing rice paddy cultivation status (AVNIR-2, PALSAR)
(2) Assessing changes in land use (AVNIR-2, PALSAR)
(3) Extracting information about vegetation categories

(1) Assessing rice paddy cultivation status (AVNIR-2, PALSAR)

Using the multi-band information from AVNIR-2 and SAR intensity images, the extraction of rice paddy status information should be possible. In analyses using LANDSAT data, large-scale rice paddies could be detected with relatively high precision. However, in many areas in Japan, the planting season coincides with the rainy season, which limits the usability of optical sensors. Because SAR can acquire data regardless of the weather, the C-band SAR in the Canadian RADARSAT satellite for example is being used in the observation of rice paddies on the Ishikari Plain in the Japanese island of Hokkaido. In this case, the SAR intensity changes according to the length of the seedlings.

(2) Assessing changes in land use (AVNIR-2, PALSAR)

AVNIR-2 provides images in 4 bands, and by assigning three of these (Red, Green, Blue) differently, the following types of images can be produced: 1) true color (R:G:B = band 3:2:1), 2) natural color (R:G:B = band 3:4:2), 3) false color (R:G:B = band 4:3:2). Land use information can be gained from these images as follows:

- True color: Image close to what would be seen by the naked eye
- Natural color: Forests (green), fields and turf (tan), built-up areas and rice paddies without water (purple), water (lavender)
- False color: Forests and grassland (red), areas without vegetation (gray)

By applying methods such as unsupervised and supervised classification to the 4-band images from AVNIR-2, land use status can be assessed, and by performing such analyses on an ongoing basis, information about changes can be obtained. An example for this is a study about land coverage categorization for all of Thailand that was conducted from 1995 to 1998 using JERS-1 OPS and LANDSAT TM. The left panel of Figure 2.3.7-1 shows an AVNIR-2 false color image of the middle and lower reaches of the Sagami River in Kanagawa Prefecture. The right panel shows a classification of vegetation obtained by applying supervised classification (maximum likelihood method) to AVNIR-2 4-band images.

There are also trials underway for creating land coverage maps from quad-polarized SAR data gained from using airborne SAR (Pi-SAR).

(3) Extracting information about vegetation categories

The above mentioned method for extracting land use information from AVNIR-2 4-band data can be applied to forest areas as well, to tentatively identify types of trees. An example for such projects is the classification of forested areas on the northern slopes of Mt. Fuji using LANDSAT data. According to reports, surveys among specialists who were shown LANDSAT images have yielded the following results:

- Using images from the fall season, it is possible to distinguish between deciduous trees and evergreen trees.
- It is possible to roughly assess distribution of various kinds of vegetation. However, detailed identification of tree types is difficult.

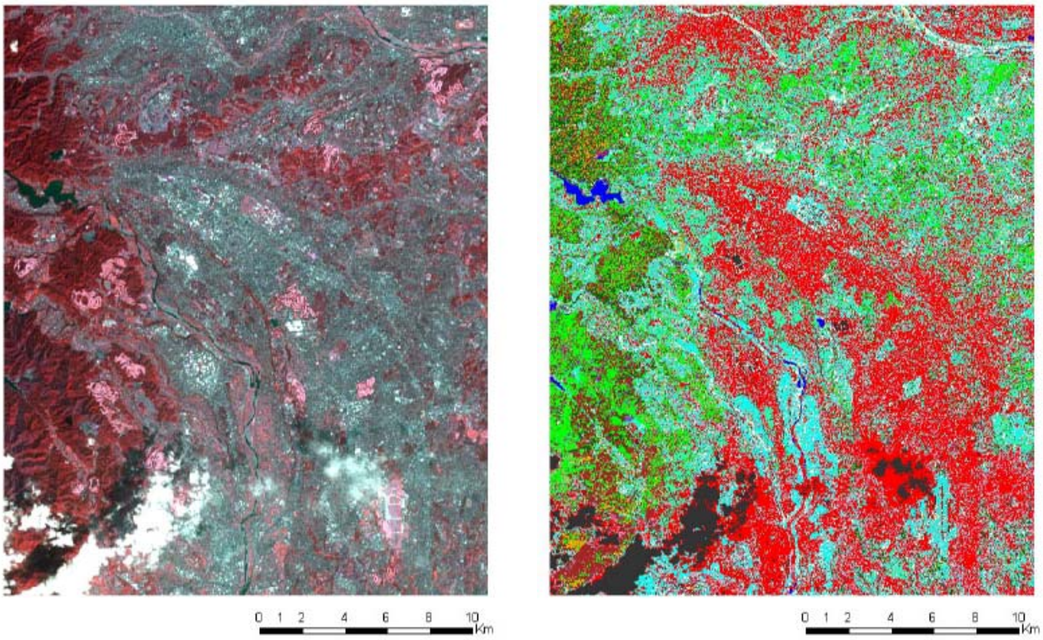

Fig. 2.3.7-1 AVNIR-2 false color image (left) and maximum likelihood method image (right) of Sagami River area, Kanagawa Prefecture

2.3.8 Application Examples from the Oceanography Field

A. Optical sensor usage examples

An example of using the optical sensors of ALOS (AVNIR-2, PRISM) is coastal zone monitoring based on visible and near infrared spectrum information (to monitor the distribution of pollution, contamination, red tide, coral shelves, and other phenomena).

Figure 2.3.8-1 shows two AVNIR-2 images from the observation of Tokyo Bay on June 1, 2006. At a spatial resolution of 10 m, AVNIR-2 has four channels: Blue (460 nm), Green (560 nm), Red (650 nm), and Near Infrared (825 nm). The left image (a) is an RGB image using the Red, Green, and Blue channels. The right image (b) is an RGB image using the Near Infrared, Red, and Green channels. Over a wide area ranging from Yokohama harbor to Chiba harbor, the color of the water is different from the surrounding sea area. According to the Yokohama Environmental Science Research Institute, a large-scale outbreak of red tide caused by Prorocentrum minimum occurred in Tokyo Bay from the end of May until the beginning of June. The different color area is thought to coincide with this red tide. Looking at Figure 2.3.8-1 (c) which plots the reflectance (TOA) in the four channels, it becomes clear that the area thought to be covered by the red tide has a markedly higher reflectance in the near infrared spectrum than other sea areas.

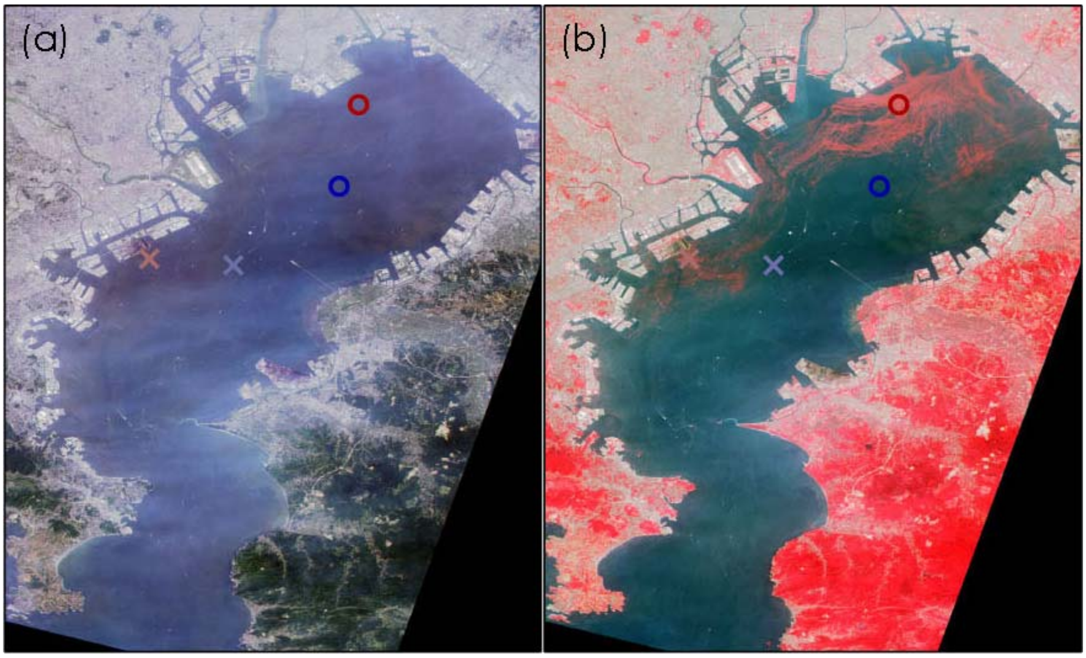

Fig. 2.3.8-1 AVNIR-2 images of Tokyo Bay on June 1, 2006

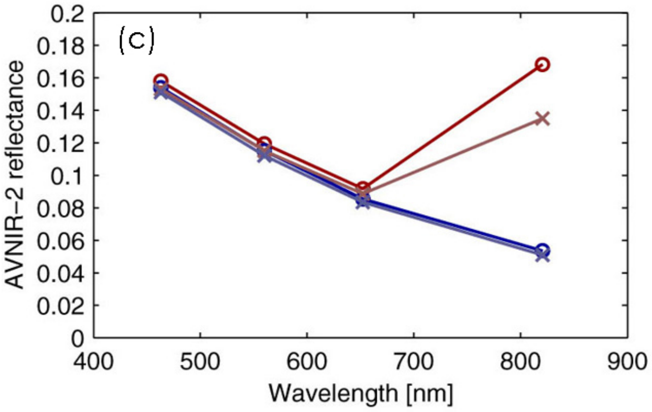

Fig. 2.3.8-1 (c)

Plot produced by taking color change (red) and non-color-change (blue) areas in image as two sets (total 4 points). Horizontal axis is wavelength and vertical axis is AVNIR-2 reflectance. Circles and crosses in plot correspond to circles and crosses in images.

Red tide observation by satellite borne sensors has the advantage of wide area coverage, but the following problems exist:

(i) Because only the sea surface "color" is represented, direct estimation of type and quantity is not possible.

(ii) Because the observation is from directly above, detection may be difficult if the color difference between red tide and surrounding areas is small.

(iii) Observation may be impaired by sun glint on the sea surface and aerosols in the atmosphere.

(iv) Observation schedule of satellite sensors and presence of clouds may prevent detection at certain times.

In spite of these difficulties, the collection of AVNIR-2 and other satellite based observation data and their correlation with specific red tide observation data, as well as the development of suitable analysis methods are expected to significantly contribute to effective red tide monitoring and process analysis.

B. SAR usage examples

Synthetic aperture radar (SAR) is a sensor type that is largely unaffected by weather conditions and allows the visualization of sea surface roughness at a spatial resolution of 10 m to 100 m. SAR is therefore capable of providing useful data for the study and monitoring of coastal areas with complex spatial fluctuations. The PALSAR carried on ALOS is an L-band SAR system which operates at a longer wavelength than the C-band commonly used for oceanography. Figure 2.3.8-2 demonstrates the difference in sea surface representation, depending on SAR wavelength (image courtesy of W.G. Pichel of NOAA).

SAR systems in satellites of various countries often employ the C-band. The radar signals are scattered even by sea surface waves on the order of several centimeters, allowing finely detailed observation. However, observation of larger phenomena is difficult. The L-band used in PALSAR will show waves on the order of about 10 centimeters. While the image will not be as detailed as with the C-band, larger phenomena can also be reliably detected. As a first for a satellite borne L-band SAR system, PALSAR has a multi-polarization mode and a wide area observation (ScanSAR) mode. Data collected by the system therefore are expected to contribute to new lines of research.

In the following sections, four examples for PALSAR application are discussed, namely (1) High-resolution sea surface wind retrieval, (2) Wave information extraction, (3) Visualization of coastal vortexes, and (4) Detection of oil spills.

- **C-band**
  - **centimeter scale**
- **L-band**
  - **decimeter scale**
- **P-band**
  - **~ meter scale**

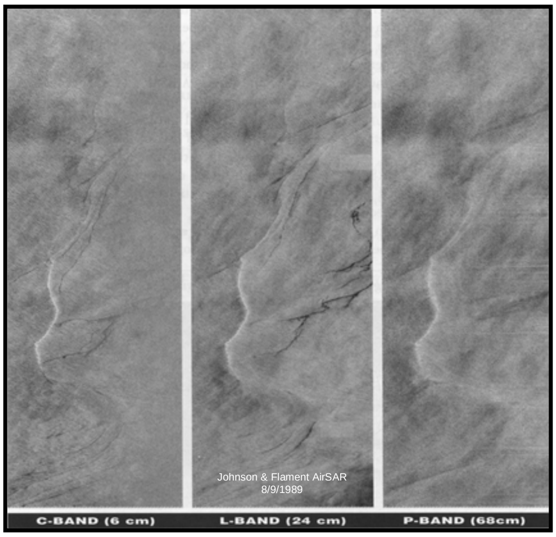

Fig. 2.3.8-2 Differences in sea surface representation according to SAR wavelength

(1) High-resolution sea surface wind retrieval

Because sea surface roughness is related to prevailing wind conditions, a relational expression between microwave backscattering intensity and sea surface wind can be established, which allows mapping of sea surface wind distribution with high resolution. A function for transforming the backscattering of microwave signals into sea surface wind speed (sea surface wind estimation model function) was established using Ku-band and C-band microwave scatterometers [2], [3]. The C-band model function has been applied to ERS and ENVISAT SAR and is being used in calculating sea surface wind distribution with high resolution. Because SAR can only obtain backscattering information from one direction, wind speed is calculated by supplying the wind direction. This is normally obtained from a separate data source such as an objective analysis or atmospheric model, but it also has been suggested that wind direction could be calculated from the SAR image pattern. For the L-band on the other hand, a model function has been developed using JERS-1 SAR [4], but this does not take the dependence on incidence angle into consideration. Because PALSAR has a wide area observation mode (ScanSAR), the development of a model taking the dependence on incidence angle into consideration has become possible. The current model function allows calculation of sea surface wind with an accuracy of about 2.6 m/s [5].

Figure 2.3.8-3 shows a wind speed field of Hokkaido for June 8, 2006, calculated from PALSAR data. The arrows indicate scatterometer-derived wind vector data close to the PALSAR observation time. Under the influence of topographic features, sea surface wind shows considerable spatial variations, but SAR makes it possible to observe sea surface wind conditions also in proximity to the coast, which is not possible with scatterometers. Coastal winds are the major driving force for wind wave development and surface circulation and therefore are a parameter with significant influence on human activities such as fisheries and leisure activities.

From Figure 2.3.8-2, it is evident that sensitivity for small sea surface waves is not as good with the C-band as with the L-band. For low wind speeds, this represents a drawback, but for retrieval of sea surface winds in areas with higher wind speeds, where saturation of C-band backscattering intensity occurs, the L-band is promising. In Figure 2.3.8-4, the Himawari (MTSAT) visible image of July 16, 2007 for the sea area to the east of Japan has been overlaid with a PALSAR (ScanSAR) image. The Himawari image clearly shows the cloud formation of typhoon No. 4, and the PALSAR backscattering intensity also demonstrates a circular pattern with a band structure. If a model function for high wind speed zones can be devised, this should enable the calculation of wind speed distribution in areas directly under the typhoon, on a scale not possible with a meteorological satellite.

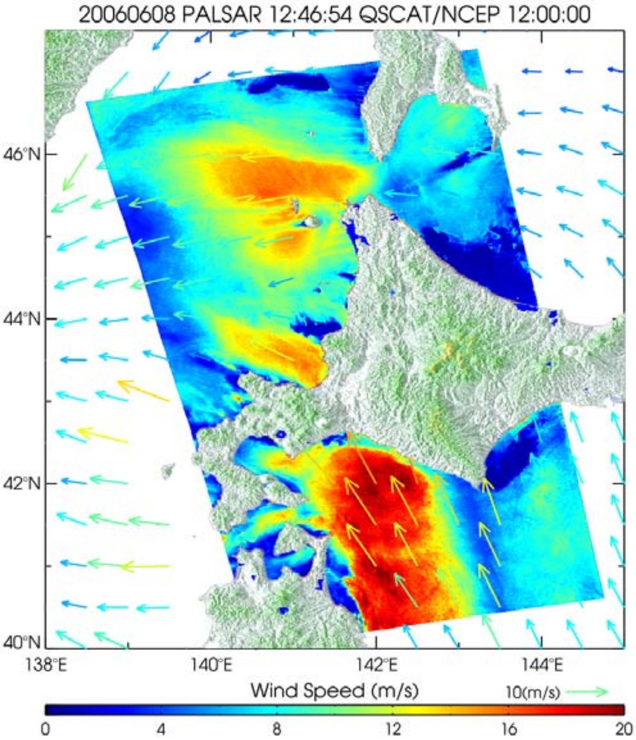

Fig. 2.3.8-3
Sea surface wind speed field for Hokkaido, June 8, 2006, calculated from PALSAR data, overlaid with arrows QSCAT/NCEP Blended Ocean Winds data supplied by Colorado Research Associates.

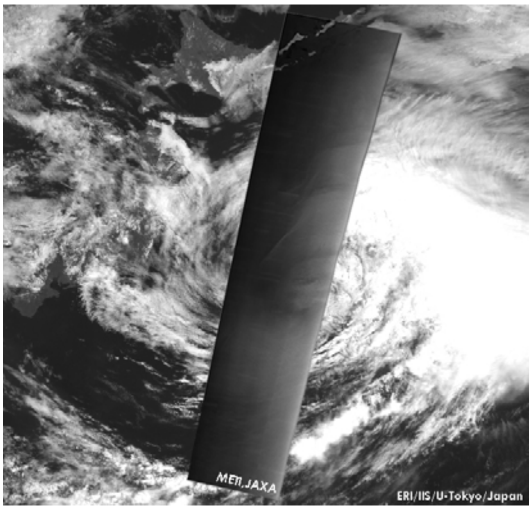

Fig. 2.3.8-4 Himawari (MTSAT) visible image of July 16, 2007 for sea area east of Japan, overlaid with PALSAR image.
MTSAT data supplied by Institute of Industrial Science, University of Tokyo.

(2) Wave information extraction

One of the maritime uses of SAR is the extraction of wave information. It goes without saying that wave monitoring and prediction are practical application areas of great importance for maritime traffic and for coastal structures. As in the case of sea surface winds and ocean currents, coastal areas are subject to a complex set of factors including topographical features of the land and the seabed, and wave conditions in these areas are less understood than conditions on the open ocean. SAR is a sensor which allows the extraction of wave parameters for coastal areas. Through combination with high-resolution wind speed data and models, progress in this area can be expected.

The left image of Figure 2.3.8-5 represents PALSAR sea surface observation data collected in high-resolution mode. Streaking undulations in the northwest-southeast direction are visualized in the image, and the two-dimensional spectrum of the SAR image (at right) allows estimation of a wave direction and a wave length. A method for estimating significant wave height from the SAR wave spectrum has also been proposed, pointing to the possibility for coastal wave parameter extraction based on L-band SAR [6].

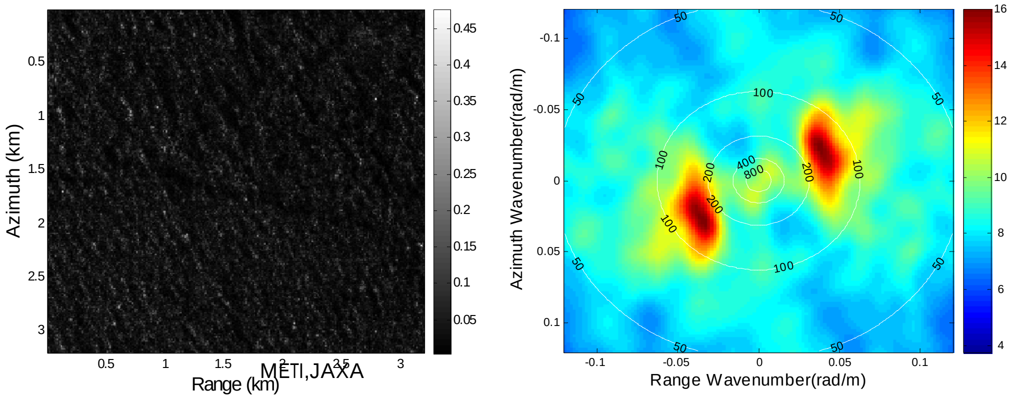

Fig. 2.3.8-5 High-resolution mode PALSAR sea surface image (left) and two-dimensional spectrum (right).

Excerpted from reference [5].

(3) Visualization of coastal eddies

Headlands, islands, and other topographical formations interact with currents, resulting in complex three-dimensional coastal currents. Mixing and dispersion processes that differ from those on the open ocean take place, forming physical and biological fronts. In recent years, satellite observation has demonstrated the existence of coastal eddies with a scale of less than 10 km, and their distribution has become more clear. Through biological processes, coastal eddies have a significant impact on fisheries, and it is therefore important to learn more about their behavior. Because SAR allows sea surface observation with high resolution without being significantly affected by weather conditions, its data are suitable for studying coastal eddies.

Figure 2.3.8-6 shows PALSAR images taken in summer 2006 of the area around Miyake-jima of the Izu Island chain. Eddy streets are visualized behind the Mikura-jima and Inamba-jima islands, of about the same size as the islands themselves. Because the

Kuroshio current was flowing in the area around Miyake-jima and Mikura-jima islands in the summer of 2006, the eddy streets are believed to have been formed by an interaction between the current and topographical features of the islands. The left image in Figure 2.3.8-7 shows sea surface temperatures (SST) as measured by MODIS on August 4, 2006. The right image plots the distribution of chlorophyll-a (Chl-a). In the colder areas (eddies) behind the islands of Miyake-jima and Mikura-jima, a dense Chl-a pattern can be observed. This can be attributed to the so-called island mass effect whereby biological productivity tends to be higher in the lee of an island. Numerical modeling has shown that the visualized eddies exhibit similar properties as Karman vortex streets [7]. In this way, SAR and other satellite data in combination with in-situ observation data and numerical modeling can be of assistance in investigating and understanding coastal phenomena such as eddy streets.

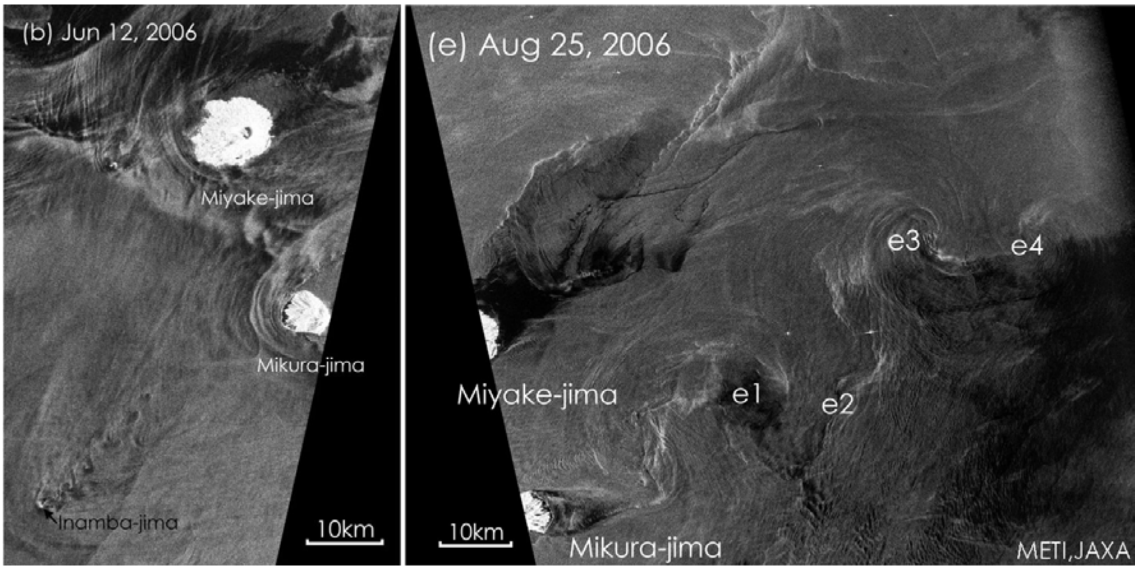

Fig. 2.3.8-6
PALSAR images of area around Miyake-jima in Izu Island chain, taken on June 12, 2006 (left) and August 25, 2006 (right)

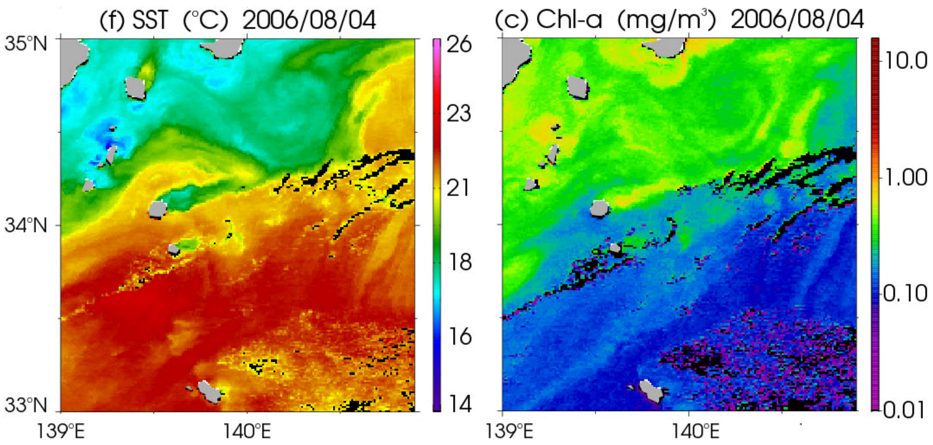

Fig. 2.3.8-7

MODIS SST and Chl-a images taken on August 4, 2006.

Data are received and processed for brightness and geometrical conversion (Level 1B) by Tokai University Research & Information Center (TRIC) and Earth Observation Research Center (EORC) of Japan Aerospace Exploration Agency (JAXA), and published in near real time by JAXA / EORC

(4) Detection of oil spills

An example of an application that is close to practical implementation is large-scale disaster monitoring. Figure 2.3.8-8 (a) shows a ScanSAR image taken on August 25, 2006. In the image, the oil spill resulting from the sinking of the tanker "Solar 1" near the island of Guimaras, Philippines, on August 11, is clearly visible. Starting at the red dot which marks the wreck position, the leaked oil appears as a dark streak. The oil film on the surface area of the spill reduces ripples and therefore shows up as a darker section on the SAR image. This oil spill disaster was monitored by several space agencies in cooperation, and an oil spill chart was created by UNOSAT, using SAR images from ENVISAT and Radarsat. In conjunction with the oil spill area as estimated from PALSAR image data, the overall distribution and changes over time can be assessed (see Figure 2.3.8-8 (b)).

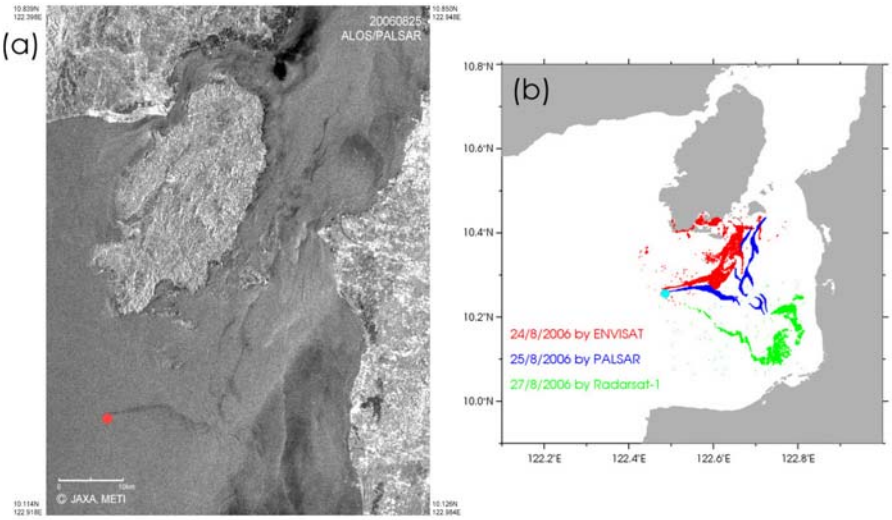

Fig. 2.3.8-8

(a) PALSAR ScanSAR image from observation on August 25,2006

(b) Estimated oil spill area based on SAR data. ENVISAT (red) and Radarsat (green) data are excerpted from distribution chart created by UNOSAT.

2.3.9 International Polar Year (IPY)

The International Polar Year focusing on the arctic and Antarctic regions is an intensive campaign of internationally coordinated, interdisciplinary, scientific research and observations organized by the International Council for Science (ICSU) and the World Meteorological Organization (WMO). The official observing period of the IPY is from March 1, 2007 until March 1, 2009. This is the fourth such event, following those of 1882-3, 1932-3, and 1957-8.

In Japan, the National Institute of Polar Research (NIPR) is actively contributing and coordinating activities planned by scientists and researchers in Japan, and a wide range of projects are being undertaken by Principal Investigators (PI) to contribute to the IPY.

The following six themes have been defined as main targets of the IPY.

- To determine the present environmental status of the Polar Regions by measuring changes in the spatial and time domain.
- To quantify and understand, past and present natural environmental and social change in the Polar Regions; and to improve projections of future change.
- To advance our understanding on all scales of the links and interactions between Polar Regions and the rest of the globe, and of the processes controlling these links.
- To investigate the frontiers of science in the Polar Regions.
- To use the unique vantage point of the Polar Regions to develop and enhance observatories from the interior of the Earth to the Sun and the cosmos beyond.
- To investigate the cultural, historical, and social processes that shape the sustainability of circumpolar human societies, and to identify their unique contributions to global cultural diversity and citizenship.

In addressing these six scientific themes, researchers from various disciplines have proposed the following six observation projects.

- A synoptic set of multidisciplinary observations to establish the status of the polar environment in 2007-2008
- The acquisition of key data sets necessary to understand factors controlling change in the polar environment
- The establishment of a legacy of multidisciplinary observational networks
- The launch of internationally coordinated, multidisciplinary investigations into new scientific frontiers
- The implementation of polar observatories to study important facets of Planet Earth and beyond
- The creation of datasets on the changing conditions of circumpolar human societies, since the first IPY (1882 - 83) until the present

JAXA ALOS Science Project plans to contribute to the IPY by making up-to-date ScanSAR browse mosaicking data of the Antarctic region after each observation cycle. It is hoped that these will be utilized by relevant researchers. In the course of the 2nd ALOS Research Announcement, the IPY was specified as one of the research categories, and three research proposals were accepted. These proposals involve detecting ice sheet movement speed using interferometric SAR images, estimating sea ice thickness using SAR, and extracting ice sheet surface height information from a combination of interferometric SAR and optical sensor data. These projects will become part of IPY activities.

At the time of the 1st ALOS Research Announcement in 2000, the IPY was not yet being considered explicitly, but a number of research proposals selected at that stage in the areas of snow and ice research have actually fit to contribute to the IPY. Some examples are SAR analysis of river flooding due to snow melting in the arctic region, ScanSAR based mapping of sea ice distribution in the Antarctic Ocean, SAR based mapping and mass balance analysis of ice sheets, and mapping of snow melt areas using SAR and other microwave sensors.

2.3.10 Cities

Earth observation data are also widely applied to urban environment observation and assessment. Advanced features provided by ALOS such as high resolution and multi-spectral observation can be helpful in understanding various aspects including land use and urban environment. The potential of data obtained by satellite observation for improving urban management and planning will be of increasing importance in the future.

An outline of how ALOS data can be applied to the field of urban development is given below.

(1) Land coverage in urban areas

By applying AVNIR-2 4-band images to unsupervised or supervised classification of land coverage, it is possible to assess the distribution of built-up areas, water surfaces, etc. Changes over time can be extracted from time-series data.

Access to NDVI or other index values and accurate land coverage classification information enables assessment of the ratio of green coverage, which can provide important insights into urban environment problems.

PALSAR data which are unaffected by clouds or day/night timing are also expected to prove useful for land coverage classification. In particular, multi-polarization observation allows the scattering characteristics of objects to be known in detail. Methods such as target analysis and entropy classification will enable in-depth evaluation of built-up areas.

(2) Urban development monitoring

Because earth observation satellites periodically survey given areas of the earth surface, they can be useful to monitor changes such as the expansion of cities and their impact on the natural and living environment. LANDSAT and other land observation satellites have revealed for example the dramatic expansion of cities in China with significant increases in built-up ratios and density. This has led to debates about differences in urban development patterns.

Well-known simulation methods of urban growth involve cell automatons and other models. In combination with satellite observation data, such models will become increasingly practical for quantitatively assessing the state of urban regions.

(3) Urban environment problems

Environmental problems in urban areas encompass a wide range of phenomena, such as water quality degradation, atmospheric pollution, heat islands, etc. Regarding water quality, direct observation is possible by analyzing images of rivers and sea water, but for other phenomena, only indirect observation is possible.

For example, the existence of a natural environment as indicated by the ratio of green coverage is thought to contribute to the reduction of atmospheric pollution and heat islands. Analysis of land coverage therefore can provide insights into urban problems. Regarding the topic of heat islands, prominent research projects aimed at predicting the temperature reducing effect of green coverage areas are using numerical simulation of urban temperature distribution in combination with direct observation data from satellites equipped with thermal infrared band sensors.

3. Overview of ALOS

3.1 Overview

The Japanese Earth observing satellite program consists of two series: those satellites used mainly for atmospheric and marine observation, and those used mainly for land observation. The Advanced Land Observing Satellite (ALOS) follows the Japanese Earth Resources Satellite-1 (JERS-1) and Advanced Earth Observing Satellite (ADEOS) and will utilize advanced land-observing technology. ALOS will be used for cartography, regional observation, disaster monitoring, and resource surveying.

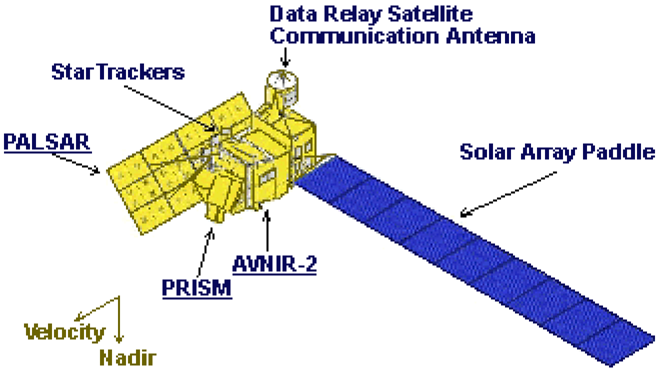

Figure 3.1-1 Overview of ALOS

The ALOS has three remote-sensing instruments: the Panchromatic Remote-sensing Instrument for Stereo Mapping (PRISM) for digital elevation mapping, the Advanced Visible and Near Infrared Radiometer type 2 (AVNIR-2) for precise land coverage observation, and the Phased Array type L-band Synthetic Aperture Radar (PALSAR) for day-and-night and all-weather land observation. In order to utilize fully the data obtained by these sensors, the ALOS was designed with two advanced technologies: the former is the high speed and large capacity mission data handling technology, and the latter is the precision spacecraft position and attitude determination capability. They will be essential to high-resolution remote sensing satellites in the next decade. ALOS have been successfully launched on an H-IIA launch vehicle from the Tanegashima Space Center, Japan. (Figure 3.1-1, Table 3.1-1)

Table 3.1-1 ALOS Characteristics

Launch Date	Jan. 24, 2006
Launch Vehicle	H-IIA
Launch Site	Tanegashima Space Center
Spacecraft Mass	Approx. 4 tons
Generated Power	Approx. 7 kW (at End of Life)
Design Life	3 -5 years
Orbit	Sun-Synchronous Sub-Recurrent
	Repeat Cycle: 46 days Sub Cycle: 2 days
	Altitude: 691.65 km (at Equator)
	Inclination: 98.16 deg.
Attitude Determination Accuracy	2.0 x 10^{-4}degree (with GCP)
Position Determination Accuracy	1m (off-line)
Data Rate	240Mbps (via Data Relay Technology Satellite) 120Mbps (Direct Transmission)
Onboard Data Recorder	Solid-state data recorder (90Gbytes)

3.2 PRISM

The Panchromatic Remote-sensing Instrument for Stereo Mapping (PRISM) is a panchromatic radiometer with 2.5m spatial resolution at nadir. Its extracted data will provide a highly accurate digital surface model (DSM).
PRISM has three independent optical systems for viewing nadir, forward and backward producing a stereoscopic image along the satellite's track. Each telescope consists of three mirrors and several CCD detectors for push-broom scanning. The nadir-viewing telescope covers a width of 70km; forward and backward telescopes cover 35km each.

The telescopes are installed on the sides of the optical bench with precise temperature control. Forward and backward telescopes are inclined +24 and -24 degrees from nadir to realize a base-to-height ratio of 1.0. PRISM's wide field of view (FOV) provides three fully overlapped stereo (triplet) images of a 35km width without mechanical scanning or yaw steering of the satellite. Without this wide FOV, forward, nadir, and backward images would not overlap each other due to the Earth's rotation. (Figure 3.2-1, Table 3.2-1, Table 3.2-2, Figure 3.2-2)

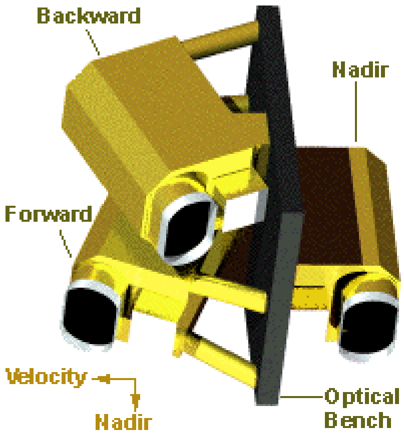

Figure 3.2-1 Overview of PRISM

Table 3.2-1 PRISM Characteristics

Number of Bands	1 (Panchromatic)
Wavelength	0.52 to 0.77 micrometers
Number of Optics	3 (Nadir; Forward; Backward)
Base-to-Height ratio	1.0 (between Forward and Backward view)
Spatial Resolution	2.5m (at Nadir)
Swath Width	70km (Nadir only) / 35km (Triplet mode)
S/N	>70
MTF	>0.2
Number of Detectors	28000 / band (Swath Width 70km) 14000 / band (Swath Width 35km)
Pointing Angle	-1.5 to +1.5 degrees (Triplet Mode, Cross-track direction)
Bit Length	8 bits

Note: PRISM cannot observe areas beyond 82 degrees south and north latitude.

Table 3.2-2 Observation Modes

Mode 1	Triplet observation mode using Forward, Nadir, and Backward views (Swath width is 35km)
Mode 2	Nadir (70km) + Backward (35km)
Mode 3	Nadir (70km)
Mode 4	Nadir (35km) + Forward (35km)
Mode 5	Nadir (35km) + Backward (35km)
Mode 6	Forward (35km) + Backward (35km)
Mode 7	Nadir (35km)
Mode 8	Forward (35km)
Mode 9	Backward (35km)

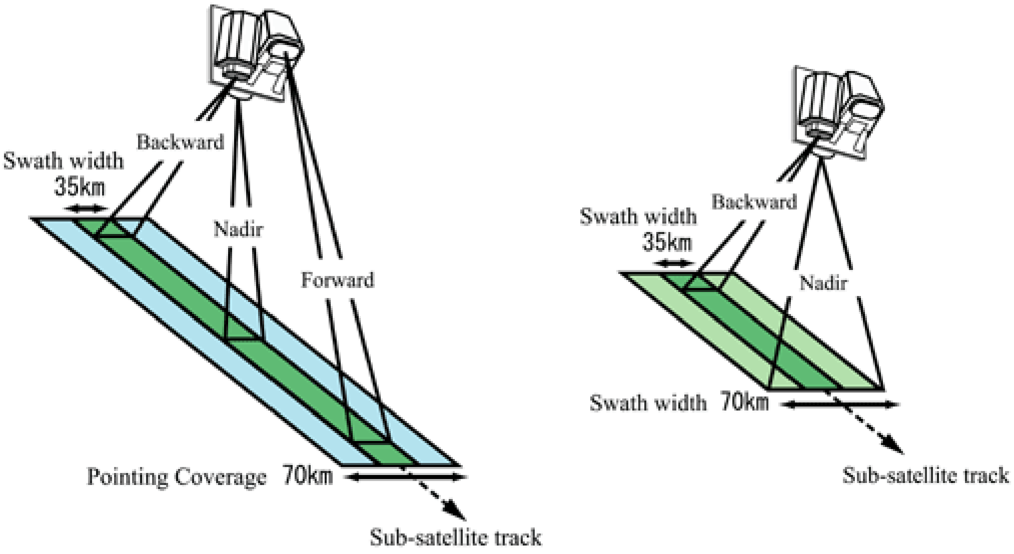

Figure 3.2-2 PRISM Observation Modes

3.3 AVNIR-2

The Advanced Visible and Near Infrared Radiometer type 2 (AVNIR-2) is a visible and near infrared radiometer for observing land and coastal zones. It provides better spatial land-coverage maps and land-use classification maps for monitoring regional environments. AVNIR-2 is a successor to AVNIR that was on board the Advanced Earth Observing Satellite (ADEOS), which was launched in August 1996.

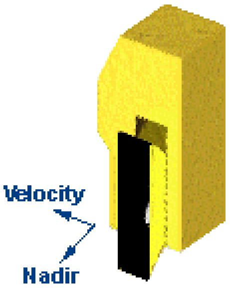

Figure 3.3-1
Overview of AVNIR-2

Its instantaneous field-of-view (IFOV) is the main improvement over AVNIR. AVNIR-2 also provides 10m spatial resolution images, an improvement over the 16m resolution of AVNIR in the multi-spectral region. Improved CCD detectors (AVNIR has 5,000 pixels per CCD; AVNIR-2 7,000 pixels per CCD) and electronics enable this higher resolution. A cross-track pointing function for prompt observation of disaster areas is another improvement. The pointing angle of AVNIR-2 is +44 and - 44 degree. (Figure 3.3-1, Table 3.3-1, Figure 3.3-2)

Table 3.3-1　AVNIR-2 Characteristics

Number of Bands	4
Wavelength	Band 1 : 0.42 to 0.50 micrometers Band 2 : 0.52 to 0.60 micrometers Band 3 : 0.61 to 0.69 micrometers Band 4 : 0.76 to 0.89 micrometers
Spatial Resolution	10m (at Nadir)
Swath Width	70km (at Nadir)
S/N	>200
MTF	Band 1 through 3 : >0.25 Band 4 : >0.20
Number of Detectors	7000/band
Pointing Angle	− 44 to + 44 degree
Bit Length	8 bits

Note: AVNIR-2 cannot observe the areas beyond 88.4 degree north latitude and 88.5 degree south latitude.

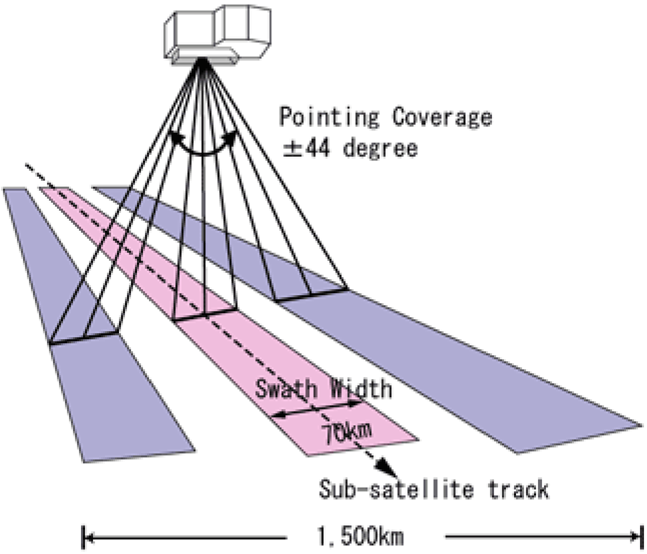

Figure 3.3-2　AVNIR-2 Observation Modes

3.4 PALSAR

The Phased Array type L-band Synthetic Aperture Radar (PALSAR) is an active microwave sensor using L-band frequency to achieve cloud-free and day-and-night land observation. It provides higher performance than the JERS-1's synthetic aperture radar (SAR). Fine resolution in a conventional mode, but PALSAR will have another advantageous observation mode. ScanSAR, which will enable us to acquire a 250 to 350km width of SAR images (depending on the number of scans) at the expense of spatial resolution. This swath is three to five times wider than conventional SAR images. (Figure 3.4-1, Table 3.4-1, Figure 3.4-2) The development of the PALSAR is a joint project between JAXA and the Japan Resources Observation System Organization (JAROS).

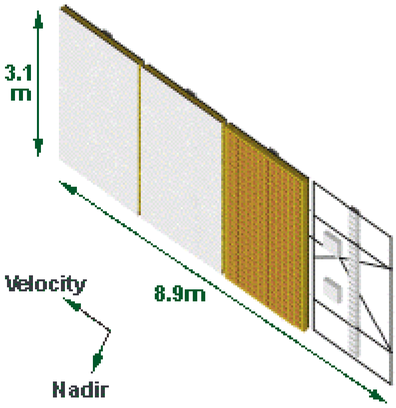

Figure 3.4-1 Overview of PALSAR

Table 3.4-1 PALSAR Characteristic

Mode	Fine		ScanSAR	Polarimetric (Experimental mode)*1
Center Frequency	1270 MHz(L-band)			
Chirp Bandwidth	28MHz	14MHz	14MHz,28MHz	14MHz
Polarization	HH or VV	HH+HV or VV+VH	HH or VV	HH+HV+VH+VV
Incident angle	8 to 60deg.	8 to 60deg.	18 to 43deg.	8 to 30deg.
Range Resolution	7 to 44m	14 to 88m	100m (multi look)	24 to 89m
Observation Swath	40 to 70km	40 to 70km	250 to 350km	20 to 65km
Bit Length	5 bits	5 bits	5 bits	3 or 5bits
Data rate	240Mbps	240Mbps	120Mbps,240Mbps	240Mbps
NE sigma zero *2	< −23dB (Swath Width 70km) < −25dB (Swath Width 60km)		< −25dB	< −29dB
S/A *2,*3	> 16dB (Swath Width 70km) > 21dB (Swath Width 60km)		> 21dB	> 19dB
Radiometric accuracy	scene: 1dB / orbit: 1.5 dB			

Note: PALSAR cannot observe the areas beyond 87.8 deg. north latitude and 75.9 deg. south latitude when the off-nadir angle is 41.5 deg.

*1 Due to power consumption, the operation time will be limited.

*2 Valid for off-nadir angle 34.3 deg. (Fine mode), 34.1 deg. (ScanSAR mode), 21.5 deg. (Polarimetric mode)

*3 S/A level may deteriorate due to engineering changes in PALSAR.

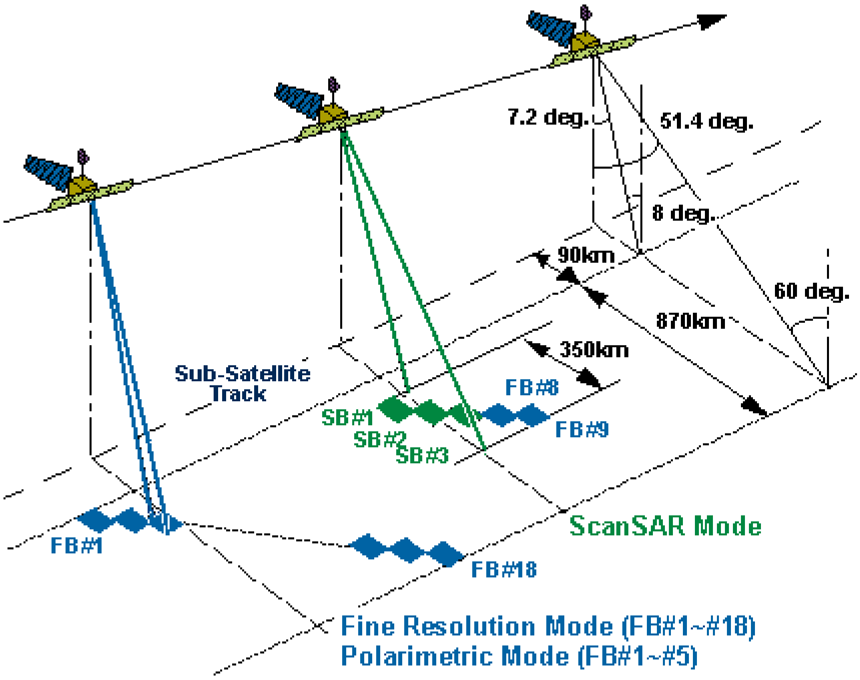

Fiure 3.4-2 PALSAR Observation Modes

4. Products

4.1 PRISM

The PRISM Processing Software accepts Level 0 data, performs radiometric and geometric corrections, and generates Level 1A, Level 1B1, and Level 1B2 products.

Table4.1-1 describes the definitions of processing level of PRISM products.

Table4.1-1 describes the definitions of processing level of PRISM products.

Level	Definitions
1A	This is a PRISM raw data extracted from the Level 0 data, expanded and generated lines. Ancillary information such as radiometric information and etc. required for the processing, superior to the Level 1B is added.
1B1	This is the data that performed radiometric correction to Level 1A data, and added the absolute calibration coefficient. Ancillary information such as radiometric information and etc. required for the processing, superior to the Level 1B2 is added.
1B2	This is the data that performed geometric correction to Level 1B1 data. The following correction options are available. R: Geo-reference data G: Geo-corded data

4.1.1 Specification of Product

(1) Scene Definitions

PRISM scene is defined by RSP (Reference System for Planning) number (Path, Frame) and scene shift distance. Each path is separated into 7200 frames on the basis of the argument of latitude of satellite. Frame number is allocated every 5 scene (approximately 28 km).

Scene shift can be carried out in the processed data, and distance of the scene shift is specified by the number of frames.

Table 4.1.2-1 Scene Size and Scene Definition (PRISM) (1/3)

Level	**Observation Mode**	**Scene Size**	**Scene Definitions and Extraction method**
1A,1B1	Nadir normal mode, forward, backward view	Approximately 35 km x 35 km (4992 pxls x 16000 lines x 4 = 305 Mbyte : Nadir 4928 pxls x 16000 lines x 4 = 301 Mbyte : Forward / Backward : Effective 4864 pxls x 3 x 16000 lines) 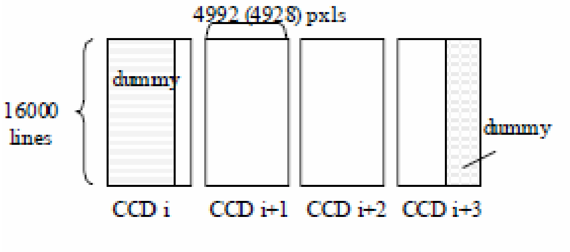	Scene position is defined by satellite RSP No. (Path and Frame) and scene shift distance. Calculate the scene center time corresponding to the frame number, and extract equidistant lines above and below from the calculated time. When scene shift is specified, the center time corresponding to the shifted frame number is calculated. Image file is created per CCD unit. Size of each file is 4992 pixels (nadir view) and 4928 pixels (forward, backward view), and areas with no data would be left as dummy data. Do not delete overlapped areas between CCDs. Even and odd pixel numbers have been already re-ordered. Usually there are 4 CCDs (4 files), but it may be occasionally 3 CCDs (3 files).
	Nadir 70 km Observation mode	Approximately 70 km x 35 km (4992 pxl x 16000 line x 6 = 457 Mbyte : Effective 4864 pxls x 6 x 16000 lines) 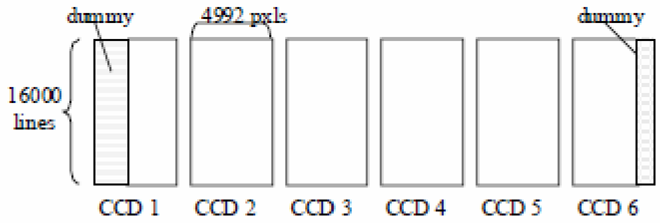	Same as above.

Table 4.1.2-1 Scene Size and Scene Definition (PRISM) (2/3)

Level	**Observation Mode**	**Scene Size**	**Scene Definitions and Extraction method**
1B2R (Geo-reference)	Nadir normal mode, forward, backward view	35 km x 35 km (Except skew area) ((14000+α) pxl x 14000 lines = 187 Mbyte) 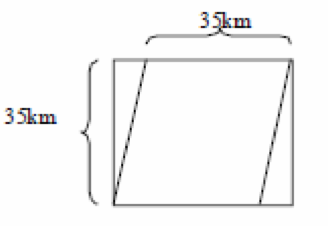	Scene position is defined by satellite RSP No. (Path and Frame) and scene shift distance. Calculate the scene center time corresponding to the frame number, and extract equidistant lines above and below from the calculated time. When scene shift is specified, the center time corresponding to the shifted frame number is calculated. There is only one image file in total, since each CCD was combined to make one scene.
1B2R (Geo-reference)	Nadir 70 km Observation mode	70 km x 35 km (Except skew area.) ((28000+α) pxl x 14000 lines = 374 Mbyte) 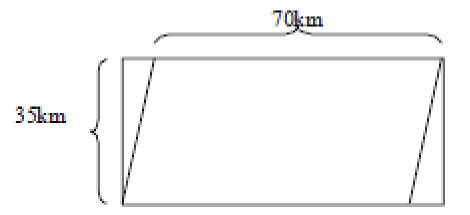	Same as above.

Table 4.1.2-1 Scene Size and Scene Definition (PRISM) (3/3)

Level	**Observation Mode**	**Scene Size**	**Scene Definitions and Extraction method**
1B2G (Geo-coded)	Nadir normal mode, forward, backward view Nadir 70 km Observation mode	Variable size (Rotated Geo-reference) 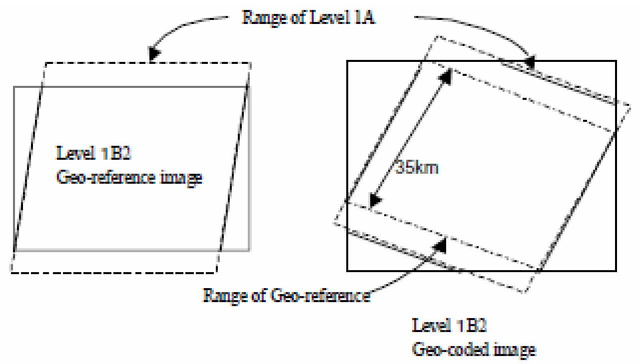	Scene position is Map north. Geo-coded is an image that rotated a Geo-reference. Each corner of the Geo-reference image touches each side of Geo-coded image. The image size will be variable and double at the maximum. There is only one image file in total, since each CCD was combined to make one scene.

(2) Definitions of scene related information

This section describes the definitions of scene related information for PRISM products.

1) Uncorrected image

PRISM has six CCD units for Nadir view and eight for Forward and Backward view. Both PRISM Level 1A and 1B1 images are created by image file of each CCD. For nadir normal mode (35km) and forward and backward view, 4864 x 3 pixels are extracted from the arbitrary pixels in CCD, and for nadir 70 km observation mode, 4864 x 6 pixels are extracted. The extracted PRISM images are transmitted to the processing system. Each image file per one line is 4992 pixels for nadir and 4982 pixels for forward and backward view. With respect to the space before extraction was started and after extraction was ended, dummy data will be set to that area. Each corner of scene is defined in the starting extraction point in the first and the last line except dummy area and the ending extraction point.

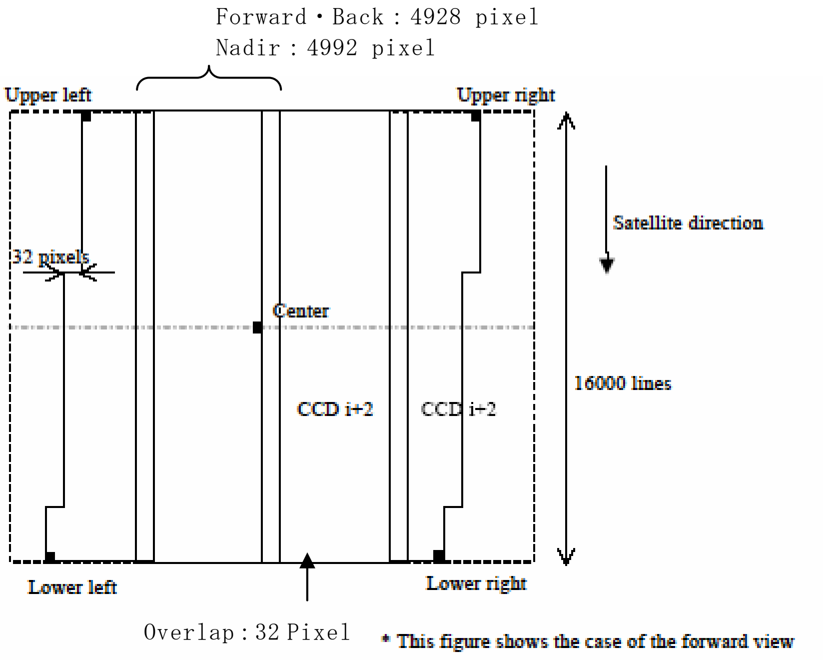

Figure 4.1.1-1 Concept of Scene Related Information for PRISM Uncorrected Image

① Latitude and longitude at each corner of scene:

Upper left : Latitude and longitude of the center point of the first pixel
for extraction at the first line
Upper right : Latitude and longitude of the center point of the end pixel

for extraction at the first line

Lower left : Latitude and longitude of the center point of the first pixel for extraction at the last line (16000th line)

Lower right : Latitude and longitude of the center point of the end pixel for extraction at the last line (16000th line)

② Pixel number of the scene center and line number:

Pixel number: Calculate the middle point between the start pixel for extraction and the end pixel at the 8000th line with an absolute pixel number. However, it is the center value allowing for overlapped pixels (32-pixel) between CCDs. The absolute pixel number is a pixel number which is given to all CCDs from CCD 1 within one scene.

Line number: Middle point between the first line and the last line. (8000.5)

③ Latitude and longitude at the scene center:

Latitude and longitude corresponding to the above address.

* There may be cases where the first pixel number for extraction is changed due to Earth location correction within one scene for forward and backward views. For nadir view, this correction is not performed.

2) Level1B2 Geo-reference image

Level 1B2 Geo-reference image is framed based on the centerline of the uncorrected image and is a map-projected image with 35 km x 14000 lines. The column direction of the Geo-reference image is framed to fit inside the effective area of the uncorrected image inside. (variable length). If the first extracted pixel is changed in the scene due to Earth rotation correction, the start of the effective area is defined in the biggest value of the absolute pixel number, on the other hand, the end of the effective area is defined in the smallest value.

For the ascending image, image direction is flipped to make nearly north of the image upward. (Satellite direction will be upward.)

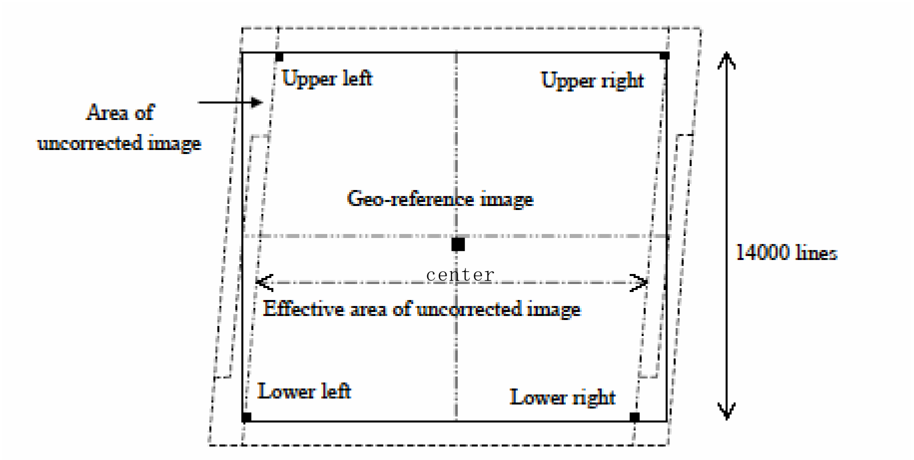

Figure 4.1.1-2-2 Concept of Scene Related Information for PRISM 1B2 Geo-reference Image

① Latitude and longitude at each corner of scene:

Upper left : Latitude and longitude of the intersection point of the first line and the first pixel of the effective area of the uncorrected image

Upper right : Latitude and longitude of the intersection point of the first line and the last pixel of the effective area of the uncorrected image

Lower left : Latitude and longitude of the intersection point of the last line (the 14000th line) and the first pixel of the effective area of the uncorrected image

Lower right : Latitude and longitude of the intersection point of the last line (the 14000th line) and the last pixel of the effective area of the uncorrected image

For the ascending image, since the image has been flipped, the first pixel of the effective area is started from the right side and the last pixel of the effective area is located in the left side. From this reason, the calculation of the intersection point will be opposite in both sides.

② Pixel number of the scene center and line number:

Pixel number: It is (s+1)/2 when size of column direction is defined as s (variable).

Line number: Center line number of image (= 7000.5)

③ Latitude and longitude at the scene center:

Latitude and longitude which correspond to the above address.

3) Level 1B2 Geo-coded image

Level 1B2 Geo-coded image is made by framing to make map-north upward. In this case, framing is done by making the four corner points of the Geo-reference image touch the Geo-coded image side.

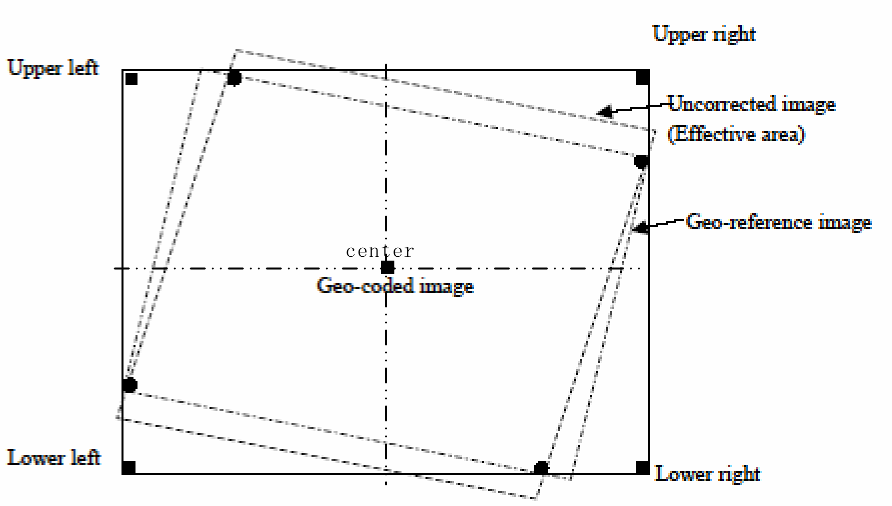

Figure 4.1.1-3 Concept of Scene Related Information for PRISM 1B2 Geo-coded Image

① Latitude and longitude at each corner of scene:

Upper left : Latitude and longitude at the corner of the upper left pixel in the whole image including dummy area

Upper right : Latitude and longitude at the corner of the upper right pixel in the whole image including dummy area

Lower left : Latitude and longitude at the corner of the lower left pixel in the whole image including dummy area

Lower right : Latitude and longitude at the corner of the lower l right pixel in the whole image including dummy area

② Pixel number of scene center and line number:

Pixel number: It is (s+1)/2 when size of the column direction is defined as s (variable).

Line number: It is (l+1)/2 when the number of lines of the image is defined as l (variable).

③ Latitude and longitude at the scene center:

Latitude and longitude which correspond to the above address.

(3) Processing Parameter

This section describes the processing parameters that can specify to PRISM products. (This extract than ALOS proccesing product for matmanualof PRISM (NEB-01006 (ALOS-DPFT-J01)) J revised edition)

① 1B2 option
② Map projection
③ Resampling
④ UTM zone number
⑤ PS projection parameter
⑥ Map direction
⑦ Accuracy of the used orbit data
⑧ Accuracy of used attitude data
⑨ Reference ellipsoid
⑩ Scene shift（along track）

(4) Product Explanation

Table 4.1.1-2 describes the products of PRISM.

Table 4.1.1-2 The products of PRISM

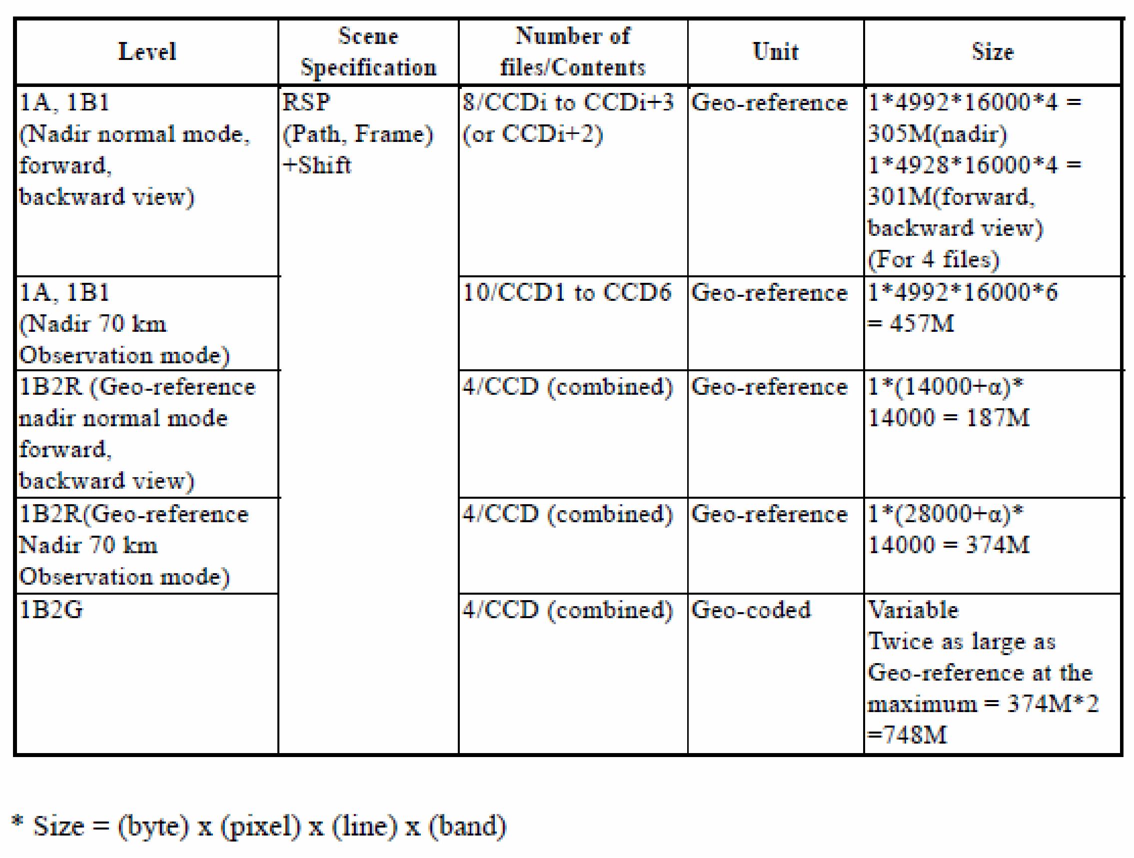

Level	Scene Specification	Number of files/Contents	Unit	Size
1A, 1B1 (Nadir normal mode, forward, backward view)	RSP (Path, Frame) +Shift	8/CCDi to CCDi+3 (or CCDi+2)	Geo-reference	1*4992*16000*4 = 305M(nadir) 1*4928*16000*4 = 301M(forward, backward view) (For 4 files)
1A, 1B1 (Nadir 70 km Observation mode)		10/CCD1 to CCD6	Geo-reference	1*4992*16000*6 = 457M
1B2R (Geo-reference nadir normal mode forward, backward view)		4/CCD (combined)	Geo-reference	1*(14000+α)* 14000 = 187M
1B2R(Geo-reference Nadir 70 km Observation mode)		4/CCD (combined)	Geo-reference	1*(28000+α)* 14000 = 374M
1B2G		4/CCD (combined)	Geo-coded	Variable Twice as large as Geo-reference at the maximum = 374M*2 =748M

* Size = (byte) x (pixel) x (line) x (band)

4.1.2 Product Format

The PRIMS product is CEOS format (BSQ: Band Sequential).

(1) Whole Structure of Product Format

PRISM product is composed of five different files; Volume directory, Leader, Image, Trailer and Supplemental, and each file consists of multiple records.

① Volume Directory file : information for identifying the logical/physical volume.
② Leader file : the geometric information. / the radiometric information.
③ Image file : Image data
④ Trailer file : The quality information of the image
⑤ Supplemental file : the geometric information. / the radiometric information. / determination and conventional orbit information（It don’t include in the case of level 1B2.)

In the geometric uncorrected image of PRISM, image file is created per CCD unit. Therefore, there are four image files at the normal observation and six image files at the 70 km observation mode.

Overlapped data (approximately 32 pixels), which have been taken at the same area of the Earth's surface, are stored in the observation data of neighboring CCDs, but these data are kept without deleting.

The number of pixels in one line of each image file will be fixed as 4992 pixels (forward and backward view: 4928 pixels); this is the same as that of the number of the elements used in CCDs, and the pixels which are not transferred are kept as dummy data.

Figure 4.1.2-1 shows the file structure of the PRISM products.

Table 4.1.2-1 describes the file name and record name that compose products and their contents, and Figure 4.1.2-2 describes the naming rule of each file.

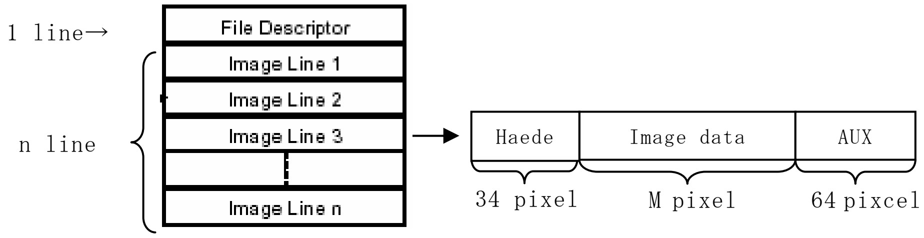

Fig. 4.1.2-1 The record staructure of image file

Table 4.1.2-1 The number of line and pixel of PRISM image file

Level	Observation mode	m	n	Image pixel number
1A、1B1	Normal observation (35km)	Nadir : 4992pixel Foward・Back : 4928pixel	16000line	3～4
	Nadir 70km	Madir : 4992pixel	16000line	6
1B2 (Geo-reference)	Normal observation (35km)	14000+αpixel ＝Image pixel number (File Descriptor Reference of 249～256byte)	14000line	1
	Nadir 70km	28000+αpixel ＝Image pixel number (File Descriptor Reference of 249～256byte)	14000line	1
1B2 (Geo-coded)		Image pixel number (File Descriptor Reference of 249～256byte)	A line number per the band (File Descriptor Reference of 237～244byte)	1

Table 4.1.2-2 Naming Rule of the PRISM File

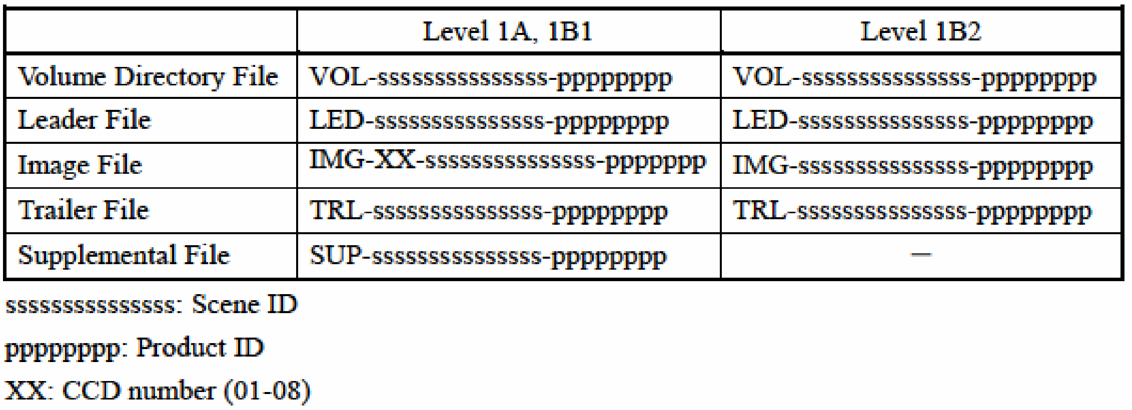

	Level 1A, 1B1	Level 1B2
Volume Directory File	VOL-sssssssssssssss-pppppppp	VOL-sssssssssssssss-pppppppp
Leader File	LED-sssssssssssssss-pppppppp	LED-sssssssssssssss-pppppppp
Image File	IMG-XX-sssssssssssssss-pppppppp	IMG-sssssssssssssss-pppppppp
Trailer File	TRL-sssssssssssssss-pppppppp	TRL-sssssssssssssss-pppppppp
Supplemental File	SUP-sssssssssssssss-pppppppp	－

sssssssssssssss: Scene ID

pppppppp: Product ID

XX: CCD number (01-08)

(2) Description of Product Records

This section describes the format of the following eight record types.

① Volume Descriptor
② File Pointer
③ Text
④ File Descriptor
⑤Scene Header
⑥ Ancillary
⑦ Image
⑧ Trailer

1) Record Data Type

Table 4.1.2-3 describes the definition of data type used for record explanation.

Table 4.1.2-3 Data Types

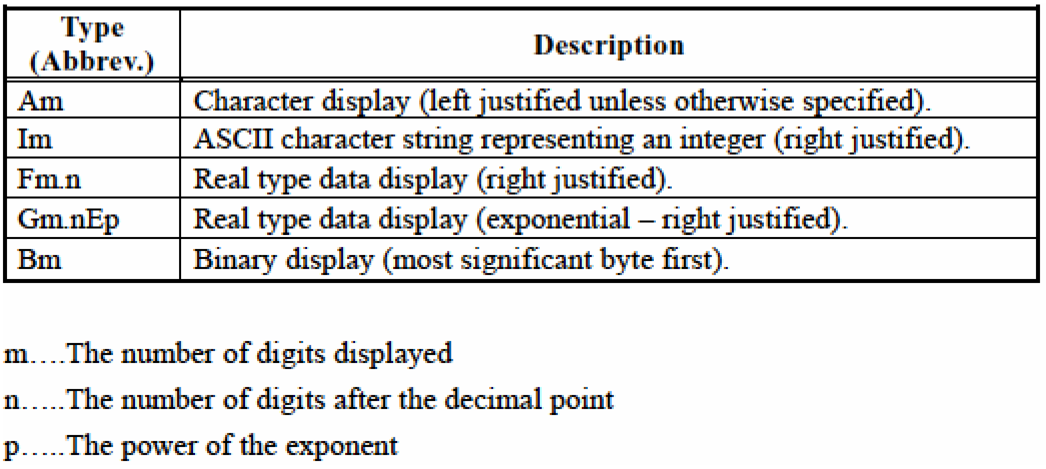

Type (Abbrev.)	Description
Am	Character display (left justified unless otherwise specified).
Im	ASCII character string representing an integer (right justified).
Fm.n	Real type data display (right justified).
Gm.nEp	Real type data display (exponential – right justified).
Bm	Binary display (most significant byte first).

m….The number of digits displayed
n…..The number of digits after the decimal point
p…..The power of the exponent

2) Product Format

Detailed format of each record is given in the product format list.

(Reference or http://www.eorc.jaxa.jp/ALOS/doc/format.htm)

4.2 AVNIR-2

The AVNIR-2 Processing Software accepts Level 0 data, performs radiometric and geometric corrections, and generates Level 1A, Level 1B1, and level LB2 products.

Table 4.2-1 show the definition of the disposal of AVNIR-2 products level.

Table4.2-1 The definitions of processing level of PRISM products

Level	Definition
1A	This is an AVNIR-2 raw data extracted from the Level 0 data, expanded and generated lines. Ancillary information such as radiometric information and etc. required for the processing, superior to the Level 1B is added.
1B1	This is the data that performed radiometric correction to Level 1A data, and added the absolute calibration coefficient. Ancillary information such as radiometric information and etc. required for the processing, superior to the Level 1B2 is added.
1B2	This is the data that performed geometric correction to Level 1B1 data. The following correction options are available. R: Geo-reference data G: Geo-corded data D: Rough DEM (Digital Elevation Model) correction: this option corrects the topographical influence to the areas where DEM was covered. DEM correction is effective only in Japanese region. Further, DEM correction error can occur with high pointing angles. Accuracy is not guaranteed since errors are complemented.

4.2.1 Specification of Product

(1) Scene Definitions

AVNIR-2 scene is defined by RSP (Reference System for Planning) number (Path, Frame) and scene shift distance. Each path is separated into 7200 frames on the basis of the argument of latitude of satellite. Frame number is allocated every 10 frame (approximately 56 km) in AVNIR-2. Scene shift can be carried out in the processed data, and the distance of scene shift is specified by distance of the scene shift is specified by the number of frames. Table 4.2.1-1 describes the scene definitions and scene size of AVNIR-2.

Table 4.2.1-1 The scene definitions and scene size of AVNIR-2.(1/2)

Processing Level	Scene Size	Scene Definitions and Extraction method
1A, 1B1	Approximately 70 km x 70 km (Nadir) (7100 pxls x 8000 lines x 4 bands = 217 Mbyte) 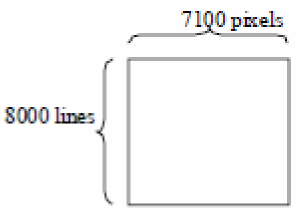	Scene position is defined by satellite RSP No. (Path and Frame) and scene shift distance. Calculate the scene center time corresponding to the frame number, and extract equidistant lines above and below from the calculated time. When scene shift is specified, the center time corresponding to the shifted frame number is calculated. The image file is composed of the data for each band, and these files are not divided by odd and even number pixel. Simple stagger liner correction is not performed in level 1B1.
1B2R (Geo-reference)	70 km x 70 km (Nadir) (Size of cross-struck direction is increased at pointing) ((7100+α) x 7000 lines x 4 bands = 190 Mbyte : Default: Pixel Spacing 10m) ((4730+α) x 4667l ines x 4 bands = 84 Mbyte : Pixel Spacing 15m) ((3550+α) x 3500 lines x 4 bands = 47 Mbyte : Pixel Spacing 20m) 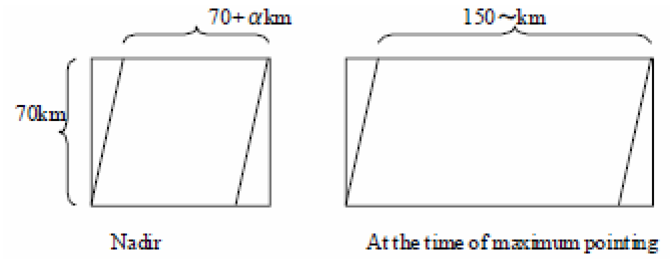	Scene position is defined by satellite RSP No. (Path and Frame) and scene shift distance. Calculate the scene center time corresponding to the frame number, and extract equidistant lines above and below from the calculated time. When scene shift is specified, the center time corresponding to the shifted frame number is calculated. The image file is composed of the data for each band.

Table 4.2.1-1 The scene definitions and scene size of AVNIR-2.(2/2)

Processing Level	Scene Size	Scene Definitions and Extraction method
1B2G (Geo-coded)	Variable size (Rotated Geo-reference) 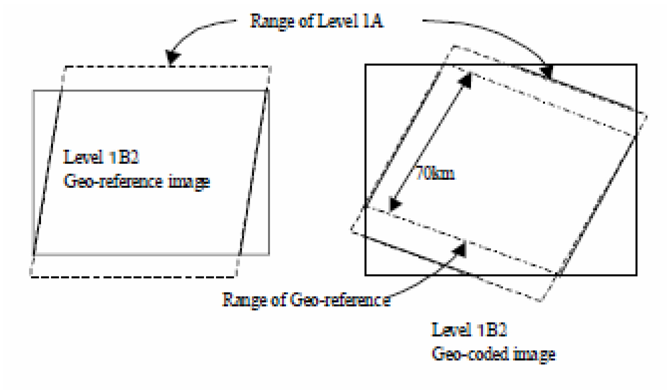	Scene position is Map north. Geo-coded is an image that rotated a Geo-reference. Each corner of the Geo-reference image touches each side of Geo-coded image. The image size will be variable and double at the maximum. The image file is composed of the data for each band.

(2) Definition of Scene Related Information

This section describes the definitions of the scene related information for AVNIR-2 products.

1) Uncorrected image

AVNIR-2 has four bands, and each band has 7100-pixel CCD. The odd number pixels and the even number pixels are arrayed by stagger alignment, where both pixels are

approximately 5 pixels away from each other. The odd number pixels come first and are located below (satellite direction). Since there is a registration error between bands, the imaging position of each band is not the same exactly. In this section, band three is described as an example.

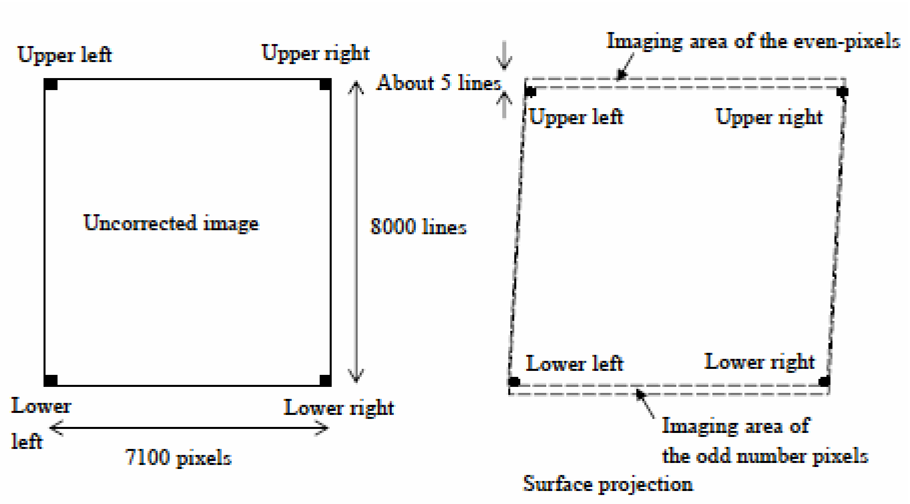

Figure 4.2.1-1 Concept of the Scene Related Information of AVNIR-2 Uncorrected Image

① Latitude and longitude at each corner of scene:

Upper left : Latitude and longitude of the first pixel (odd pixel) at the first line

Upper right : Latitude and longitude of the position corresponding to odd number pixel of the 7100th pixel at the first line. (Even number pixel is actually placed in this position, but it is assumed that odd number pixel exists there.)

Lower left : Latitude and longitude of the position corresponding to even number pixel of the first pixel at the last line (8000th line). (Odd number pixel is actually placed in this position, but it is assumed that even number pixel exists there.)

Lower right : Latitude and longitude of the 7100th pixel (even pixel) at the last line (8000th line)

② Pixel number of scene center and line number:

Pixel number: middle point between 7100 pixels (3550.5)
Line number: middle point between 8000 lines (4000.5)

③ Latitude and longitude at the scene center:

Latitude and longitude of the middle point between the imaging point corresponding to the odd number pixel and the imaging point corresponding to the even number pixel. Each imaging point corresponds to the above address.

2) Level1B2 Geo-reference Image

Level 1B2 Geo-reference image is framed based on the centerline of an uncorrected image and is a map-projected image with 70 km x 7000 lines (when pixel spacing is 10 m). Column direction of the Geo-reference image is framed to fit inside the effective area of the uncorrected image in the Geo-referenced image (variable length). Band three is used for framing. For the ascending image, image direction is flipped to make nearly north of the image upward. (Satellite direction will be upward.)

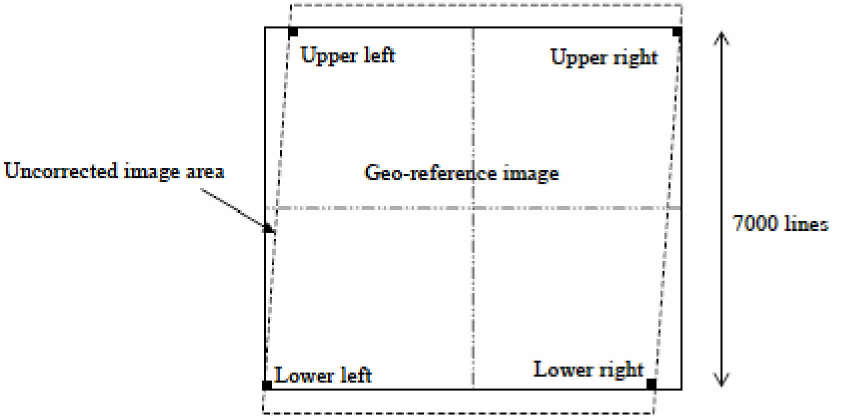

Figure 4.2.1-2 Concept of the Scene Related Information of AVNIR-2 1B2 Geo-referenced Image

① Latitude and longitude at each corner of scene:

Upper left : Latitude and longitude of the intersection point of the first line and the first pixel of the uncorrected image (it is the line connecting the upper left and lower left of the uncorrected image).

Upper right : Latitude and longitude of the intersection point of the first line and the end pixel of the uncorrected image (it is the line connecting the upper right and lower right of the uncorrected image).

Lower left : Latitude and longitude of the intersection point of the last line and the first pixel of the uncorrected image.

Lower right : Latitude and longitude of the intersection point of the last line and the last pixel of the uncorrected image.

For ascending image, since the image has been flipped, the first pixel of the uncorrected image is started from the right side and the last pixel of the uncorrected image is located in the left side. From this reason, the calculation of the intersection point is opposite in both sides

② Pixel number of scene center and line number:

Pixel number: It is (s+1)/2 when size of the column direction is defined as s (variable).

Line number: Center line number of the image. Pixel spacing value, the number of lines, and the center line number are described as follows:

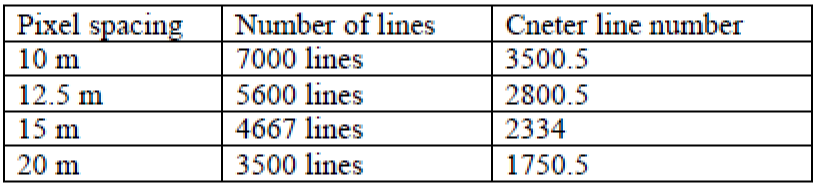

Pixel spacing	Number of lines	Cneter line number
10 m	7000 lines	3500.5
12.5 m	5600 lines	2800.5
15 m	4667 lines	2334
20 m	3500 lines	1750.5

(Default of the pixel spacing depends on the pointing angle)

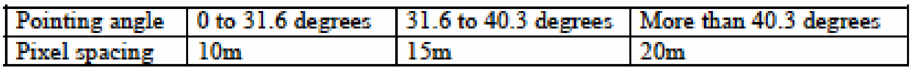

Pointing angle	0 to 31.6 degrees	31.6 to 40.3 degrees	More than 40.3 degrees
Pixel spacing	10m	15m	20m

③ Latitude and longitude at the scene center:

Latitude and longitude which correspond to the above address.

3) Lebeleo-coded Image

Level 1B2 Geo-coded image is made by framing to make map-north upward. In this case, framing is done by making the four corner points of the Geo-reference image touch the Geo-coded image sides.

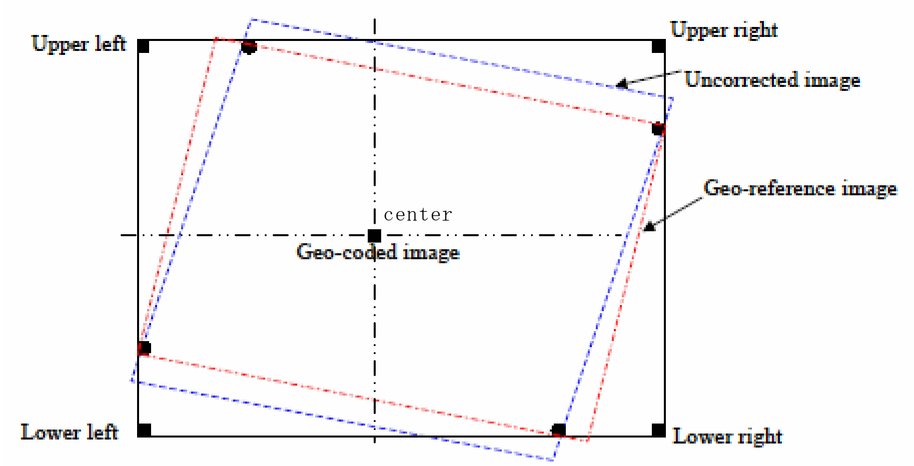

Figure 4.2.1-3 Concept of the Scene Related Information of AVNIR-2 1B2 Geo-coded Image

① Latitude and longitude at each corner of scene:

Upper left : Latitude and longitude at the corner of the upper left pixel in the whole
image including dummy area
Upper right : Latitude and longitude at the corner of the upper right pixel in the whole image including dummy area
Lower left : Latitude and longitude at the corner of the lower left pixel in the whole
image including dummy area
Lower right : Latitude and longitude at the corner of the lower right pixel in the whole image including dummy area

② Pixel number of scene center and line number:

Pixel number: It is (s+1)/2 when size of the column direction is defined as s (variable).
Line number: It is (l+1)/2 when the number of lines of the image is defined as l (variable).

③ Latitude and longitude at the scene center:

Latitude and longitude which correspond to the above address.

(3) Processing Parameters

This section describes the processing parameters that can specify to AVNIR-2 products.

（This extract than ALOS proccesing product for matmanualof AVNIR-2（NEB-01006 (ALOS-DPFT-J02)）J revised edition）

① 1B2 option
② Map projection
③ Resampling
④ UTM zone number
⑤ PSProjection parameter
⑥ Map direction
⑦ Accuracy of the used orbit data
⑧ Accuracy of the used orbit attitude data
⑨ Reference ellipsoid
⑩ Scene shift（along track）
⑪ Pixel spacing

Table 4.2.1-2 describes the products of AVNIR-2 and scene unit.

Table 4.2.1-2 The products of AVNIR-2

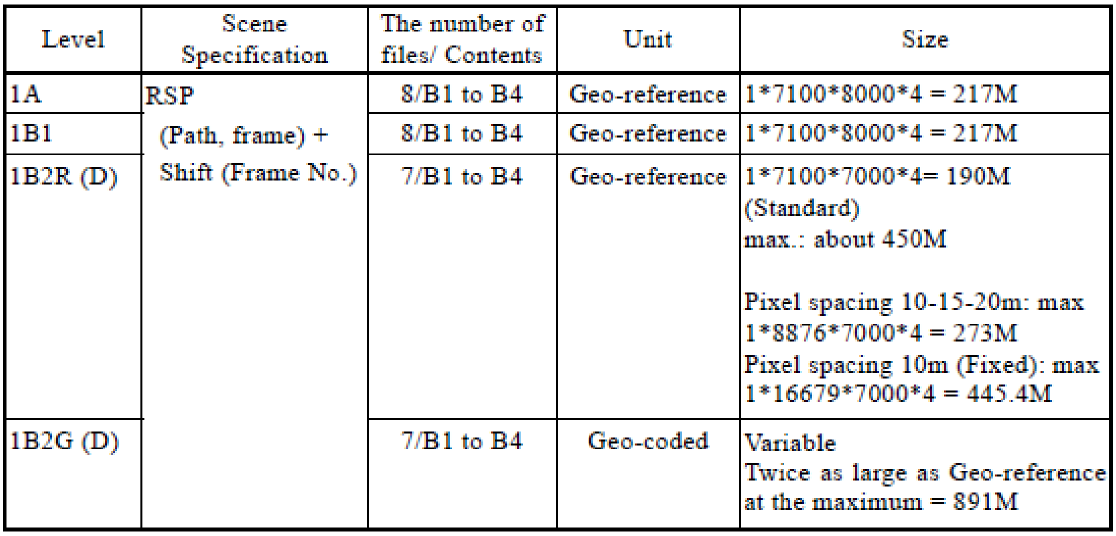

Level	Scene Specification	The number of files/ Contents	Unit	Size
1A	RSP (Path, frame) + Shift (Frame No.)	8/B1 to B4	Geo-reference	1*7100*8000*4 = 217M
1B1		8/B1 to B4	Geo-reference	1*7100*8000*4 = 217M
1B2R (D)		7/B1 to B4	Geo-reference	1*7100*7000*4= 190M (Standard) max.: about 450M Pixel spacing 10-15-20m: max 1*8876*7000*4 = 273M Pixel spacing 10m (Fixed): max 1*16679*7000*4 = 445.4M
1B2G (D)		7/B1 to B4	Geo-coded	Variable Twice as large as Geo-reference at the maximum = 891M

* Size = (byte) x (pixel) x (line) x (band)

4.2.2 Product Format

AVNIR-2 product is CEOS format (BSQ). It show below it about the details.

(1) Whole Structure of Product Format

AVNIR-2 product is composed of five different files as shown below, and each file consists of multiple records.

① Volume Directory file : information for identifying the logical/physical volume.
② Leader file : the geometric information.／the radiometric information.
③ Image file : Image data
④ Trailer file : The quality information of the image
⑤ Supplemental file : the geometric information.／the radiometric information.／determination and conventional orbit information（It don’t include in the case of level 1B2.）

In the geometrically uncorrected image of AVNIR-2, image file is not separated into odd number pixels and even number pixels, and simple correction for stagger-linear between odd and even number pixel is not performed. That is, the data on the same line consist of the same observation time.

Figure 4.2.2-1 shows the file structure of the AVNIR-2 products.

Table 4.2.2-1 describes the file name and record name that compose products and their contents, and Table 4.2.2-2 describes the naming rule of each file.

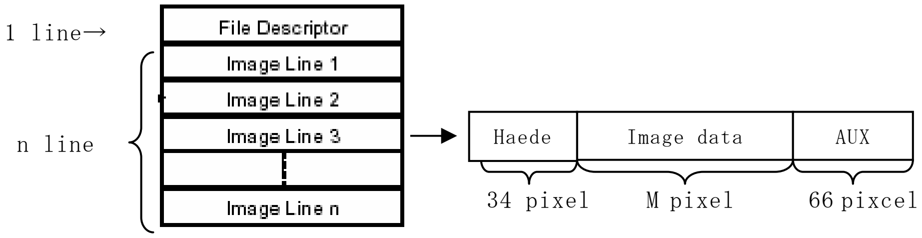

Fig. 4.2.2-1 The record staructure of image file

Table 4.1.2-1 The number of line and pixel of AVNIR-2 image file

Level	Observation Mode	m	n	The number of image file
1A、1B1	Normal observation	7100pixel	8000 line	4
1B2 (Geo-reference)	Pixel spacing 10m	7100+α pixel =image pixel number (File Descriptor Reference of 249～256byte))	7000 line	4
	Pixel spacing 12.5m	?+α pixel =image pixel number (File Descriptor Reference of 249～256byte)	5600 line	4
	Pixel spacing 15m	4730+α pixel =image pixel number (File Descriptor Reference of 249～256byte)	4667 line	4
	Pixel spacing 20m	3550+α pixel = image pixel number (File Descriptor Reference of 249～256byte)	3500 line	4
1B2 (Geo-coded)		image pixel number (File Descriptor Reference of 249～256byte)	A line number per the band (File Descriptor Reference of 237～244byte)	4

Table4.2.2-2 Naming Rule of AVNIR-2 File

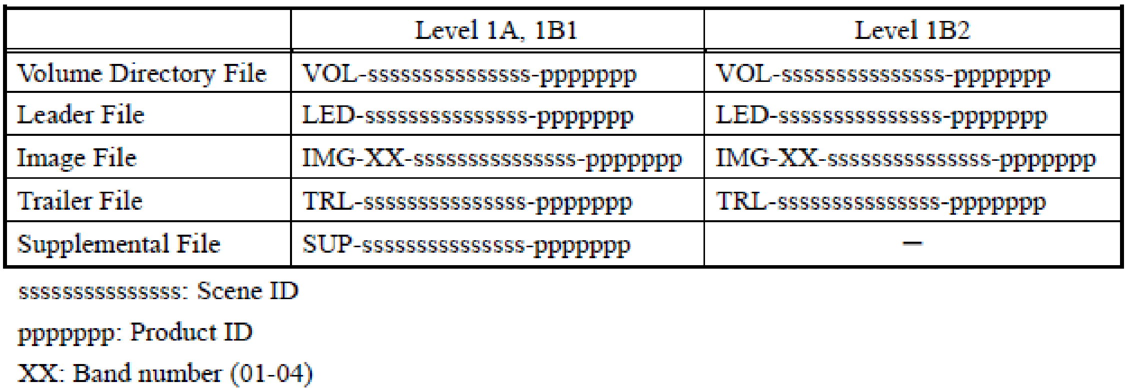

	Level 1A, 1B1	Level 1B2
Volume Directory File	VOL-sssssssssssssss-ppppppp	VOL-sssssssssssssss-ppppppp
Leader File	LED-sssssssssssssss-ppppppp	LED-sssssssssssssss-ppppppp
Image File	IMG-XX-sssssssssssssss-ppppppp	IMG-XX-sssssssssssssss-ppppppp
Trailer File	TRL-sssssssssssssss-ppppppp	TRL-sssssssssssssss-ppppppp
Supplemental File	SUP-sssssssssssssss-ppppppp	—

sssssssssssssss: Scene ID

ppppppp: Product ID

XX: Band number (01-04)

(2) Description of Product Records

This section describes the format of the following eight record types.

(1) Volume Descriptor
(2) File Pointer
(3) Text
(4) File Descriptor
(5) Scene Header
(6) Ancillary
(7) Image
(8) Trailer

1) Record Data Types

Table 4.2.2-3 describes the definition of the data type used for record explanation.

Table 4.2.2-3 Data Types

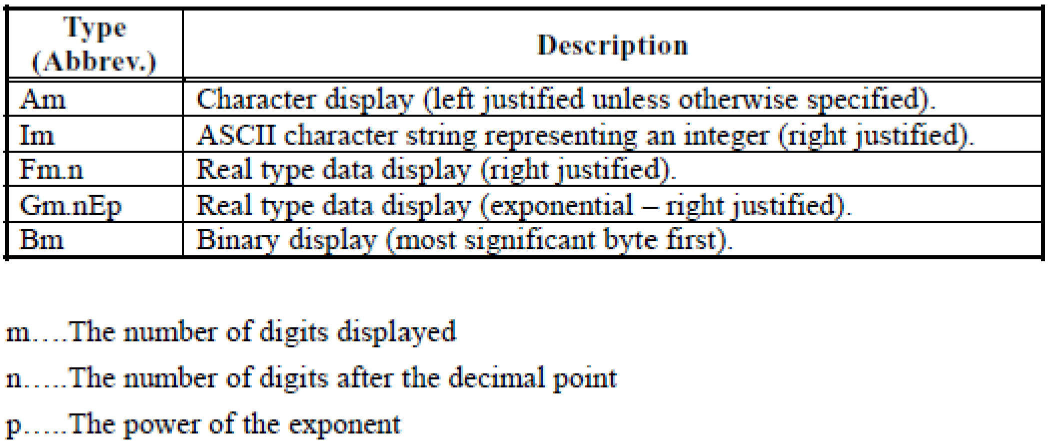

Type (Abbrev.)	Description
Am	Character display (left justified unless otherwise specified).
Im	ASCII character string representing an integer (right justified).
Fm.n	Real type data display (right justified).
Gm.nEp	Real type data display (exponential – right justified).
Bm	Binary display (most significant byte first).

m….The number of digits displayed
n…..The number of digits after the decimal point
p…..The power of the exponent

2) Product Format

Detailed format of each record is given in the product format list.

(Reference or http://www.eorc.jaxa.jp/ALOS/doc/format.htm)

4.3 PALSAR

The definitions of PALSAR data products for processing levels are shown in Table 4.3-1.

Table 4.3-1 Processing Levels and Their Definitions

Processing Level	Definition
1.0	The data of 1 scene area is extracted from received data. Data type is 8 bit. The number of SAR data files is the same as the number of polarizations in the case of dual polarization and polarimetry modes. The data in SCAN SAR mode is not divided into individual scans.
1.1	Range compression and 1 look azimuth compression are performed. Data is complex data on the slant range coordinate. The phase history is included.
1.5	After range and multi-look azimuth compression are performed, radiometric and geometric corrections are performed according to the map projection. Pixel spacing can be selected for the Fine mode

4.3.1 Product Overview

The processing levels of observational modes are given in Table 4.3.1-1.

Table 4.3.1-1 Processing Levels of Observational Modes

Observation Mode		Processing Level			Remarks
		1.0	1.1	1.5	
Fine mode	Single polarization	O	O	O	18 beams
	Dual polarization	O	O	O	18 beams
Scan SAR mode	Burst mode 1	O	-	O	3 scans, 4 scans, 5 scans
	Burst mode 2	O	-	O	3 scans, 4 scans, 5 scans
Direct Downlink mode		O	O	O	18 beams
Polarimetry mode		O	O	O	12 beams

Remark : Level 1.0 data sometimes includes calibration data as well as observation data.

(1) Definition of a scene

PALSAR scene is defined by RSP (Reference System for Planning) number (Path, Frame) and scene shift distance. Each path is separated into 7200 frames on the basis of the argument of latitude of satellite. Frame number is allocated every 10 frames (approximately 56 km) except for Scan SAR mode, and every 50 frames for Scan SAR mode. Scene shift can be carried out in the processed data, and the distance of scene shift is specified by distance of the scene shift is specified by the number of frames.

The scene sizes of some typical modes are shown in Table 4.3.1-2, Table 4.3.1-3, Table 4.3.1-4 and Table 4.3.1-5.

Table 4.3.1-2 Image Size of PALSAR Level 1.0Products

Mode	Offnadir／Scan number	Azimuth	Range			Scene size (MB)
		Record number	Sample number	Sample record size (byte)	Record length (byte)	
Fine mode (Single polarization)	21.5	28572～31060	7008	14428	14500	395.1～429.51
	34.3	33402～35575	10304	21020	21100	672.13～715.86
	41.5	29656～31660	11936	24284	24300	678.26～8733.70
Fine mode (Dual polarization)	21.5	28572～31060	3504	7420	7500	408.73～444.32
	34.3	33402～35575	5152	10716	10800	688.06～732.82
	41.5	29656～31660	5968	12348	12400	350.70～374.40
Direct Down Link mode	21.5	28572～31060	3504	7420	7500	204.36～222.16
	34.3	33402～35575	5152	10716	10800	344.03～366.41
	41.5	29656～31660	5968	12348	12400	350.70～374.40
Polarimetry mode	21.5	29927～31907	1584	3580	3600	410.98～438.18
Scan SAR mode (Burst mode 1) 5Scan	1	14244～15624	4976	10364	11200	1148.77～1236.57
	2	29250～31064	4720	9852	11200	
	3	16080～17483	5376	11164	11200	
	4	26435～28339	4432	9276	11200	
	5	21542～23260	4688	9788	11200	

notes;

The scene size depends on the record number which change by pulse repeat frequency.

The scene size of FBD/PLR is the total size of each polarization files.

Reference: ALOS/PALSAR Level 1 Product Format Description (NEB-01006 (ALOS-DPFT-J03))

Table 4.3.1-3 Image Size of PALSAR Level 1.1 Products (typical values)

Fine and Direct downlink modes			
Off-nadir angle (deg)	Range Samples		Azimuth samples
	Single	Dual, Direct Downlink mode	
9.9	3,936	1,824	18,432
14.0	5,088	2,400	18,432
18.0	6,144	2,944	18,432
21.5	7,168	3,456	18,432
25.8	8,288	4,000	18,432
28.8	9,056	4,384	18,432
30.8	9,568	4,640	18,432
34.3	10,400	5,088	18,432
36.9	10,816	5,376	18,432
38.8	11,296	5,600	18,432
41.5	11,680	5,792	18,432
43.4	12,256	6,080	18,432
45.2	9,248	4,576	18,432
46.6	9,472	4,704	18,432
47.5	9,664	4,800	18,432
49.0	9,824	4,864	18,432
50.0	9,952	4,928	18,432
50.8	8,224	4,064	18,432

Polarimetry mode		
Off-nadir angle (deg)	Range Samples	Azimuth samples
9.7	1,344	18,432
13.8	1,472	18,432
16.2	736	18,432
17.3	768	18,432
17.9	800	18,432
19.2	832	18,432
20.5	1,312	18,432
21.5	1,344	18,432
23.1	1,216	18,432
24.2	1,024	18,432
25.2	1,056	18,432
26.2	1,120	18,432

Remark 1: The output size for one processing segment in the azimuth direction is 9216 samples. The number of output azimuth samples is 18,432, corresponding to a size of two segments.

Remark 2: The Sampling Window Start Time (SWST) may vary slightly which can result in the number of output range samples changing by approximately 256 samples during processing.

Remark 3: For level 1.1 products, each data record corresponds to 1 image range line. Each range line begins at the nearest-range pixel and ends at the farthest-range pixel. Also, the first image record contains the earliest range line, and the last record contains the latest line.

Table 4.3.1-4 Data Capacity (rough estimation) of Level 1.5 Products (Geo-reference)

Mode	Pixel Spacing	Image Size Range x Azimuth	East – West Frame Size (Pixels)	South - North Frame Size (Pixels)	Data Capacity (MB)
Fine beam /Direct Downlink Mode	6.25m	70×52～78km	8900～13100	11200	280
		50×64～79km	10300～13100	8000	200
		40×75～79km	12000～13100	6400	160
	12.5m	70×52～78km	4500～6600	5600	71
		50×64～79km	5200～6600	4000	50
		40×75～79km	6000～6600	3200	40
Scan SAR		250×350km	3500	2500	17
		300×350km	3500	3000	21
		350×350km	3500	3500	24

- Above table shows maximum capacities without considering data capacity increase due to methods of map projection and processing scene latitude.
- In PS (Polar Stereographic) projection, maximum capacity (at scene latitude of +/- 25deg.) may be twice as large as the values in the table.
- Reference: ALOS/PALSAR Level 1 Product Format Description (NEB-01006 (ALOS-DPFT-J03))

Table 4.3.1-5 Data Capacity (rough estimation) of Level 1.5 Products (Geo-code)

Mode	Pixel Spacing	Image Size Range x Azimuth	East – West Frame Size (Pixels)	South - North Frame Size (Pixels)	Data Capacity (MB)
Fine beam /Direct Downlink Mode	6.25m	70×52～78km	8300～17200	11200～17200	558
		50×64～79km	10300～15300	8000～15300	400
		40×75～79km	12000～14600	6400～14600	320
	12.5m	70×52～78km	4200～8600	5600～8600	140
		50×64～79km	5200～7700	4000～7700	101
		40×75～79km	6000～7300	3200～7300	81
Scan SAR		250×350km	4300	4300	36
		300×350km	4600	4600	41
		350×350km	5000	5000	48

- Above table shows maximum capacities without considering data capacity increase due to methods of map projection and processing scene latitude.
- In PS (Polar Stereographic) projection, maximum capacity (at scene latitude of +/- 25deg.) may be twice as large as the values in the table.
- Reference: ALOS/PALSAR Level 1 Product Format Description (NEB-01006 (ALOS-DPFT-J03))

(2) Pixel Spacing

Table 4.3.1-6 shows the pixel spacing of level 1.5 products for each observational mode.

Table 4.3.1-6 Pixel Spacing of Level 1.5 Products

Fine mode		SCAN SAR mode		Direct Downlink mode	Polarimetry mode
Single polarization	Dual polarization	Burst mode 1	Burst mode 2		
6.25m(2look) 12.5m(4look)	12.5m(4look)	100m	100m	12.5m(4look)	12.5m(4look)

(3) Processing Parameters

The processing parameters of each level are given in Table 4.2.1-7.

Table 4.2.1-7 Summary of Processing Parameters

Items	Processing level		
	1.0	1.1	1.5
Map projection	-	-	UTM,PS MER, LCC(*3)
Framing (*1)	-	-	GR,GC
Image direction (*2)	-	-	Map
Resampling	-	-	NN,BL,CC
Geodetic coordinate (Earth model)	-	-	ITRF97(GRS80)
Scene Shift	-5 to 4	-5 to 4	-5 to 4
Window Function	-	rectangle	rectangle
Multi-look Number	-	1	depending on observational mode
Pixel Spacing	-	-	depending on observational mode and multi-look number

(*1)GR: Geo-reference、GC: Geo-code

(*2)valid in the case of Geo-coded

(*3)UTM, PS, MER or LCC can be chosen in the case of SCAN SAR mode and UTM or PS can be chosen in other cases.

4.3.2 Product Formats

PALSAR product formats are based on the CEOS (Committee on Earth Observation Satellites) revised standardized formats.

(1) File Composition

An image volume consists of 4 kinds of files. The file names and their contents are shown in Table 4.3.2-1, the records composing those files are shown in Table 4.3.2-2.

Table 4.3.2-1 File Composition and Definitions of File Names

File Name	Definition of File Name	Contents
Volume Directory File	VOL-Scene ID-Product ID	This file is located at the beginning of the image volume and stores the volume and file management information.
Leader File	LED-Scene ID-Product ID	This file is located before image file and stores annotation data, ancillary data and other types of data related to the image data in the succeeding image file.
Image File	IMG-XX-Scene ID-Product ID	This file is located after the leader file and stores the image data.
Trailer File	TRL-Scene ID-Product ID	This file is located after the image file and stores the final information related to the image data.

XX: polarization (HH, HV, VH, VV) (order of transmitting, receiving)

Table 4.3.2-2 Record Composition of Each File

File / Record name	Processing Level		
	1.0	1.1	1.5
a) Volume directory file			
1) Volume descriptor	O	O	O
2) File pointer	O	O	O
3) Text	O	O	O
b) SAR leader file			
1) File descriptor	O	O	O
2) Data set summary	O	O	O
3) Map projection data	-	-	O
4) Platform position data	O	O	O
5) Attitude data	O	O	O
6) Radiometric data	-	O	O
7) Data quality summary	-	O	O
8) Calibration data	O	-	-
9) Facility related data	O	O	O
c) SAR Image file			
1) File descriptor	O	O	O
2) Signal data	O	O	-
3) Processed data	-	-	O
d) Trailer file			
1) File descriptor	O	O	O
2) Low resolution image data (*1)	-	O	O

(*1) This record is not included in the products of Scan SAR mode

The record composition of SAR image file is shown in Fig. 4.3.2-1. The line number, pixel number and data size is shown in Table 4.3.2-3.

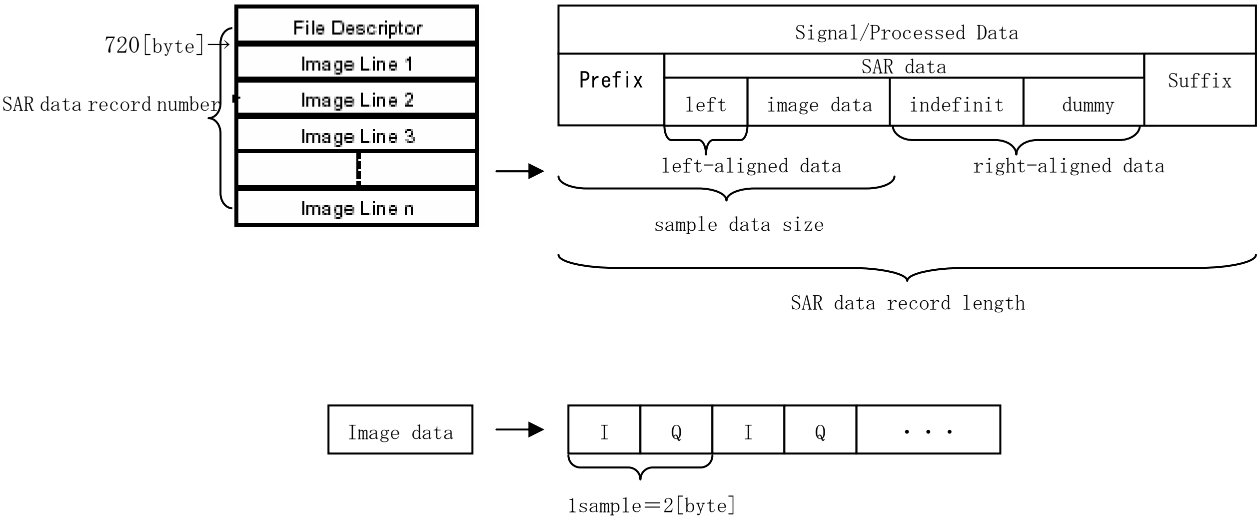

Fig. 4.3.2-1 Record composition of SAR image file

Table 4.3.2-3 Line number, pixel number and data size

Processed Level	Prefix [byte]	Left-aligned [byte]	Image data		Data record [line]	Right-aligned [byte]	Suffix [byte]
			Sample number	Data size[byte]			
1.0／1.1	412	0	Pixel number (= sample number) (See 25～28 byte in Signal data)	Sample number × 2[byte]	SAR data record number (See 181～186 byte in file descriptor)	SAR data length－image data size (See 187～192 byte in file descriptor)	0
1.5	192	0	Pixel number (= sample number) (See 25～28 byte in Processed data)	Sample number × 2[byte]	SAR data record number (See 181～186 byte in file descriptor)	SAR data length－image data size (See 187～192 byte in file descriptor)	0

(2) Description of Product Records

This section describes the format of the SAR image file.

1) Record Data Type

Table 4.3.2-4 describes the definition of data type used for record explanation.

Table 4.3.2-4 Data Types

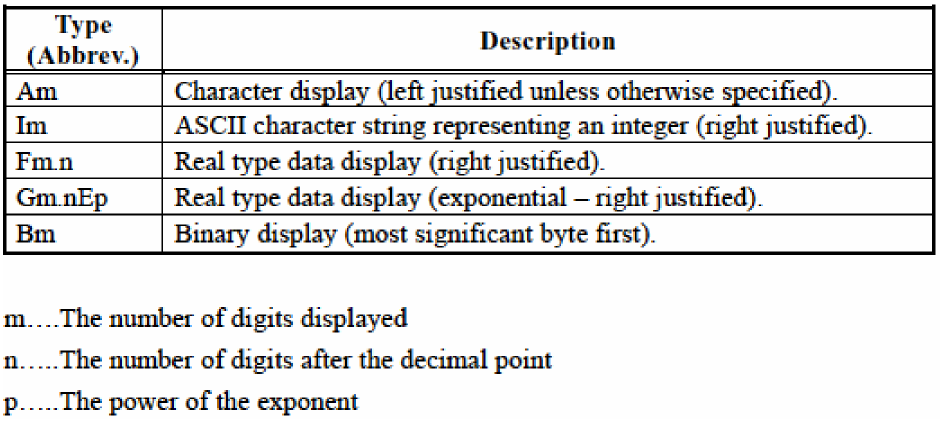

Type (Abbrev.)	Description
Am	Character display (left justified unless otherwise specified).
Im	ASCII character string representing an integer (right justified).
Fm.n	Real type data display (right justified).
Gm.nEp	Real type data display (exponential – right justified).
Bm	Binary display (most significant byte first).

m….The number of digits displayed

n…..The number of digits after the decimal point

p…..The power of the exponent

2) Product Format

Detailed format of each record is given in the product format list.

(Reference or http://www.eorc.jaxa.jp/ALOS/doc/format.htm)

5. Operation

5.1 Sensor Operation Outline

Mission equipment operation scheduling is planned as follows.

- Land and Daytime: Observation with one to three sensors of PRISM, AVNIR-2, PALSAR
- Land and Night-time: Observation with PALSAR, Calibration of PRISM and AVNIR-2

During nominal operations, PRISM and AVNIR-2 observe nadir mainly and PALSAR observation observes at 34.3 degrees of off-nadior typically.

When disaster monitoring, AVNIR-2 and PALSAR quickly observe target area with the cross track pointing function of AVNIR-2 and the variable off-nadir angle function of PALSAR.

Table 5.1-1 Basic Operation of each Sensor

	Observation Condition		
	Land		Ocean
	Night time	Day time	
PRISM	x	H	L
AVNIR-2	x	H	L
PALSAR	H	M	L

H: High Priority, M: Mid Priority, L: Low Priority, x: Calibration

Information about simultaneous operation control and required conditions for the three sensors are listed below. Table 5.1-2 lists the data rates for each sensor.

Sensor control

- The three sensors are simultaneously operational
- Two kinds of data rates for one sensor such as 120 Mbps and 240Mbps are operational exclusively

HSSR control

- HSSR has two channels for recording and one channel for reproduction. Two–channel simultaneous recording (120 Mbps + 240 Mbps) is possible. (120 Mbps + 120 Mbps is also possible, but this is not used.)
- Simultaneous HSSR recording and direct downlink (120 Mbps) is possible.

* HSSR: High-speed solid-state data recorder carried in ALOS allows recording and playback of compressed and multiplexed data.

Table 5.1-2 Source Data and Output Systems concerning the Three Sensors and HSSR Operations

	Data/Systems	Rate	Comments
Source Data	PRISM	240Mbps	1/4.5 compressed data (independent from kinds of observation modes)
		120Mbps	1/9 compressed data (independent from kinds of observation modes)
	AVNIR-2	120Mbps	All modes of AVNIR-2
	PALSAR	240Mbps	All observation modes except following 120Mbps mode
		120Mbps	Direct Downlink mode and ScanSAR mode (Burst Type 1)

5.1.1 PRISM

PRISM is a panchromatic radiometer operating in the visible near infrared region, and has three telescopes for forward, nadir and backward view. PRISM has an Earth rotation correction function to correct distortion of observation views by the three telescopes due to the Earth's rotation and obtains images by selecting automatically the best image extraction position.

Each telescope of PRISM has over 70km of field of view; observation width will be 35km in the normal observation mode with the three telescopes. The FOV can be pointed electrically ±1.5 deg. (approx. 17.5km). The nadir telescope can output data with a 70km swath width. For this mode, 35km swath width data of the backward telescope can be output simultaneously.

Table 5.1.1-1 PRISM Operation Modes

Mode		Content	Remarks
Observation	1	Nadir / Forward / Backward views simultaneous observation	Possible to request
	2	Nadir 70km + Backward 35km simultaneous observation	Ditto
	3	Nadir 70km	Ditto
	4	Nadir / Forward 35km simultaneous observation	Ditto
	5	Nadir / Backward 35km simultaneous observation	Ditto
	6	Forward/ Backward 35km simultaneous observation	Ditto
	7	Nadir 35km observation	Ditto
	8	Forward 35km observation	Ditto
	9	Backward 35km observation	Ditto
Calibration*	1	Electrical Calibration Mode	
	2	Blackbody Calibration Mode	
Standby	1	Keep a condition to transit into standby mode-2	
	2	Set a condition to transit into observation mode	
Sleep		Keep a temperature avoiding defect, trouble or degradation of function or performance which the sensor could not recover	
Survival		In the anomalous case of ALOS attitude or power supply, maintain survival condition – avoiding defect, trouble or degradation of function or performance from which the sensor could not recover.	
All-off		All-off - all power supplies	

5.1.2 AVNIR-2

AVNIR-2 obtains high resolution image data in four bands of visible and near infrared. AVNIR-2 has a cross track pointing function in the range ±44˚ (positive for left of satellite flight direction).

Table 5.1.2-1 AVNIR-2 Operation Modes

Mode		Content	Remarks
Observation		Observation	Possible to request
Standby		Set and keep a condition to transit into observation mode or calibration modes	
Calibration	1	Calibration using internal lamp A	
	2	Calibration using internal lamp B	
	3	Calibration using both internal lamps A and B	
Sleep		Maintains a temperature state which will avoid defect, trouble or degradation of function or performance from which the sensor could not recover	
Survival		In an anomalous case of ALOS attitude or power supply, maintains a survival condition which will avoid defect, trouble or degradation of function or performance from which the sensor could not recover	
All-off		All-off - all power supplies	

5.1.3 PALSAR

PALSAR is an L band Synthetic Aperture Radar which can change incidence angle in the range from 9.7 to 50.8 degrees. Spatial resolution at off-nadir 34.3 degrees is 10m for the high resolution mode. PALSAR also has a wide area observation mode called ScanSAR.

Table 5.1.3-1 lists the PALSAR operation modes.

Mode		**Content**	**Remarks**
Observation	High resolution mode	High resolution observation by single polarization (HH/HV) or simultaneous receiving of two polarizations (HH+HV/VV+VH)	Possible to request
	ScanSAR mode	Wide area observation by ScanSAR (single polarization) The same data rate as that of High resolution mode or its half rate.	Ditto
	Direct Downlink mode	Direct Downlink observed without using data recoder or DRTS (single polarization) Observation with half rate of that of the high resolution mode (single polarization)	Ditto
	Polarimetric mode	Observation with four polarizations simultaneously (HH+HV+VV+VH) Incidence angle is in the range from 9.7 to 26.2 degrees	Ditto
Calibration	Periodic	Noise Measure 1,Noise Measure 2	
	Every observation	Noise Measure 3,Transmitter Power Monitor,Transmitter Wave Pattern Monitor	
	Option	Receiving and Transmission REV,Total Characteristics of Receiving and Transmission System,I/O Characteristics when Receiving , ATT Characteristics of Receiving System , Frequency Characteristic Measure of Receiving System	
Antenna Development		Unfolding of antenna, setting of off-nadir, and development	
Standby		Keep a condition to transit into observation mode or calibration modes. When changing from the survival mode or the sleep mode to the standby mode, set a condition to transit into observation mode or calibration modes.	
Sleep		Keep PALSAR in the allowed temperature range for non-operation	
Survival			
All-off		PALSAR Off	

5.2 Operation Scenarios

The ALOS Basic Observation Scenarios are devised with the aim of joint observation. By selecting common-use modes that meet the requirements of as many users as possible, the need for individual acquisition requests will be reduced, and overall achievement of observation targets will be improved.

In order to meet the requirements of a multitude of users, comprehensive and efficient observation scenarios to cover the entire land surface of the earth are necessary. For monitoring purposes and to allow for the detection of crustal deformation and other events, observation of an area needs to be completed within a short time and repeated on a regular basis. Taking these requirements into consideration, the Basic Observation Scenarios provide for global coverage as follows: PALSAR Fine mode: three times per year; Wide mode: once per year; PRISM and AVNIR-2: once per year. For Japan and other designated regions, special observation activities are planned.

Tables 5.2-1 and 5.2-2 list the basic concepts that were applied for setting observation areas, observation modes, and observation frequencies.

Table 5.2-1 ALOS Basic Observation Scenarios (Global)

	Area	**Frequency**	**Mode**	**Basic Concept**
PALSAR (Ascending)	Global	2 times/year	FBD(HH+HV,34.3)	Global monitoring, forest observation, crustal deformation monitoring. With a view to interferometric observation, observation for two continuous repeat cycles (*) is performed.
		1 time/year	FBS(HH,34.3)	Forest observation, resources prospecting
	Regional	1 time/2 years	Polarimetry(21.5)	Polarimetric InSAR
	Regional	7 times/2 years	FBD(HH+HV,34.3) & FBS(HH,34.3)	Crustal deformation monitoring
PALSAR (Descending)	Global	1 time/year	ScanSAR(HH,5-beam)	Global monitoring
	Regional	Irregular	FBS(HH,34.3)	Crustal deformation monitoring34.3° selected for continuity from JERS-1 (35°). PALSAR adjusted for optimum performance at 34.3°.
	Wetlands	8 times/year continuously	ScanSAR(HH,5-beam)	Wetlands monitoring
PRISM	Global	1 time/year	3-direction (triplet) mode	Taking into account data for average monthly cloud cover (**) for each area Single-pass cover by pointing adjustment of ±1.2° (2 repeat cycles (*))
AVNIR-2	Global	1 time/year	Nadir	Taking into account data for average monthly cloud cover (**) for each area
PALSAR+ AVNIR-2	Regional	1 time/year	FBS(HH,34.3) & 34.3°	Simultaneous observation with PALSAR and AVNIR-2 at 34.3°

* Repeat cycle: Period until satellite returns to exact same position; 46 days for ALOS.

** Using monthly average cloud cover data for 1989 - 1995 from ISCCP (International Satellite Cloud Climatology Program), for respective observation timing of each area.

Table 5.2-2 ALOS Basic Observation Scenarios (Japan)

	Areas	Frequency	Mode	Basic Concept
PALSAR (Ascending)	Japan	6 times/year	FBD(HH+HV,34.3)	Forest observation, crustal deformation monitoring. With a view to interferometric observation, observation for two continuous repeat cycles (*) is performed.
		5 times/2 years	FBS(HH,34.3)	Crustal deformation monitoring, resources prospecting
		1 time/2 years	Polarimetry(21.5)	Polarimetric InSAR
		1 time	FBS(HH,21.5)	Emergency InSAR (at beginning of regular operation)
		1 time	FBS(HH,34.3)	Emergency InSAR (at beginning of regular operation)
PALSAR (Descending)	Japan	1 time/year	ScanSAR(HH,5-beam)	Global monitoring
	Eastern Japan	3 times/year	FBS(HH,34.3)	Crustal deformation monitoring
	Hokkaido and adjacent waters	3 times/year	ScanSAR(HH,5-beam)	Drift ice monitoring
PRISM	Japan	3.5 times/year	3-direction (triplet) mode	Taking into account data for average monthly cloud cover (**) for each area Single-pass cover by pointing adjustment of ±1.2° (2 repeat cycles (*))
AVNIR-2	Japan	7 times/year	Nadir	Taking into account data for average monthly cloud cover (**) for each area
PALSAR+ AVNIR-2	Japan	1 time/year	FBS(HH,34.3) & 34.3°	Simultaneous observation with PALSAR and AVNIR-2 at 41.5°

* Repeat cycle: Period until satellite returns to exact same position; 46 days for ALOS.

** Using monthly average cloud cover data for 1989 - 1995 from ISCCP (International Satellite Cloud Climatology Program), for respective observation timing of each area.

The ALOS Basic Observation Scenarios divide the earth into the areas shown in Figures 5.2-1, 5.2-2, 5.2-3, and 5.2-4. The division takes various factors into consideration, such as geographical and environmental characteristics, ALOS data node location, sensor operation, and wide area observation mode key areas.

The data acquisition plans for each sensor type by area are given as follows: Table 5.2-3 PRISM Basic Observation Scenario; Table 5.2-4 AVNIR-2 Basic Observation Scenario; Table 5.2-5 PALSAR Basic Observation Scenario for Ascending Mode; Table 5.2-6 and Table 5.2-7 PALSAR Basic Observation Scenario for Descending Mode. The numbers under the year/month indication on the horizontal axis indicate the repeat cycle number. Taking the block of 46 days after launch (one ALOS orbit) as Cycle 1, the cycle number is incremented by one on each subsequent orbit. The first three months after launch were defined as the checkout phase, and the following five months were the initial calibration phase. The Basic Observation Scenarios therefore start at Cycle 7. Table 5.2-8 shows the correspondence between cycle numbers and actual dates. Because the initial checkout phase was extended by 20 days, the start of Cycle 3 falls on May 16, 2006.

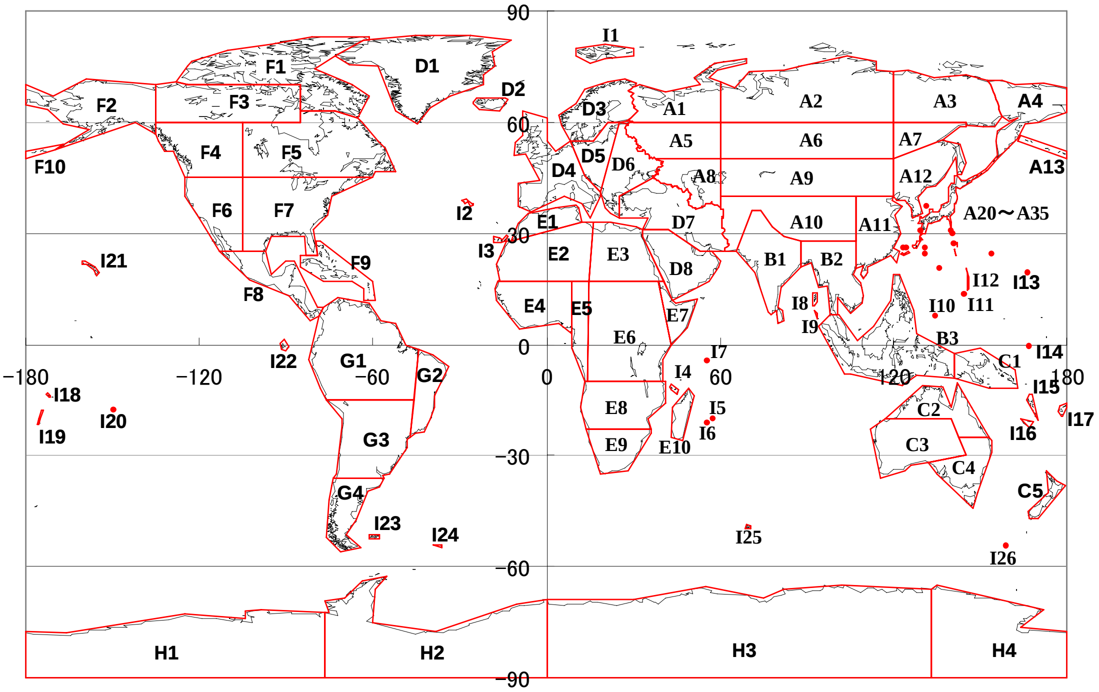

Fig. 5.2-1 ALOS Basic Observation Scenario Area Map (Ascending)

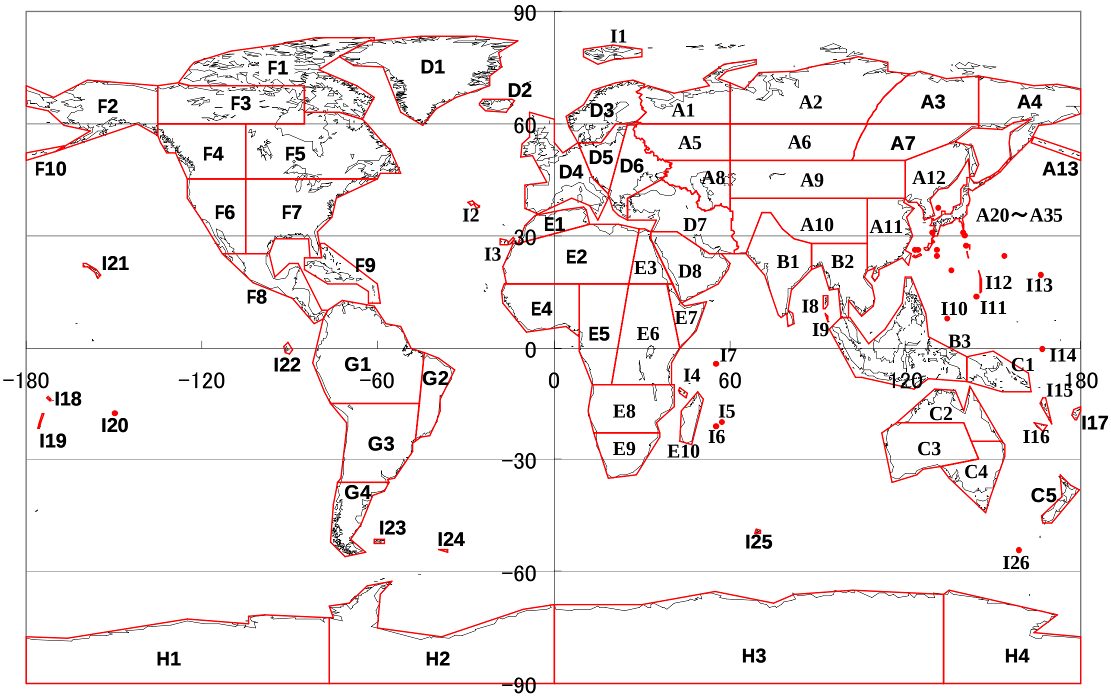

Fig. 5.2-2 ALOS Basic Observation Scenario Area Map (Descending)

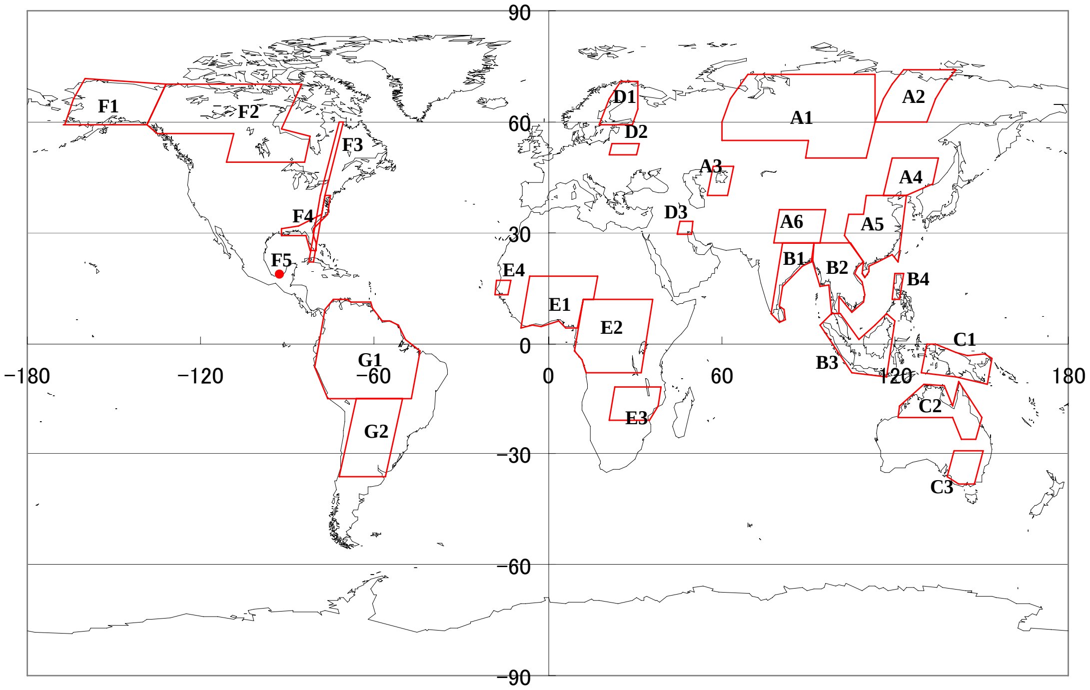

Fig. 5.2-3 ALOS Basic Observation Scenario Area Map (Wetland ScanSAR)

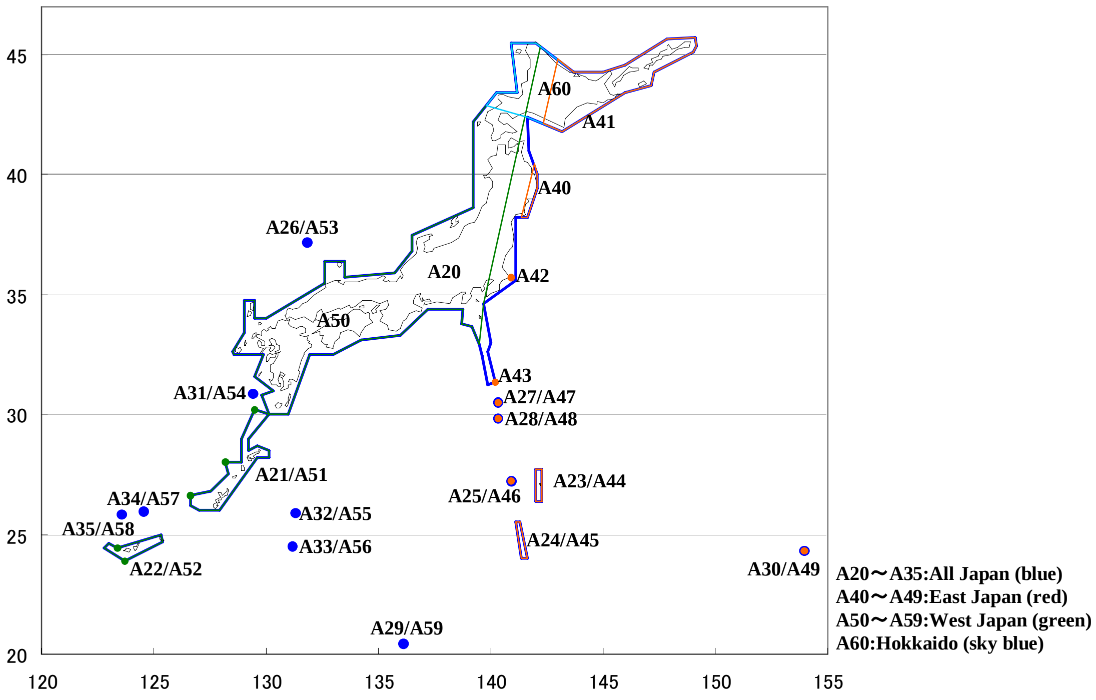

Fig. 5.2-4 ALOS Basic Observation Scenario Area Map (Enlarged Japan Map)

Table 5.2-3 PRISM Basic Observation Scenario (as of October 16, 2007)

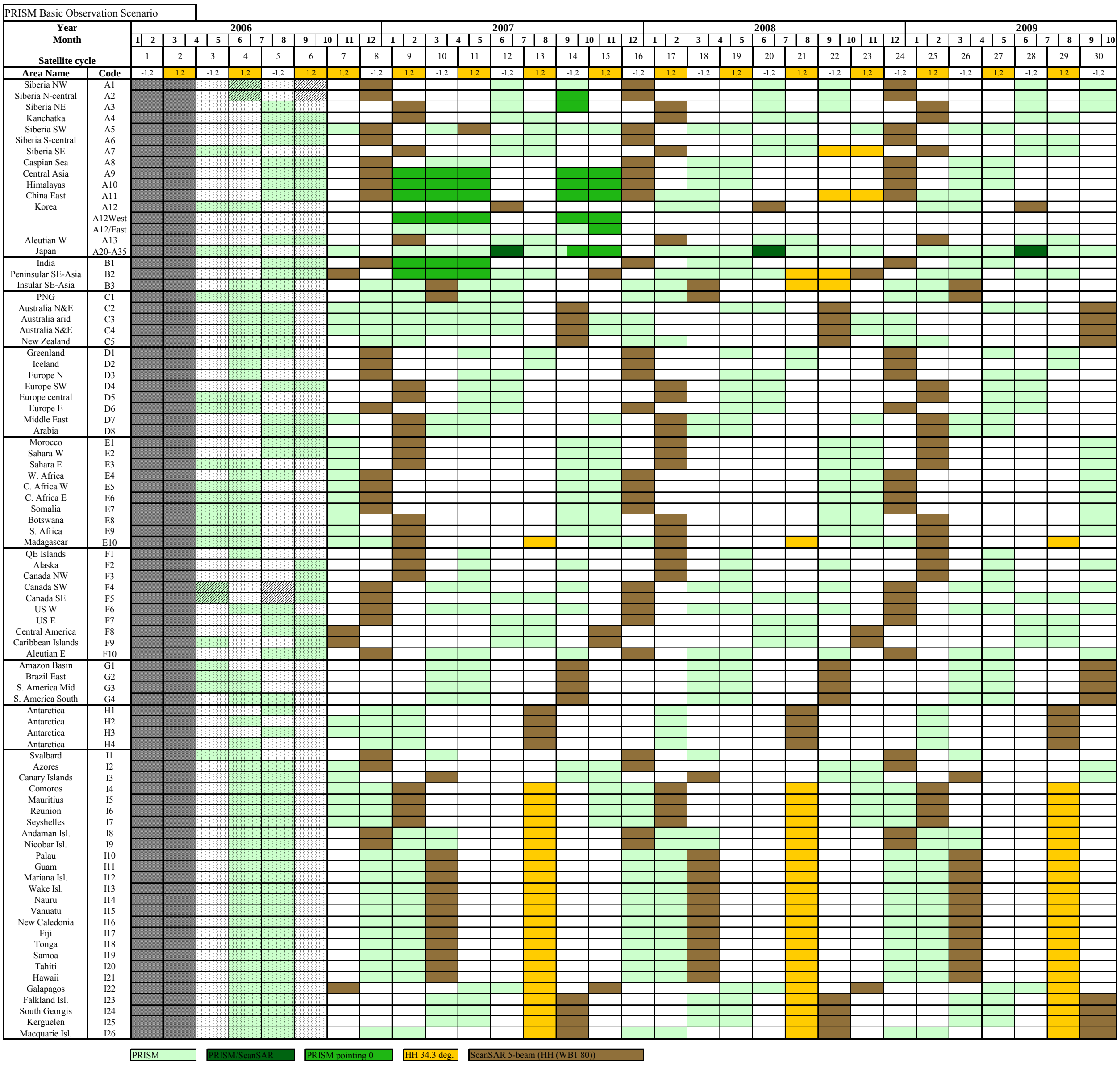

PRISM Basic Observation Scenario

Year: 2006, 2007, 2008, 2009

Month: 2006: 1 2 3 4 5 6 7 8 9 10 11 12; 2007: 1 2 3 4 5 6 7 8 9 10 11 12; 2008: 1 2 3 4 5 6 7 8 9 10 11 12; 2009: 1 2 3 4 5 6 7 8 9 10

Satellite cycle: 1 2 3 4 5 6 7 8 9 10 11 12 13 14 15 16 17 18 19 20 21 22 23 24 25 26 27 28 29 30

-1.2 1.2 -1.2 1.2 -1.2 1.2 1.2 -1.2 1.2 -1.2 1.2 -1.2 1.2 -1.2 1.2 -1.2 1.2 -1.2 1.2 -1.2 1.2 -1.2 1.2 -1.2 1.2 -1.2 1.2 -1.2 1.2 -1.2

Area Name	Code
Siberia NW	A1
Siberia N-central	A2
Siberia NE	A3
Kanchatka	A4
Siberia SW	A5
Siberia S-central	A6
Siberia SE	A7
Caspian Sea	A8
Central Asia	A9
Himalayas	A10
China East	A11
Korea	A12
	A12West
	A12/East
Aleutian W	A13
Japan	A20-A35
India	B1
Peninsular SE-Asia	B2
Insular SE-Asia	B3
PNG	C1
Australia N&E	C2
Australia arid	C3
Australia S&E	C4
New Zealand	C5
Greenland	D1
Iceland	D2
Europe N	D3
Europe SW	D4
Europe central	D5
Europe E	D6
Middle East	D7
Arabia	D8
Morocco	E1
Sahara W	E2
Sahara E	E3
W. Africa	E4
C. Africa W	E5
C. Africa E	E6
Somalia	E7
Botswana	E8
S. Africa	E9
Madagascar	E10
QE Islands	F1
Alaska	F2
Canada NW	F3
Canada SW	F4
Canada SE	F5
US W	F6
US E	F7
Central America	F8
Caribbean Islands	F9
Aleutian E	F10
Amazon Basin	G1
Brazil East	G2
S. America Mid	G3
S. America South	G4
Antarctica	H1
Antarctica	H2
Antarctica	H3
Antarctica	H4
Svalbard	I1
Azores	I2
Canary Islands	I3
Comoros	I4
Mauritius	I5
Reunion	I6
Seyshelles	I7
Andaman Isl.	I8
Nicobar Isl.	I9
Palau	I10
Guam	I11
Mariana Isl.	I12
Wake Isl.	I13
Nauru	I14
Vanuatu	I15
New Caledonia	I16
Fiji	I17
Tonga	I18
Samoa	I19
Tahiti	I20
Hawaii	I21
Galapagos	I22
Falkland Isl.	I23
South Georgis	I24
Kerguelen	I25
Macquarie Isl.	I26

PRISM | PRISM/ScanSAR | PRISM pointing 0 | HH 34.3 deg. | ScanSAR 5-beam (HH (WB1 80))

Table 5.2-4 AVNIR-2 Basic Observation Scenario (as of September 6, 2007)

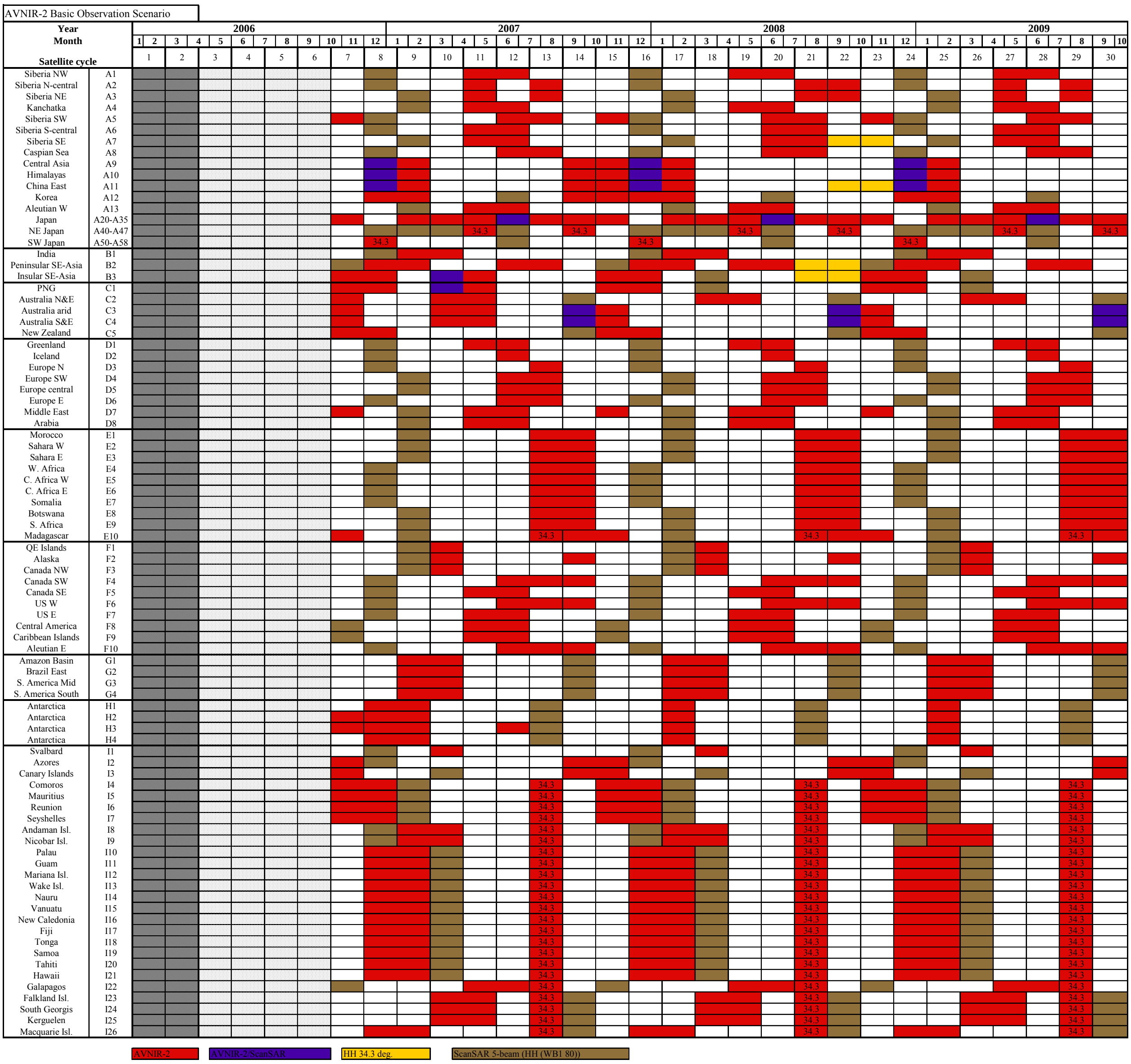

AVNIR-2 Basic Observation Scenario

Year	2006												2007												2008												2009									
Month	1	2	3	4	5	6	7	8	9	10	11	12	1	2	3	4	5	6	7	8	9	10	11	12	1	2	3	4	5	6	7	8	9	10	11	12	1	2	3	4	5	6	7	8	9	10

Satellite cycle		1	2	3	4	5	6	7	8	9	10	11	12	13	14	15	16	17	18	19	20	21	22	23	24	25	26	27	28	29	30
Siberia NW	A1	▓	▓	░	░	░	░		🟫			🟥	🟥				🟫			🟥	🟥				🟫			🟥	🟥		
Siberia N-central	A2	▓	▓	░	░	░	░		🟫			🟥		🟥			🟫					🟥	🟥		🟫			🟥		🟥	
Siberia NE	A3	▓	▓	░	░	░	░			🟫		🟥		🟥				🟫				🟥	🟥			🟫		🟥		🟥	
Kanchatka	A4	▓	▓	░	░	░	░			🟫		🟥	🟥					🟫		🟥	🟥					🟫		🟥	🟥		
Siberia SW	A5	▓	▓	░	░	░	░	🟥	🟫				🟥	🟥		🟥	🟫				🟥	🟥		🟥	🟫				🟥	🟥	
Siberia S-central	A6	▓	▓	░	░	░	░		🟫			🟥	🟥				🟫				🟥	🟥			🟫			🟥	🟥		
Siberia SE	A7	▓	▓	░	░	░	░			🟫		🟥	🟥					🟫			🟥	🟥	🟨	🟨		🟫		🟥	🟥		
Caspian Sea	A8	▓	▓	░	░	░	░		🟫				🟥	🟥			🟫				🟥	🟥			🟫				🟥	🟥	
Central Asia	A9	▓	▓	░	░	░	░		🟪	🟥					🟥	🟥	🟪	🟥							🟪	🟥					
Himalayas	A10	▓	▓	░	░	░	░		🟪	🟥					🟥	🟥	🟪	🟥							🟪	🟥					
China East	A11	▓	▓	░	░	░	░		🟪	🟥					🟥	🟥	🟪	🟥					🟨	🟨	🟪	🟥					
Korea	A12	▓	▓	░	░	░	░		🟥	🟥			🟫		🟥	🟥	🟥	🟥			🟫				🟥	🟥			🟫		
Aleutian W	A13	▓	▓	░	░	░	░			🟫		🟥	🟥					🟫		🟥	🟥					🟫		🟥	🟥		
Japan	A20-A35	▓	▓	░	░	░	░	🟥		🟥	🟥	🟥	🟪	🟥	🟥	🟥		🟥	🟥	🟥	🟪	🟥	🟥	🟥		🟥	🟥	🟥	🟪	🟥	🟥
NE Japan	A40-A47	▓	▓	░	░	░	░		🟫	🟫	🟫	🟥 34.3	🟫		🟥 34.3		🟫	🟫	🟫	🟥 34.3	🟫		🟥 34.3		🟫	🟫	🟫	🟥 34.3	🟫		🟥 34.3
SW Japan	A50-A58	▓	▓	░	░	░	░		🟥 34.3				🟫				🟥 34.3				🟫				🟥 34.3				🟫		
India	B1	▓	▓	░	░	░	░		🟫	🟥	🟥						🟫	🟥	🟥						🟫	🟥	🟥				
Peninsular SE-Asia	B2	▓	▓	░	░	░	░	🟫	🟥	🟥			🟥	🟥		🟫	🟥	🟥		🟥	🟥	🟨	🟨	🟫	🟥	🟥			🟥	🟥	
Insular SE-Asia	B3	▓	▓	░	░	░	░	🟥	🟥		🟪	🟥				🟥	🟥		🟫			🟨	🟨	🟥	🟥		🟫				
PNG	C1	▓	▓	░	░	░	░	🟥	🟥		🟪	🟥				🟥	🟥		🟫					🟥	🟥		🟫				
Australia N&E	C2	▓	▓	░	░	░	░	🟥			🟥	🟥			🟫				🟥	🟥			🟫				🟥	🟥			🟫
Australia arid	C3	▓	▓	░	░	░	░	🟥			🟥	🟥			🟪	🟥							🟪	🟥							🟪
Australia S&E	C4	▓	▓	░	░	░	░	🟥			🟥	🟥			🟪	🟥							🟪	🟥							🟪
New Zealand	C5	▓	▓	░	░	░	░	🟥	🟥						🟫	🟥	🟥						🟫	🟥	🟥						🟫
Greenland	D1	▓	▓	░	░	░	░		🟫			🟥	🟥				🟫			🟥	🟥				🟫			🟥	🟥		
Iceland	D2	▓	▓	░	░	░	░		🟫				🟥				🟫				🟥				🟫				🟥		
Europe N	D3	▓	▓	░	░	░	░		🟫					🟥			🟫					🟥			🟫					🟥	
Europe SW	D4	▓	▓	░	░	░	░			🟫			🟥	🟥				🟫			🟥	🟥				🟫			🟥	🟥	
Europe central	D5	▓	▓	░	░	░	░			🟫			🟥	🟥				🟫			🟥	🟥				🟫			🟥	🟥	
Europe E	D6	▓	▓	░	░	░	░		🟫				🟥	🟥			🟫				🟥	🟥			🟫				🟥	🟥	
Middle East	D7	▓	▓	░	░	░	░	🟥		🟫		🟥	🟥			🟥		🟫		🟥	🟥			🟥		🟫		🟥	🟥		
Arabia	D8	▓	▓	░	░	░	░			🟫		🟥	🟥					🟫		🟥	🟥					🟫		🟥	🟥		
Morocco	E1	▓	▓	░	░	░	░			🟫				🟥	🟥			🟫				🟥	🟥			🟫				🟥	🟥
Sahara W	E2	▓	▓	░	░	░	░			🟫				🟥	🟥			🟫				🟥	🟥			🟫				🟥	🟥
Sahara E	E3	▓	▓	░	░	░	░			🟫				🟥	🟥			🟫				🟥	🟥			🟫				🟥	🟥
W. Africa	E4	▓	▓	░	░	░	░		🟫					🟥	🟥		🟫					🟥	🟥		🟫					🟥	🟥
C. Africa W	E5	▓	▓	░	░	░	░		🟫					🟥	🟥		🟫					🟥	🟥		🟫					🟥	🟥
C. Africa E	E6	▓	▓	░	░	░	░		🟫					🟥	🟥		🟫					🟥	🟥		🟫					🟥	🟥
Somalia	E7	▓	▓	░	░	░	░		🟫					🟥	🟥		🟫					🟥	🟥		🟫					🟥	🟥
Botswana	E8	▓	▓	░	░	░	░			🟫				🟥	🟥			🟫				🟥	🟥			🟫				🟥	🟥
S. Africa	E9	▓	▓	░	░	░	░			🟫				🟥	🟥			🟫				🟥	🟥			🟫				🟥	🟥
Madagascar	E10	▓	▓	░	░	░	░	🟥		🟫				🟥 34.3	🟥	🟥		🟫				🟥 34.3	🟥	🟥		🟫				🟥 34.3	🟥
QE Islands	F1	▓	▓	░	░	░	░			🟫	🟥							🟫	🟥							🟫	🟥				
Alaska	F2	▓	▓	░	░	░	░			🟫	🟥				🟥			🟫	🟥				🟥			🟫	🟥				🟥
Canada NW	F3	▓	▓	░	░	░	░			🟫	🟥							🟫	🟥							🟫	🟥				
Canada SW	F4	▓	▓	░	░	░	░		🟫				🟥	🟥	🟥		🟫				🟥	🟥	🟥		🟫				🟥	🟥	🟥
Canada SE	F5	▓	▓	░	░	░	░		🟫			🟥	🟥				🟫			🟥	🟥				🟫			🟥	🟥		
US W	F6	▓	▓	░	░	░	░		🟫				🟥	🟥	🟥		🟫				🟥	🟥	🟥		🟫				🟥	🟥	🟥
US E	F7	▓	▓	░	░	░	░		🟫			🟥	🟥				🟫			🟥	🟥				🟫			🟥	🟥		
Central America	F8	▓	▓	░	░	░	░	🟫				🟥	🟥			🟫				🟥	🟥			🟫				🟥	🟥		
Caribbean Islands	F9	▓	▓	░	░	░	░	🟫				🟥	🟥			🟫				🟥	🟥			🟫				🟥	🟥		
Aleutian E	F10	▓	▓	░	░	░	░		🟫				🟥	🟥	🟥		🟫				🟥	🟥	🟥		🟫				🟥	🟥	🟥
Amazon Basin	G1	▓	▓	░	░	░	░			🟥	🟥				🟫			🟥	🟥				🟫			🟥	🟥				🟫
Brazil East	G2	▓	▓	░	░	░	░			🟥	🟥				🟫			🟥	🟥				🟫			🟥	🟥				🟫
S. America Mid	G3	▓	▓	░	░	░	░			🟥	🟥				🟫			🟥	🟥				🟫			🟥	🟥				🟫
S. America South	G4	▓	▓	░	░	░	░			🟥	🟥				🟫			🟥	🟥				🟫			🟥	🟥				🟫
Antarctica	H1	▓	▓	░	░	░	░		🟥	🟥				🟫				🟥				🟫				🟥				🟫	
Antarctica	H2	▓	▓	░	░	░	░	🟥	🟥	🟥				🟫				🟥				🟫				🟥				🟫	
Antarctica	H3	▓	▓	░	░	░	░	🟥	🟥	🟥			🟥	🟫				🟥				🟫				🟥				🟫	
Antarctica	H4	▓	▓	░	░	░	░		🟥	🟥				🟫				🟥				🟫				🟥				🟫	
Svalbard	I1	▓	▓	░	░	░	░		🟫		🟥						🟫		🟥						🟫		🟥				
Azores	I2	▓	▓	░	░	░	░	🟥	🟫						🟥	🟥	🟫						🟥	🟥	🟫						🟥
Canary Islands	I3	▓	▓	░	░	░	░	🟥			🟫				🟥	🟥			🟫				🟥	🟥			🟫				🟥
Comoros	I4	▓	▓	░	░	░	░	🟥	🟥	🟫				🟥 34.3		🟥	🟥	🟫				🟥 34.3		🟥	🟥	🟫				🟥 34.3	
Mauritius	I5	▓	▓	░	░	░	░	🟥	🟥	🟫				🟥 34.3		🟥	🟥	🟫				🟥 34.3		🟥	🟥	🟫				🟥 34.3	
Reunion	I6	▓	▓	░	░	░	░	🟥	🟥	🟫				🟥 34.3		🟥	🟥	🟫				🟥 34.3		🟥	🟥	🟫				🟥 34.3	
Seyshelles	I7	▓	▓	░	░	░	░	🟥	🟥	🟫				🟥 34.3		🟥	🟥	🟫				🟥 34.3		🟥	🟥	🟫				🟥 34.3	
Andaman Isl.	I8	▓	▓	░	░	░	░		🟫	🟥	🟥			🟥 34.3			🟫	🟥	🟥			🟥 34.3			🟫	🟥	🟥			🟥 34.3	
Nicobar Isl.	I9	▓	▓	░	░	░	░		🟫	🟥	🟥			🟥 34.3			🟫	🟥	🟥			🟥 34.3			🟫	🟥	🟥			🟥 34.3	
Palau	I10	▓	▓	░	░	░	░		🟥	🟥	🟫			🟥 34.3			🟥	🟥	🟫			🟥 34.3			🟥	🟥	🟫			🟥 34.3	
Guam	I11	▓	▓	░	░	░	░		🟥	🟥	🟫			🟥 34.3			🟥	🟥	🟫			🟥 34.3			🟥	🟥	🟫			🟥 34.3	
Mariana Isl.	I12	▓	▓	░	░	░	░		🟥	🟥	🟫			🟥 34.3			🟥	🟥	🟫			🟥 34.3			🟥	🟥	🟫			🟥 34.3	
Wake Isl.	I13	▓	▓	░	░	░	░		🟥	🟥	🟫			🟥 34.3			🟥	🟥	🟫			🟥 34.3			🟥	🟥	🟫			🟥 34.3	
Nauru	I14	▓	▓	░	░	░	░		🟥	🟥	🟫			🟥 34.3			🟥	🟥	🟫			🟥 34.3			🟥	🟥	🟫			🟥 34.3	
Vanuatu	I15	▓	▓	░	░	░	░		🟥	🟥	🟫			🟥 34.3			🟥	🟥	🟫			🟥 34.3			🟥	🟥	🟫			🟥 34.3	
New Caledonia	I16	▓	▓	░	░	░	░		🟥	🟥	🟫			🟥 34.3			🟥	🟥	🟫			🟥 34.3			🟥	🟥	🟫			🟥 34.3	
Fiji	I17	▓	▓	░	░	░	░		🟥	🟥	🟫			🟥 34.3			🟥	🟥	🟫			🟥 34.3			🟥	🟥	🟫			🟥 34.3	
Tonga	I18	▓	▓	░	░	░	░		🟥	🟥	🟫			🟥 34.3			🟥	🟥	🟫			🟥 34.3			🟥	🟥	🟫			🟥 34.3	
Samoa	I19	▓	▓	░	░	░	░		🟥	🟥	🟫			🟥 34.3			🟥	🟥	🟫			🟥 34.3			🟥	🟥	🟫			🟥 34.3	
Tahiti	I20	▓	▓	░	░	░	░		🟥	🟥	🟫			🟥 34.3			🟥	🟥	🟫			🟥 34.3			🟥	🟥	🟫			🟥 34.3	
Hawaii	I21	▓	▓	░	░	░	░		🟥	🟥	🟫			🟥 34.3			🟥	🟥	🟫			🟥 34.3			🟥	🟥	🟫			🟥 34.3	
Galapagos	I22	▓	▓	░	░	░	░	🟫				🟥	🟥	🟥 34.3		🟫				🟥	🟥	🟥 34.3		🟫				🟥	🟥	🟥 34.3	
Falkland Isl.	I23	▓	▓	░	░	░	░				🟥	🟥		🟥 34.3	🟫				🟥	🟥		🟥 34.3	🟫				🟥	🟥		🟥 34.3	🟫
South Georgis	I24	▓	▓	░	░	░	░				🟥	🟥		🟥 34.3	🟫				🟥	🟥		🟥 34.3	🟫				🟥	🟥		🟥 34.3	🟫
Kerguelen	I25	▓	▓	░	░	░	░				🟥	🟥		🟥 34.3	🟫				🟥	🟥		🟥 34.3	🟫				🟥	🟥		🟥 34.3	🟫
Macquarie Isl.	I26	▓	▓	░	░	░	░		🟥	🟥				🟥 34.3	🟫		🟥	🟥				🟥 34.3	🟫		🟥	🟥				🟥 34.3	🟫

🟥 AVNIR-2
🟪 AVNIR-2/ScanSAR
🟨 HH 34.3 deg.
🟫 ScanSAR 5-beam (HH (WB1 80))

Table 5.2-5 PALSAR Basic Observation Scenario (Ascending) (as of January 18, 2007)

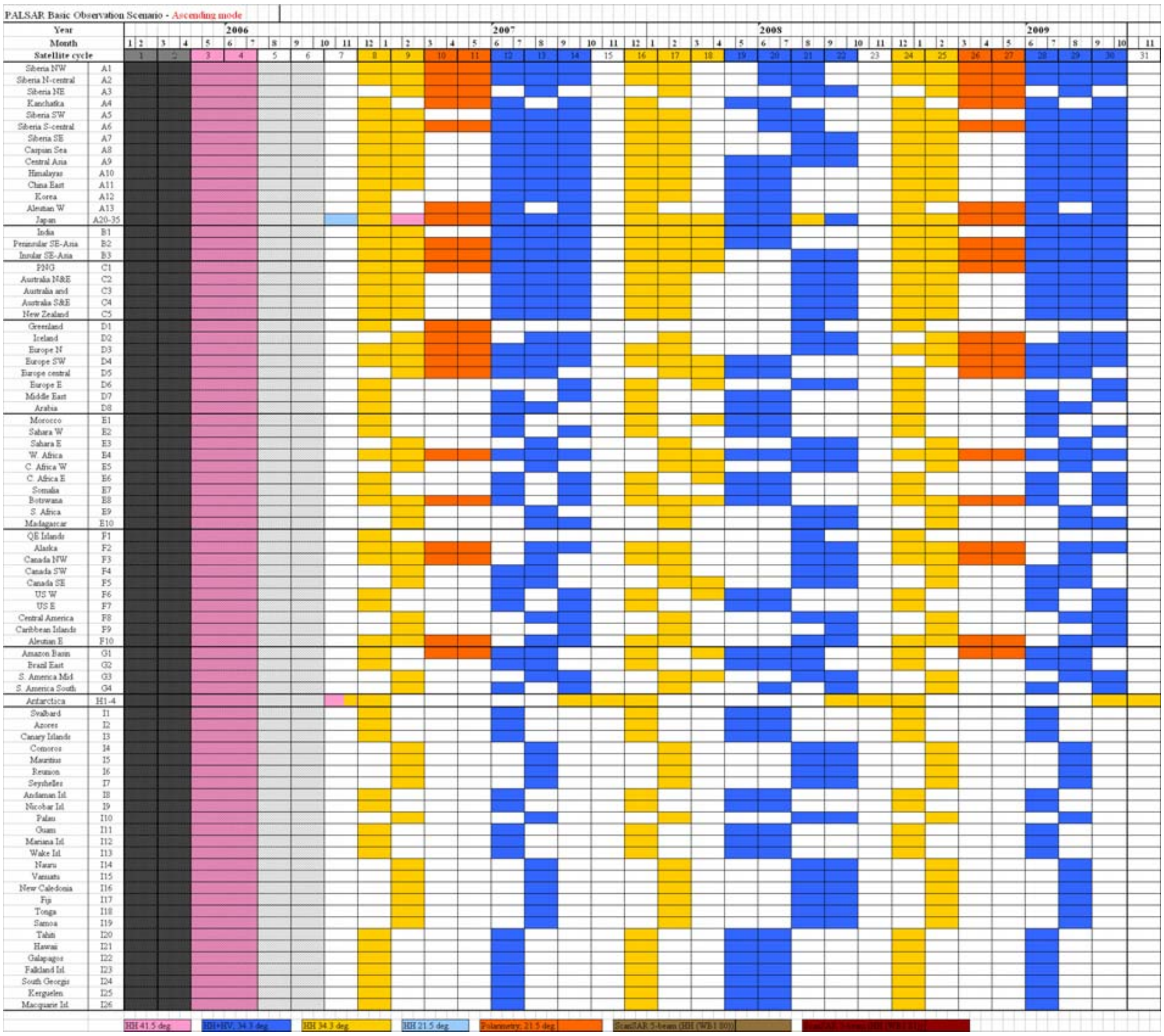

Table 5.2-6 PALSAR Basic Observation Scenario (Descending)
(as of January 18, 2007)

PALSAR Basic Observation Scenario - Descending mode

Year	2006												2007												2008												2009									
Month	1	2	3	4	5	6	7	8	9	10	11	12	1	2	3	4	5	6	7	8	9	10	11	12	1	2	3	4	5	6	7	8	9	10	11	12	1	2	3	4	5	6	7	8	9	10

Satellite cycle		1	2	3	4	5	6	7	8	9	10	11	12	13	14	15	16	17	18	19	20	21	22	23	24	25	26	27	28	29	30
Siberia NW	A1	▓	▓	░	░	░	░		🟫								🟫								🟫						
Siberia N-central	A2	▓	▓	░	░	░	░		🟫								🟫								🟫						
Siberia NE	A3	▓	▓	░	░	░	░			🟫								🟫								🟫					
Kanchatka	A4	▓	▓	░	░	░	░			🟫								🟫								🟫					
Siberia SW	A5	▓	▓	░	░	░	░		🟫								🟫								🟫						
Siberia S-central	A6	▓	▓	░	░	░	░		🟫								🟫								🟫						
Siberia SE	A7	▓	▓	░	░	░	░			🟫								🟫					🟨	🟨		🟫					
Caspian Sea	A8	▓	▓	░	░	░	░		🟫								🟫								🟫						
Central Asia	A9	▓	▓	░	░	░	░		🟫								🟫								🟫						
Himalayas	A10	▓	▓	░	░	░	░		🟫								🟫								🟫						
China East	A11	▓	▓	░	░	░	░		🟫								🟫						🟨	🟨	🟫						
Korea	A12	▓	▓	░	░	░	░						🟫								🟫								🟫		
Aleutian W	A13	▓	▓	░	░	░	░			🟫								🟫								🟫					
Japan	A20-35	▓	▓	░	░	░	░						🟫								🟫								🟫		
NE Japan	A40-47/A60	▓	▓	░	░	░	░		🟫	🟫	🟫	🟨	🟫	🟨	🟨		🟫	🟫	🟫	🟨	🟫	🟨	🟨		🟫	🟫	🟫	🟨	🟫	🟨	🟨
SW Japan	A50-58	▓	▓	░	░	░	░		🟨				🟫				🟨				🟫				🟨				🟫		
India	B1	▓	▓	░	░	░	░		🟫								🟫								🟫						
Peninsular SE-Asia	B2	▓	▓	░	░	░	░	🟫								🟫						🟨	🟨	🟫							
Insular SE-Asia	B3	▓	▓	░	░	░	░				🟫								🟫			🟨	🟨				🟫				
PNG	C1	▓	▓	░	░	░	░				🟫								🟫								🟫				
Australia N&E	C2	▓	▓	░	░	░	░								🟫								🟫								🟫
Australia arid	C3	▓	▓	░	░	░	░								🟫								🟫								🟫
Australia S&E	C4	▓	▓	░	░	░	░								🟫								🟫								🟫
New Zealand	C5	▓	▓	░	░	░	░								🟫								🟫								🟫
Greenland	D1	▓	▓	░	░	░	░		🟫								🟫								🟫						
Iceland	D2	▓	▓	░	░	░	░		🟫								🟫								🟫						
Europe N	D3	▓	▓	░	░	░	░		🟫								🟫								🟫						
Europe SW	D4	▓	▓	░	░	░	░			🟫								🟫								🟫					
Europe central	D5	▓	▓	░	░	░	░			🟫								🟫								🟫					
Europe E	D6	▓	▓	░	░	░	░		🟫								🟫								🟫						
Middle East	D7	▓	▓	░	░	░	░			🟫								🟫								🟫					
Arabia	D8	▓	▓	░	░	░	░			🟫								🟫								🟫					
Morocco	E1	▓	▓	░	░	░	░			🟫								🟫								🟫					
Sahara W	E2	▓	▓	░	░	░	░			🟫								🟫								🟫					
Sahara E	E3	▓	▓	░	░	░	░			🟫								🟫								🟫					
W. Africa	E4	▓	▓	░	░	░	░		🟫								🟫								🟫						
C. Africa W	E5	▓	▓	░	░	░	░		🟫								🟫								🟫						
C. Africa E	E6	▓	▓	░	░	░	░		🟫								🟫								🟫						
Somalia	E7	▓	▓	░	░	░	░		🟫								🟫								🟫						
Botswana	E8	▓	▓	░	░	░	░			🟫								🟫								🟫					
S. Africa	E9	▓	▓	░	░	░	░			🟫								🟫								🟫					
Madagascar	E10	▓	▓	░	░	░	░			🟫				🟨				🟫				🟨				🟫				🟨	
QE Islands	F1	▓	▓	░	░	░	░			🟫								🟫								🟫					
Alaska	F2	▓	▓	░	░	░	░			🟫								🟫								🟫					
Canada NW	F3	▓	▓	░	░	░	░			🟫								🟫								🟫					
Canada SW	F4	▓	▓	░	░	░	░		🟫								🟫								🟫						
Canada SE	F5	▓	▓	░	░	░	░		🟫								🟫								🟫						
US W	F6	▓	▓	░	░	░	░		🟫								🟫								🟫						
US E	F7	▓	▓	░	░	░	░		🟫								🟫								🟫						
Central America	F8	▓	▓	░	░	░	░	🟫								🟫								🟫							
Caribbean Islands	F9	▓	▓	░	░	░	░	🟫								🟫								🟫							
Aleutian E	F10	▓	▓	░	░	░	░			🟫								🟫								🟫					
Amazon Basin	G1	▓	▓	░	░	░	░								🟫								🟫								🟫
Brazil East	G2	▓	▓	░	░	░	░								🟫								🟫								🟫
S. America Mid	G3	▓	▓	░	░	░	░								🟫								🟫								🟫
S. America South	G4	▓	▓	░	░	░	░								🟫								🟫								🟫
Antarctica	H1-4	▓	▓	░	░	░	░							🟫								🟫								🟫	
Svalbard	I1	▓	▓	░	░	░	░		🟫								🟫								🟫						
Azores	I2	▓	▓	░	░	░	░		🟫								🟫								🟫						
Canary Islands	I3	▓	▓	░	░	░	░				🟫								🟫								🟫				
Comoros	I4	▓	▓	░	░	░	░			🟫				🟨				🟫				🟨				🟫				🟨	
Mauritius	I5	▓	▓	░	░	░	░			🟫				🟨				🟫				🟨				🟫				🟨	
Reunion	I6	▓	▓	░	░	░	░			🟫				🟨				🟫				🟨				🟫				🟨	
Seyshelles	I7	▓	▓	░	░	░	░			🟫				🟨				🟫				🟨				🟫				🟨	
Andaman Isl.	I8	▓	▓	░	░	░	░		🟫					🟨			🟫					🟨			🟫					🟨	
Nicobar Isl.	I9	▓	▓	░	░	░	░		🟫					🟨			🟫					🟨			🟫					🟨	
Palau	I10	▓	▓	░	░	░	░				🟫			🟨					🟫			🟨					🟫			🟨	
Guam	I11	▓	▓	░	░	░	░				🟫			🟨					🟫			🟨					🟫			🟨	
Mariana Isl.	I12	▓	▓	░	░	░	░				🟫			🟨					🟫			🟨					🟫			🟨	
Wake Isl.	I13	▓	▓	░	░	░	░				🟫			🟨					🟫			🟨					🟫			🟨	
Nauru	I14	▓	▓	░	░	░	░				🟫			🟨					🟫			🟨					🟫			🟨	
Vanuatu	I15	▓	▓	░	░	░	░				🟫			🟨					🟫			🟨					🟫			🟨	
New Caledonia	I16	▓	▓	░	░	░	░				🟫			🟨					🟫			🟨					🟫			🟨	
Fiji	I17	▓	▓	░	░	░	░				🟫			🟨					🟫			🟨					🟫			🟨	
Tonga	I18	▓	▓	░	░	░	░				🟫			🟨					🟫			🟨					🟫			🟨	
Samoa	I19	▓	▓	░	░	░	░				🟫			🟨					🟫			🟨					🟫			🟨	
Tahiti	I20	▓	▓	░	░	░	░				🟫			🟨					🟫			🟨					🟫			🟨	
Hawaii	I21	▓	▓	░	░	░	░				🟫			🟨					🟫			🟨					🟫			🟨	
Galapagos	I22	▓	▓	░	░	░	░	🟫						🟨		🟫						🟨		🟫						🟨	
Falkland Isl.	I23	▓	▓	░	░	░	░							🟨	🟫							🟨	🟫							🟨	🟫
South Georgis	I24	▓	▓	░	░	░	░							🟨	🟫							🟨	🟫							🟨	🟫
Kerguelen	I25	▓	▓	░	░	░	░							🟨	🟫							🟨	🟫							🟨	🟫
Macquarie Isl.	I26	▓	▓	░	░	░	░							🟨	🟫							🟨	🟫							🟨	🟫

🟨 HH 34.3 deg.

🟫 ScanSAR 5-beam (HH (WB1 80))

Table 5.2-7 PALSAR Basic Observation Scenario (Descending/Wetland ScanSAR) (as of January 18, 2007)

PALSAR Basic Observation Scenario - ScanSAR Wetlands - Descending mode

Year: **2006** | **2007** | **2008** | **2009**

Month: **1 2 3 4 5 6 7 8 9 10 11 12** | **1 2 3 4 5 6 7 8 9 10 11 12** | **1 2 3 4 5 6 7 8 9 10 11 12** | **1 2 3 4 5 6 7 8 9 10**

Satellite cycle		1	2	3	4	5	6	7	8	9	10	11	12	13	14	15	16	17	18	19	20	21	22	23	24	25	26	27	28	29	30
West Siberia	Scan_A1	▓	▓	░	░	░	░			🟫	🟫	🟫	🟫	🟫	🟫	🟫	🟫														
Lena Delta	Scan_A2	▓	▓	░	░	░	░											🟫	🟫	🟫	🟫	🟫	🟫	🟫	🟫						
Volga Delta	Scan_A3	▓	▓	░	░	░	░											🟫	🟫	🟫	🟫	🟫	🟫	🟫	🟫						
Amur	Scan_A4	▓	▓	░	░	░	░			🟫	🟫	🟫	🟫	🟫	🟫	🟫	🟫														
East China paddy	Scan_A5	▓	▓	░	░	░	░			🟫	🟫	🟫	🟫	🟫	🟫	🟫	🟫														
Tibet	Scan_A6	▓	▓	░	░	░	░											🟫	🟫	🟫	🟫	🟫	🟫	🟫	🟫						
India paddy	Scan_B1	▓	▓	░	░	░	░									🟫	🟫	🟫	🟫	🟫	🟫	🟫	🟫								
Mainland SE-Asia	Scan_B2	▓	▓	░	░	░	░	🟫	🟫	🟫	🟫	🟫	🟫	🟫	🟫	🟫	🟫	🟫	🟫	🟫	🟫	🟫	🟫	🟫	🟫	🟫	🟫	🟫	🟫	🟫	🟫
Insular SE-Asia	Scan_B3	▓	▓	░	░	░	░	🟫	🟫	🟫	🟫	🟫	🟫	🟫	🟫	🟫	🟫	🟫	🟫	🟫	🟫	🟫	🟫	🟫	🟫	🟫	🟫	🟫	🟫	🟫	🟫
Luzon	Scan_B4	▓	▓	░	░	░	░	🟫	🟫	🟫	🟫	🟫	🟫	🟫	🟫																
New Guinea	Scan_C1	▓	▓	░	░	░	░	🟥	🟫	🟫	🟥	🟫	🟫	🟫	🟫	🟫	🟫	🟫	🟫	🟫	🟫	🟫	🟫	🟫	🟫	🟫	🟫	🟫	🟫	🟫	🟫
North Australia	Scan_C2	▓	▓	░	░	░	░	🟥	🟫	🟫	🟥	🟫	🟫	🟫	🟫																
Murray-Darling	Scan_C3	▓	▓	░	░	░	░											🟫	🟫	🟫	🟫	🟫	🟫	🟫	🟫						
Finland	Scan_D1	▓	▓	░	░	░	░	🟫	🟫	🟫	🟫	🟫	🟫	🟫	🟫																
Pripet-Biebrza	Scan_D2	▓	▓	░	░	░	░			🟫	🟫	🟫	🟫	🟫	🟫	🟫	🟫														
Tigris marshes	Scan_D3	▓	▓	░	░	░	░								🟫	🟫	🟫	🟫	🟫	🟫	🟫	🟫									
Niber Basin	Scan_E1	▓	▓	░	░	░	░											🟫	🟫	🟫	🟫	🟫	🟫	🟫	🟫						
Congo Basin	Scan_E2	▓	▓	░	░	░	░						🟫	🟫	🟫	🟫	🟫	🟫	🟫	🟫	🟫										
Okavango-Mozambique	Scan_E3	▓	▓	░	░	░	░	🟫	🟫	🟫	🟫	🟫	🟫	🟫	🟫	🟫	🟫	🟫	🟫	🟫	🟫	🟫	🟫								
Senegal wetlands	Scan_E4	▓	▓	░	░	░	░											🟫	🟫	🟫	🟫	🟫	🟫	🟫	🟫						
ASF mask	Scan_F1	▓	▓	░	░	░	░			🟫	🟫	🟫	🟫	🟫	🟫	🟫	🟫														
Canada W	Scan_F2	▓	▓	░	░	░	░			🟫	🟫	🟥	🟥	🟫	🟫	🟫	🟫														
Quebec-Everglades	Scan_F3	▓	▓	░	░	░	░			🟫	🟫	🟫	🟫	🟫	🟫	🟫	🟫														
SE USA	Scan_F4	▓	▓	░	░	░	░			🟫	🟫	🟫	🟫	🟫	🟫	🟫	🟫														
Mexico	Scan_F5	▓	▓	░	░	░	░											🟫	🟫	🟫	🟫	🟫	🟫	🟫	🟫						
Amazon Basin	Scan_G1	▓	▓	░	░	░	░	🟫	🟫	🟥	🟫	🟫	🟫	🟫	🟫	🟫	🟫	🟥	🟫	🟫	🟫	🟫	🟫					🟫	🟫	🟫	🟫
Pantanal	Scan_G2	▓	▓	░	░	░	░	🟫	🟫	🟥	🟫	🟫	🟫	🟫	🟫	🟫	🟫						🟫	🟫	🟫	🟥	🟫	🟫	🟫	🟫	🟫

🟫 ScanSAR 5-beam (HH (WB1 80))

🟥 ScanSAR 5-beam (HH (WB1 81))

Table 5.2-8 Definition of Cycle

Cycle Number	**Term**	**Remarks**
Cycle1	2006/1/24 − 2006/3/10	Initial Mission Phase
Cycle2	2006/3/11 − 2006/4/24	
Cycle3	2006/5/15 − 2006/6/30	Initial CAL Phase
Cycle4	2006/7/1 − 2006/8/15	
Cycle5	2006/8/16 − 2006/9/30	
Cycle6	2006/10/1 − 2006/10/19	
Cycle7	2006/10/20 − 2006/12/04	Operations Phase
Cycle8	2006/12/05 − 2007/1/19	
Cycle9	2007/1/20 − 2007/3/6	
Cycle10	2007/3/7 − 2007/4/21	
Cycle11	2007/4/22 − 2007/6/6	
Cycle12	2007/6/7 − 2007/7/22	
Cycle13	2007/7/23 − 2007/9/6	
Cycle14	2007/9/7 − 2007/10/22	
Cycle15	2007/10/23 − 2007/12/7	
Cycle16	2007/12/8 − 2008/1/22	
Cycle17	2008/1/23 − 2008/3/8	
Cycle18	2008/3/9 − 2008/4/23	
Cycle19	2008/4/24 − 2008/6/8	
Cycle20	2008/6/9 − 2008/7/24	
Cycle21	2008/7/25 − 2008/9/8	
Cycle22	2008/9/9 − 2008/10/24	
Cycle23	2008/10/25 − 2008/12/9	
Cycle24	2008/12/10 − 2009/1/24	
Cycle25	2009/1/25 − 2009/3/11	
Cycle26	2009/3/12 − 2009/4/26	
Cycle27	2009/4/27 − 2009/6/11	
Cycle28	2009/6/12 − 2009/7/27	
Cycle29	2009/7/28 − 2009/9/11	
Cycle30	2009/9/12 − 2009/10/27	

5.3 Operation Priority Ranking

The priority ranking for ALOS satellite operation is as shown below.

1) Satellite emergency operation

2) Housekeeping (HK) operation

3) Disaster status assessment operation

4) Calibration and validation operation

5) Basic operation (basic observation scenario)

6) Autonomous use by Japanese organization based on agreement

7) Autonomous data node use

8) Autonomous research use

9) Other observation request

6. User Services

6.1 User Services

The various services related to ALOS data are described below.

6.1.1 Service Outline

Users can obtain various kinds of services, according to user status: satellite data search, order, observation request, information verification and lookup.

For general users, these services are provided by RESTEC as the Primary Distributor (PD) of ALOS data.

User service area: Asia region (except Thailand), Oceania region, North and South Americas region (except Canada) (See Fig. 6.1.3-1)

Contact information for RESTEC and the URL for on-line services are indicated below.

Data Promotion Section, Application & Service Dept.,
Remote Sensing Technology Center (RESTEC)
Roppongi First Bldg., 12F, 1-9-9, Roppongi, Minato-ku, Tokyo 106-0032, Japan
TEL: +81-3-5561-9777
FAX: +81-3-5574-8515
E-mail: data@restec.or.jp

On-line service: CROSS
http://cross.restec.or.jp

For researchers or representatives of a research organization working on joint projects, referred to as Principal Investigators (PI), and for external institution users, the services are mainly provided via AUIG (ALOS User Interface Gateway), an on-line information service that provides access to various services via an Internet browser.

6.1.2 User Types

Users are divided into the following three categories.

(1) General users

General users of data who do not have a special status and do not require product orders.

(2) Joint project researchers and PI users

Researchers engaged in joint projects for which a contract or agreement with JAXA exists. Representatives of research projects which were approved within the framework of the JAXA/EORC Research Announcement process and which use ALOS data for application research and scientific research are called PI users.

(3) External institution users

Research institutions which have a contract or agreement with JAXA.

6.1.3 Data Policy

ALOS data are provided under one of two purpose categories, as outlined below. The method in which the data are provided and the pricing differ, according to the category.

(1) Data provision method

1) Non-commercial use

Data are provided to aid in research for the purposes listed below. Based on a contractual agreement with JAXA, data are provided directly by JAXA to government institutions, universities, and other research institutions in Japan. For worldwide use, data will be provided based on the ALOS Data Node concept.

(a) Technology development: technical research aimed at satellite and sensor evaluation or at the advancement of analysis methods, etc.
(b) Practical application development and implementation research: study and practical application activities in fields such as map creation, area observation, disaster assessment, resource prospecting, and others.
(c) Data provision in case of emergencies and disasters.
(d) Geoscience and related fields: research contributing to solving environmental problems.
(e) Other activities contributing to JAXA's mission: public relations activities aimed at promoting JAXA and informing the public about its projects, and use of data for educational purposes.

Regarding (c), data that fall under the International Disaster Charter to which JAXA is a signatory will be provided according to the framework defined by the Charter.

2) Commercial use

This refers to the provision of data to a non-specified number of users for purposes other than defined in section 1). In principle, data will be provided through private-sector companies. For worldwide use, data will be provided based on the ALOS Data Node concept, similar to non-commercial use.

(2) ALOS Data Nodes (ADN)

Originally, earth observation satellite data were exchanged among international institutions on a global basis without sub-dividing the data for separate areas. However, because of the immense processing loads involved, and to facilitate the use of data tailored to regional needs, the ALOS Data Node (ADN) concept was created, dividing the earth into four main geographical zones, with the capability for local data processing and handling. Consequently, data are provided jointly by JAXA and the ADN organization or sub data node organization which has a contractual agreement with JAXA. Regarding the commercial use of data, this is in principle handled by Regional Distributors (RD) under each ADN organization. The PD, RESTEC serves an interface between JAXA and the ADNs (and their RDs) for the management and administration of all issues relating to commercial use of ALOS data for all zones.

The ALOS Data Nodes for the major regions are as follows.

1) Asia: JAXA (Geo-Informatics and Space Technology Development Agency [GISTDA] of Thailand serves as Asian Sub-Node handling Thailand, Myanmar, Laos, Vietnam, Cambodia, Malaysia, Indonesia, Singapore, Brunei, and the Philippines.)
2) Europe and Africa: European Space Agency (ESA)
3) North and South America: National Oceanic and Atmospheric Administration (NOAA) and University of Alaska, Alaska Satellite Facility (ASF)
4) Oceania: Geoscience Australia (GA)

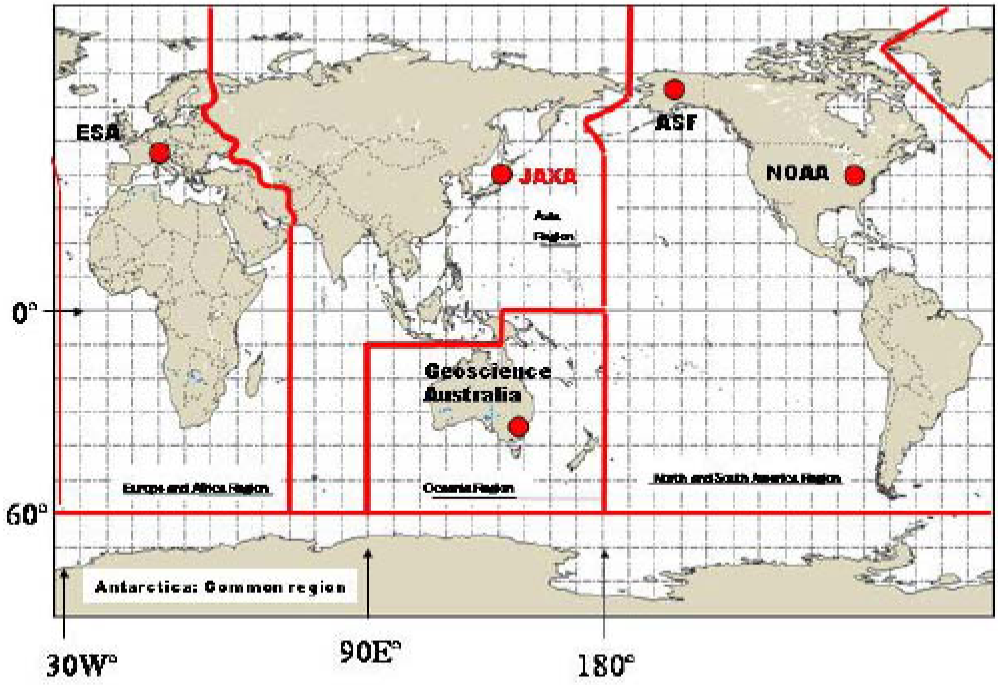

Fig. 6.1.3-1 Zone definition and organizations serving as ALOS Data Nodes

(3) Costs for data

1) Non-commercial use

When data are provided by JAXA, actual expenses for data handling and copying will be charged. This includes the cost of media, labor costs for handling and copying, utility charges, indirect costs to JAXA, and JAXA general management costs. When data are provided by ADNs other than JAXA, the actual expenses incurred by the ADN organizations will be charged. These costs are set by the respective organizations.

2) Commercial use

Costs are set by the private-sector companies that provide the data. Costs will therefore differ according to the node region.

(4) Basic conditions for use of data

1) Rights and obligations with regard to use of data by licensed users

① Users have the right to alter data to create added value data or added value products and use these internally.

② Users have the right to copy, use, and provide to third parties high-level added value products * from altered data as described above. When providing to third parties (including publication), the fact that JAXA is the source of the original data must be clearly stated.

③ Users have the right to provide data to third parties (including publication) in a form where the pixel structure of the original data cannot be reconstructed without high-level processing, as defined in a) and b) below. When providing to third parties (including publication), the fact that JAXA is the source of the original data must be clearly stated. This excludes cases where the data were simply put into image form, or otherwise not processed significantly, and cases where data are provided to third parties for a fee (separate contract required).

a) Output to paper media for creation of posters, calendars, pamphlets, etc. (including for publicity and advertising purposes)
b) Images in the form of JPEG or bitmap files for use as illustrations in research papers and other documents (including pages on websites)

④ With the permission of JAXA, users have the right to create catalog data (decimated data) or limited sample data for publication on websites, etc.

* High-level value added products: Data altered by means of advanced data processing (data analysis or combination of data from several satellites, image processing based on external information other than the data itself, transformation

of physical quantities etc.), where the pixel structure of the original data is not preserved and restoration of the original data is not possible.

2) Prohibited actions

① Copying of data (except for backup and in cases as defined in 1) (b) and (c) above).

② Providing data to third parties (except in cases as defined in 1) (b) and (c) above).

(5) Conditions for use of data by non-commercial users

In addition to the basic conditions given in (3) above, such users are subject to the following additional conditions.

1) Data may not be used for purposes other than those defined in the agreement with JAXA. Data provided to PIs may only be used for research activities as defined in the Research Announcement.

2) The results of research performed using the data or the results of using the data must be reported to JAXA, and JAXA has the right to use these results for its own activities without compensation.

(6) Data rights

1) JAXA holds the copyrights and all other associated intellectual property rights for all data provided by JAXA. (Regarding PALSAR, the rights revert to JAXA and the Ministry of Economy, Trade and Industry.)

2) When users have created high-level added value data, JAXA does not exert its copyright to the relevant data, allowing the user to freely use the relevant data.

(7) Other items (limitations, etc.)

1) The provided data may only be used for peaceful purposes.

2) Satellite operation conditions, DRTS (Data Relay and Tracking Satellite) position, and other conditions may impose limitations on the number of scenes and observation regions for which data are made available.

3) JAXA does not bear responsibility for any problems such as missing data, impaired data quality, or data delays due to problems at the satellite or ground-based equipment, or for instances where data cannot be provided due to weather conditions or other conditions beyond the control of JAXA.

* Section 6.1.3 above is excerpted from "Advanced Land Observing Satellite (ALOS) Data Policy (SDA-040006)" (published by Earth Observation Research Center, Japan Aerospace Exploration Agency, October 2004).

6.2 AUIG

6.2.1 AUIG Outline

AUIG (ALOS User Interface Gateway) is an on-line information service that gives access to various ALOS services via an Internet browser. Users can obtain information about the satellite, order observation data, and perform other actions.

AUIG services related to observation data are as follows:

- Search past observation data and observation requests, using a simple search function (free of charge)
- Order past observation data (images, etc.), (fee-based)
- Search and view the latest high-quality images of Japan (free of charge)
- AUIG services related to information about ALOS are as follows:
- Display map information about current position and flight path (free of charge)
- Display map information about past observation locations (free of charge)

For some satellite data services, user registration is required, either in the PI user or external institution user category.

6.2.2 Service Limitations

Table 6.2.2-1 lists limitations that apply to the services provided by AUIG.

Table 6.2.2-1 AUIG Services

	Outline of service	Joint project researcher/PI	External institution user	General user
User Registration	Perform user registration	○	○	×
Change User Registration	Change user registration details	○	○	×
Change Password	Change Password	○	○	×
Customize	Set up or change the screen shown when using AUIG	○	○	×
Order Product	Order data or issue observation requests in three categories (*): archived data, scheduled observation scenes, and observation requests (Observation requests can be searched only)	○ (Up to 50 scenes per year free of charge)	○ (According to agreement)	×
Order Status	Check status of product order or observation request	○	○	×
Japan Area Data Set	Browse latest high-quality images (processed data in GeoTiff format) of Japanese land areas	○	○	○
Search Observation/Catalog	Browse data in three categories: archived data, scheduled observation scenes, and observation requests	○	○	○
Observation Result	Check observation results in ALOS operation period (for each sensor)	○	○	○
Observation Plan	Browse ALOS observation plans	○	○	○
Satellite Orbit	Browse information about ALOS flight path control	○	○	○
Search Flight Position	Check ALOS flight position (trajectory)	○	○	○
Urgent Observation Image	Browse images taken by ALOS during urgent observation	○	○	○
FAQ	Provides answers to frequently asked questions by users of AUIG	○	○	○
What's New	Shows changes and additions to the site	○	○	○
LINK	Provides links to other sites related to AUIG, ALOS, and space development	○	○	○

○: Available, ×: Not available

* Archived data: Data acquired in the past by ALOS

Scheduled observation scenes: Products for which observation planning is complete

Observation requests: Observation requests for which observation planning is not complete

6.2.3 Usage Procedures

All users can access the site and obtain AUIG services via the Internet, using an Internet browser. Joint project researchers and PIs as well as external institution users who are not yet registered can initiate the registration process on the site.

The URLs for AUIG are as follows:

- Japanese language version: https://auig.eoc.jaxa.jp/auigs/jp/top/index.html
- English language version: https://auig.eoc.jaxa.jp/auigs/en/top/index.html

6.2.4 Notes and Limitations

Notes and limitations with regard to using AUIG are listed below.

(1) Notes

Restriction on the number of search queries (product order and observation request service) Taking into account the time required for searches, the number of scenes that can be searched in one operation while using the product ordering and observation request service is limited as follows:

Archive data only: 3,000 scenes

Other searches: 1,000 scenes each for archived data, scheduled observation scenes, and observation requests.

Searches exceeding these numbers will be automatically discontinued, and search results up to that point will be displayed.

1) Specifying an area range for searching (product order and observation request service, catalog search service) Due to the search logic implemented by the system, specifying an area range for the search will produce results as follows:

   If the latitude of the specified area range extends beyond 40 degrees, scenes from outside the apparent area will also be searched.

   When an elongated area in the direction of longitude is specified, the search results may include hits from outside the specified area.

   These points should be kept in mind when searching.

2) Changing or canceling orders (order status service) The entire process from receipt of an order to the issuing of the product is carried out automatically. Therefore please note that changing or canceling an order is not possible after the date/time shown on the order status screen. Regarding scheduled observation scenes and observation requests, the "Hold" option should be specified at the time of ordering if there is a possibility that a change or cancellation may become necessary.

3) Display of observation results (observation result display service) Observation results are displayed in two formats, namely "Wide Mesh Unit" or "GRS Mesh Unit," with the format being selected automatically depending on the map scale. The "Wide Mesh Unit" format displays summarized maximum values based on the "GRS Mesh Unit" format and should be used for approximate evaluations. The "GRS Mesh Unit" format also is different from the actual scene and may contain errors. For scenes that require precise evaluation, the "Observation and Catalog Search" can be used.

(2) Limitations

1) Browser requirements

Browser	Version	Windows	Mac	UNIX(Solaris)
Internet Explorer	5.0	×	−	−
	5.1.X, 5.2.X	−	×	−
	5.5, 6.0	○	−	−
Netscape	4.0 - 4.6	×	−	−
	4.76	−	−	×
	4.78	×	×	−
	6.23	○	○	−
	7.02	○	○	−
	7.1	○	○	−

○ : OK × : Not supported - : N/A

- About Internet Explorer 5.1.x, 5.2.x (Mac) Map display is not supported.
- About Netscape 4.78 (Windows) Changing the window size will result in a blank display. This is due to browser inherent specifications.

6.3 ALOS Research Announcement

6.3.1 Introduction

Japan Aerospace Exploration Agency (JAXA) Research Announcement (RA) is soliciting research proposals for science and utilization research. The first RA was issued in 1999 for researchers all over the world, and the second RA was issued in 2007. JAXA decided to issue this second RA specifically for researchers in Asia and Russia. This change was based on the successful construction of the ALOS Data Node (ADN), the worldwide data-distribution strategy, newly developed for the ALOS project.

This research will support the ALOS Research Plan to be carried out by members of the ALOS Science Project exploiting PRISM, AVNIR-2 and PALSAR sensor data. Membership in this team will be conferred on successful respondents to this RA.

Taking the 2nd ALOS Research Announcement as an example, fields in which research is solicited are as follows.

Proposals are solicited for conducting research in the following three categories:

- Calibration and Validation of ALOS data products and sensors
- Utilization research
- Scientific research

The Principal Investigators (PIs) can cover the full range of ALOS science and applications, including

(1) land use and land cover research, (2) topography and geology, (3) terrestrial (vegetation) ecosystem, agriculture and forestry research, (4) climate system, hydrological processes and water resources related research, (5) oceanography and coastal zone related research, (6) disaster and earthquakes, (7) resource exploration, (8) development of spatial data infrastructure, (9) basic studies on scattering and interferometric characteristics, (10) basic studies for accurate observation with high-resolution optical sensors, and (11) Polar research.

Participation as an ALOS Principal Investigator (PI) was open to researchers in the Asian and Russian region, shown in Fig. 6.1.3-1, with the exception of the Democratic People's Republic of Korea, from all categories of organizations: educational institutions, research institutes, private enterprises and government institutions and any other organizations.

Funds for PIs are not available under this RA.

The advantages of a PI are:

- access to relevant ALOS data (50 scenes per Japanese Fiscal Year) at no cost.

6.3.2 Research goals and objectives

The various products derived from ALOS data are expected to contribute significantly to the advancement of science. The research results in this RA will be utilized effectively for various applications such as Earth environment monitoring, natural resource exploration, disaster monitoring, and regional development planning. This RA specifically solicited research that uses ALOS data alone or in conjunction with other datasets in three categories, (1) Calibration and Validation, (2) Utilization Research, and (3) Scientific Research.

(1) Calibration and Validation of ALOS data products and sensors

The three imaging sensors onboard ALOS are designed for superior performance in various aspects of high-resolution Earth observation.

These sensors must be calibrated and validated for us to achieve

- realistic performance in measuring an image's radiance (radar back scattering) and locations and
- the potential of retrieving geophysical parameters (digital elevation model, geo-location, forest distribution, ice-monitoring, interferometry, disaster monitoring) for Earth environmental monitoring.

In this RA, we have set two research goals related to the above. We would like to solicit your research proposals for achieving these goals.

1) Calibrate Individual Sensors

This category seeks to clarify the sensor's input and output relationship (including determining calibration coefficients) as well as the sensor characterization with or without ground truth data.

The target sensors are PRISM, AVNIR-2, and PALSAR.

More detailed research items are given below.

PRISM

- Sensor performance evaluation (including image quality evaluation)
- Geometric calibration
- Radiometric calibration (including stripe removal and determining calibration coefficients)

AVNIR-2

- Sensor performance evaluation (including image quality evaluation)
- Geometric calibration

- Radiometric calibration (including stripe removal and determining calibration coefficients)

PALSAR

- Sensor performance evaluation (including image quality evaluation)
- Geometric calibration
- Radiometric calibration (including antenna pattern determination and polarimetry)

2) Develop and Validate Algorithms for Extracting Physical Parameters

It is important to develop algorithms that extract geophysical parameters from the calibrated images and truth data. It is also important to validate the estimated geophysical parameters using the above algorithms.

JAXA defined 1) DEM/DSM and 2) orthophoto images are the geographical products to be produced preferentially, however, proposals on developing and validating the other geophysical parameters were also welcomed.

(2) Utilization Research

The objectives of the earlier Japanese Earth Observation Satellites emphasized the scientific element. However, except for a limited category of data that is already being used operationally, this satellite data has not been used operationally due to many technical and operational issues. Therefore, in the preparatory operational phase of Earth observation data, utilization technology must be urgently established, and operational use in social systems is expected. A significant effort will thus be made to enhance opportunities fully employing data processing technology cultivated by JERS-1 and ADEOS as well as for promoting new developments.

The integration of ALOS data with numerical prediction models of sea ice, sea state, and disasters as well as monitoring and managing agricultural products, forestry, and fishery will directly lead to national benefits. Providing ALOS data for international utilization will also lead to the discovery of potential users and the enhancement of the market. Moreover, a wide range of provided data and user-oriented or value-added services will be able to satisfy a variety of market needs from personal to commercial applications.

Examples of utilization research are given below.

- Land use and land cover change monitoring
- Forecasting of sea-state conditions and sea ice for off-shore applications
- Ship traffic monitoring and fishery management in coastal waters
- Agriculture and forestry management (planting status, agricultural productivity

estimation, vegetation changes)

- Natural disasters (forest fires, flooding, landslide, earthquakes)
- Pollution monitoring (oil spill, red tide)
- Geology and natural resources exploration
- Applications related to SAR interferometry (digital elevation models, crustal movements, vegetation distribution)
- Development of the Geographic Information System (GIS) database of national land
- Educational use

(3) Scientific Research

The data products obtained by ALOS will contribute to promoting of science. It will be essential to address many environmental issues (such as vegetation change, biomass burning, water resource management, resource assessment, disaster and earthquake mitigation, and cryosphere monitoring) in a broad range of Earth science disciplines. Our current knowledge of the complex interactions between the various components of the Earth system is not yet sufficient to predict environmental changes with the accuracy required for effective strategic development.

The researches in this category address one or several Earth Science domains including both basic scientific research (e.g. land surface properties, measurement principles, and algorithm development for derivation of geophysical parameters) and studies of Earth Science processes. The targets have various time and spatial scales from local to regional and global.

It may be possible to compare these analyses with analyses for other satellite data (such as from JERS-1 or ADEOS). Examples of major objectives are presented below.

- Land use and land cover change
- Topography and geology
- Terrestrial ecosystem, agriculture and forestry
- Climate system, hydrological processes, and water resource related research
- Oceanography and coastal zone related research
- Process studies for microwave scattering and SAR interferometry
- Basic studies for measuring accuracy by optical sensors with fine spatial resolution
- Polar research to correspond with the International Polar Year (IPY)

6.3.3 Data distribution

(1) Data Policy

For this RA, the data will be provided free of charge to PIs who agree to the following.

1) JAXA (JAXA and METI for PALSAR data) possesses all intellectual property rights of the provided data and products.
2) Provided data shall be utilized only for peaceful and non-commercial purposes.
3) Provided data shall be utilized only for conducting RA activities that comply with the research proposal.
4) Provided data shall not be transferred to any unauthorized third party or person without JAXA's prior written consent, with the exception of authorized Co-Investigators (CIs).

Other detailed conditions, such as the number of data scenes, shall be determined through review by JAXA.

PIs must realize that data for PIs will be limited by satellite operations, the position of the Data Relay and Tracking Satellites (DRTS) and other eventualities.

JAXA shall not be liable for data loss, deterioration in data quality, or delay of data supply resulting from problems of ALOS or ground facilities, or for not providing ALOS data due to bad weather or matters beyond JAXA's control.

(2) Data Distribution

The PIs can utilize the archived JAXA data acquired from observation by ALOS, other satellites, and airborne SAR. The ALOS data for use in the ALOS standard operation plan, is primarily based on the ALOS Operation Concept and Observation Strategy. JAXA will not accept observation requests from the selected PIs in principle.

1) Standard Data Products

The PIs will be provided the following data after the conclusion of their research agreements.

- PRISM Level 1A, Level 1B1 and Level 1B2
- AVNIR-2 Level 1A, Level 1B1 and Level 1B2
- PALSAR Level 1.0, Level 1.1 and Level 1.5

2) Higher-Level Data Products of EORC

The data products from JAXA's selected area may be provided to PIs as sample datasets. Other products may also be provided for some requests. However, PIs should not base their research plans on the expectation of such products, and should be responsible for utilizing such products.

- PRISM DSM, Orthophoto Image
- AVNIR-2 Orthophoto Image
- PALSAR DEM, Orthophoto Image

3) Satellite data belonging to JAXA

Satellite data here means sensor data from MOS, JERS, ADEOS, TRMM, ADEOS-II,

ERS*, SPOT*, RADARSAT*, LANDSAT* and IRS*.

*: Regarding observation data from satellites of countries other than Japan, areas of reception are limited to Japan and immediate surroundings, and observation periods may also be limited.

6.3.4 Funding

JAXA will not provide funds to PIs.

6.3.5 Qualifications of applicants

We welcome all researchers in the Asian and Russian regions shown in Fig. 6.1.3-1 above (with the exception of the Democratic People's Republic of Korea) from educational institutions, research institutes, private enterprises, government institutions, and any other organizations, domestic or foreign, to submit research proposals for peaceful, non-commercial purposes.

6.3.6 BENEFITS AND RESPONSIBILITIES OF PIS

(1) Benefits

Upon acceptance by JAXA, PIs may request satellite data and airborne SAR data listed in section 6.3.3 at no cost.

(2) Responsibilities

1) Interim Report

The PIs must submit interim reports by 31 January 2008 on the status of their research in the format given by JAXA. They are highly recommended to participate in PI symposiums held jointly by JAXA and ADN organizations annually, and present the progress and accomplishments of their research.

2) Final Report

All PIs must submit their final reports to JAXA in English in accordance with the instructions in the agreement. The submission due data is currently planned in the end of July 2009. They must present their results or part of their results at a meeting, symposium or workshop conducted by JAXA.

6.3.7 Research organizations

The organizational framework within the Japan Aerospace Exploration Agency, Earth Observation Research Center (hereinafter EORC) regarding research using ALOS data is as follows.

The ALOS Research Group, led by the ALOS Science Project Manager, is an organization within EORC which supports research projects. The activities of PIs selected through the RAs form part of the activities of the ALOS Research Group.

Initial selection and evaluation of research proposals was performed by the Research Evaluation Committee which was chaired by an ALOS program scientist and comprised of experts in the respective fields. The JAXA Research Selection Committee (Research Board) then made the final decision, based on the recommendations from the evaluation committee. At the time of the Interim Evaluation, the establishment of a committee to evaluate results based on interim reports from PIs is planned, and the successful PIs through the evaluation can continue their research projects.

* ALOS Research Announcement Office:

Earth Observation Research Center (EORC)

Japan Aerospace Exploration Agency (JAXA)

2-1-1, Sengen, Tsukuba, Ibaraki 305-8505, Japan

Tel: +81-29-868-2475 Fax: +81-29-868-2961

Email: aproject@jaxa.jp

Appendix 1　Abbreviation Table

Abbreviation Table

Abbreviation	Name
ADEOS	Advanced Earth Observing Satellite
ADEOS-Ⅱ	Advanced Earth Observing Satellite-Ⅱ
AIRSAR	NASA/JPL DC-8 Aircraft SAR
ALOS	Advanced Land Observing Satellite
ATT	Attenuator
AUIG	ALOS User Interface Gateway
AVNIR	Advanced Visible and Near Infrared Radiometer
AVNIR-2	Advanced Visible and Near Infrared Radiometer type 2
bps	bit per second
BSQ	Band Sequential
CAL/VAL	Calibration/Validation
CCD	Charge Coupled Device
CEOS	Committee on Earth Observation Satellites
CPU	Central Processing Unit
dB	decibel
DEM	Digital Elevation Model
DRTS	Data Relay Test Satellite
DSM	Digital Surface Model
DTM	Digital Terrain Model
EOC	Earth Observation Center
EORC	Earth Observation Research and application Center
ERS	European Remote Sensing Satellite

Abbreviation	Name
ETM+	Enhanced Thematic Mapper,Plus
FAO	Food and Agriculture Organization
FBD	Fine mode Beam Dual-polarimetric
FBS	Fine mode Beam Single-polarimetric
GA	Geoscience Australia
GBFM	Global Boreal Forest Mapping
GCP	Ground Control Point
GIS	Geographic Information System
GISTDA	Geo-Informatics and Space Technology Development Agency
GLI	Global Imager
GOFC-GOLD	Global Observation of Forest and Land Cover Dynamics
GPS	Global Positioning System
GRFM	Global Rain Forest Mapping
GRS	Ground Reference System
GSFC	Goddard Space Flight Center
GSI	Geographical Survey Institute
GSJ	Geological Survey of Japan
GTOS	Global Terrestrial Observation System
GUI	Graphical User Interface
HDDR	High Density Digital Recorder
HDDT/HDT	High Density Digital Tape
HDF	Hierarchical Data Format
H-Ⅱ	H-Ⅱ

Abbreviation	Name
H-ⅡA	H-ⅡA
HK	Housekeeping
HSSR	High-speed Solid State Data Recorder
HTTP	Hyper Text Transfer Protocol
IC	Integrated Circuit
IDCP	InterDAQ Control Protocol
IGBP	International Geosphere-Biosphere Program
IGOS	Integrated Global Observation Strategy
IGOS-P	Integrated Global Observation Strategy partnership
INSAR	Interferometric Synthetic Aperture Radar (=IFSAR)
IRS	Information Retrieval Subsystem
ISAS	Institute of Space and Astronautical Science
ISCCP	International Satellite Cloud Climatology Project
JAROS	Japan Resources Observation System Organization
JAXA	Japan Aerospace Exploration Agency
JERS-1	Japanese Earth Resources Satellite-1
JPEG	Joint Photographic coding Experts Group
JPL	Jet Propulsion Laboratory
JTWC	Joint Typhoon Warning Center
JWA	Japan Weather Association
KAIST	Korea Advanced Institute of Science and Technology
KSA	Ka-band Single Access
KOMPSAT-1	Korean Multi-Purpose Satellite-1

Abbreviation	Name
LAI	Leaf Area Index
LANDSAT	Land Satellite
MODIS	Moderate Resolution Imaging Spectrometer
MOS	Marine Observation Satellite
MTF	Modulation Transfer Function
NASA	National Aeronautics and Space Administration
NASDA	National Space Development Agency of Japan
NOAA	National Oceanic and Atmospheric Administration
ODA	Official Development Assistance
OPS	Optical Sensor
OS	Operating System
PALSAR	Phased Array type L-band Synthetic Aperture Radar
PI	Principal Investigator
Pi-SAR	Polarimetric and Interferometric Airborne Synthetic Aperture Radar
PRF	Pulse Repetition Frequency
PRISM	Panchromatic Remote-sensing Instrument for Stereo Mapping
RADAR	Radio Detection and Ranging
RADARSAT	Radar Satellite
RESTEC	Remote Sensing Technology Center of Japan
Rev	Revolution
RGB	Red/Green/Blue
SAR	Synthetic Aperture Radar
Scan-SAR	Scan-Synthetic Aperture Radar

Abbreviation	Name
sigma-SAR	Sigma Synthetic Aperture Radar Processor
SPOT	Satellite Probatoire d'Observation de la Terre
TBD	To Be Determined
TCO	Terrestrial Carbon Observations
TIFF	Tagged Image File Format
TKSC	Tsukuba Space Center
TM	Thematic Mapper
TRMM	Tropical Rainfall Measuring Mission
UA	University of Alaska
UNFCCC	United Nations Framework Convention on Climate Change
UTM	Universal Transverse Mercator
VCDU	Virtual Channel Data Unit
VCID	Virtual Channel Identification
WWW	World Wide Web

Appendix2 Pertinent information

Bibliography and Related document

[1] United Nations. “World Cartography” New York, vol. XX, 1990, ISBN-9211004322.

[2] A. Stoffelen, and D. Anderson, ″Scatterometer data interpretation: Estimation and validation of the transfer function CMOD4″, J. Geophys. Res., vol. 102, pp.5767-5780, 1997.

[3] F. J. Wentz, and D. K. Smith, ″A model function for the ocean-normalized radar cross section at 14 GHz derived from NSCAT observations″, J. Geophys. Res., vol. 104, pp.11499-11514, 1999.

[4] T. Shimada, H. Kawamura, M. Shimada, ″An L-band geophysical model function for SAR wind retrieval using JERS-1 SAR″, IEEE Trans. Geosci. Remote Sensing, vol. 41, pp.518-531, 2003.

[5] O. Isoguchi, and M. Shimada, ″Relationship between wind vectors and L-band radar cross sections examined using PALSAR″, Proceedings of 2007 IGARSS (DVD), Barcelona, Spain, 2007.

[6] H. Kawamura, J. Sun, and T. Shimada, “Retrieval of surface wave parameters from PALSAR images”, submitted to J. Geophys. Res., 2007.

[7] O. Isoguchi, M. Shimada, F. Sakaida, and H. Kawamura, “Kuroshio-induced cold eddy streets in the lee of isolated islands”, Proceedings of 2007 IGARSS (DVD), Barcelona, Spain, 2007.

[8] IPY, ″A Framework for the International Polar Year 2007-2008″, IPY framework document, 2004

[9] EORC, JAXA. “ALOS PRISM Level 1 Product Format Descriptions Rev.J,” Tokyo, 2006, NEB-01006(ALOS-DPFT-E01).

[10] EORC, JAXA. “ALOS AVNIR-2 Level 1 Product Format Descriptions Rev.J” Tokyo, 2006, NEB-01006(ALOS-DPFT-E02).

[11] EORC, JAXA. “ALOS PALSAR Level 1 Product Format Description (Vol.1: Level 1.0)Rev.J” Tokyo, 2006, NEB-01006(ALOS-DPFT-E03).

[12] EORC, JAXA. “ALOS PALSAR Level 1 Product Format Description (Vol.2: Level 1.1/1.5) Rev.I” Tokyo, 2006, NEB-01006(ALOS-DPFT-E04).

Organizing Committee of Sixth International Carbon Dioxide Conference. “6th International Carbon Dioxide Conference vol. I” Tokyo, 2001, ISBN-4-9901002-0-4.

Organizing Committee of Sixth International Carbon Dioxide Conference. “6th International Carbon Dioxide Conference vol. II” Tokyo, 2001, ISBN-4-9901002-1-2.

NASDA, European Space Agency (ESA), Committee on Earth Observation Satellites (CEOS). “CEOS SAR Workshop 2001 ABSTRACTS” Tokyo, 2001, NDX-000238.

NASDA, ESA, CEOS. “CEOS SAR Workshop 2001 Proceedings” Tokyo, 2001, NDX-000306.

MITI, NASDA. “FINAL REPORT OF JERS-1 / ERS-1 SYSTEM VERIFICATION PROGRAM VOLUME 1” Tokyo, 1995.

MITI, NASDA. “FINAL REPORT OF JERS-1 / ERS-1 SYSTEM VERIFICATION PROGRAM VOLUME 2” Tokyo, 1995.

NASDA, EOC. “JERS-1: Earth Visitor’s Guide” Tokyo, 1996, NCX-000119.

Earth Observation Center (EOC), NASDA. “JERS-1 DATA USERS HANDBOOK” Tokyo, 1994.

EORC, JAXA. “JERS-1 Research Invitation Program Final Report” Tokyo, 2004, NDX-030063.

EORC, NASDA. “JERS-1 SCIENCE PROGRAM ’99 PI REPORTS Global Forest Monitoring and SAR Interferometry” Tokyo, 1999.

EORC, NASDA. “Proceedings of 1st ALOS PI Workshop” Tokyo, 2001, NDX-000264.

EORC, JAXA. “Proceedings of 2nd ALOS PI Workshop” Tokyo, 2004, NDX-030064.

Earth Science and Technology Organization (ESTO), “Proceedings of The Second Workshop on SAR Interferometry -SAR WORKSHOP ’97 TSUKUBA- : Auditorium of AIST Tsukuba Research Center, Tsukuba, Japan; November 18-20, 1997 / Disaster Prevention Science Team, Committee for Earth Observation Systems, Earth Science and Technology Forum” Tokyo, 1997.

National Institute of Agro-Environmental Sciences, Science Technology Agency of Japan (Japan International Science and Technology Exchange Center). “Proceedings of The International Workshop on Investigation of Tropical Environments using New Remote Sensing Sensors such as Micro wave Sensors (IWITERS) -SAR WORKSHOP ’97 TSUKUBA-” Tokyo, 1997.

Ministry of International Trade and Industry (MITI), NASDA. “Result Reporting Meeting of JERS-1 / ERS-1 System Verification Program Abstracts” Tokyo, 1994.

NASDA. “SAR Workshop 2003” Tokyo, 2003.

Related Homepage

Japan Aerospace Exploration Agency（JAXA）

- http://www.jaxa.jp/index_e.html

Office of Space Applications, JAXA

- http://www.satnavi.jaxa.jp/index_e.html

Earth Observation Research Center（EORC）

- http://www.eorc.jaxa.jp/en/index.html

Earth Observation Center（EOC）

- http://www.eorc.jaxa.jp/hatoyama/homepage.html

ALOS Project Team, JAXA

- http://alos.jaxa.jp/index-e.html

EORC ALOS

- http://www.eorc.jaxa.jp/ALOS/index.htm

Earth Remote Sensing Data Analysis Center（ERSDAC）

- http://www.ersdac.or.jp/eng/index.E.html

International Polar Year（IPY）

- http://www.ipy.org/

Contact

ALOS Research Announcement Office:
Earth Observation Research Center (EORC)
Japan Aerospace Exploration Agency (JAXA)
E-mail: aproject@jaxa.jp

2-1-1, Sengen, Tsukuba-city, Ibaraki 305-8505 Japan